

RESPONSE OF APS STORAGE RING BASEMAT TO AMBIENT VIBRATION

by

J. A. Jendrzejczyk, M. W. Wambsganss, and R. K. Smith

INTRODUCTION

The storage ring of the Advanced Photon Source (APS) facility at Argonne is very sensitive to vibration. Large vibration amplitudes would result in degraded machine performance. Because the storage ring assembly is supported on the storage ring basemat, the dynamics of the basemat are critical to successful operation. Before construction began, a survey of site ground vibration [1] indicated that the site was acceptable from a vibration standpoint. When construction of the linear accelerator (Linac) floor slab and shielding walls was completed, dynamic-response measurements were conducted [2]. The slab/wall system showed attenuation of soilborne vibrations in the horizontal directions, but an amplification (approximately a factor of 1.5) of vertical vibration at a frequency of 7.7 Hz. Vibration response of the slab/wall system at all other frequencies showed attenuation of soilborne vibrations. Dynamic-response measurements were also conducted on an incomplete section of the storage ring basemat [3]. Although this section was not prototypical, results were similar to those of the Linac floor in the horizontal direction, showing large damping and attenuation of horizontal soilborne vibrations. While the basemat followed the soil vibration in the vertical direction, no large amplification was observed. However, measured vertical amplitudes on the basemat were a function of location, indicating a modal response. A series of vibration response measurements was conducted on a completed section of the storage ring basemat/tunnel adjacent and to the west of the Early Assembly Area (EAA) on May 21, 1992, and is the subject of this report.

THIS DOCUMENT IS UNCLASSIFIED

The submitted manuscript has been authored by a contractor of the U. S. Government under contract No. W-31-109-ENG-38. Accordingly, the U. S. Government retains a nonexclusive, royalty-free license to publish or reproduce the published form of this contribution, or allow others to do so, for U. S. Government purposes.

MASTER

OBJECTIVES

To measure the dynamic response of a completed section of the storage ring basemat/tunnel system. Specific objectives are to (a) measure vertical basemat response over a large area to determine general response and attenuation characteristics; (b) measure vertical basemat response over a limited area to detect any rocking motion; (c) measure three axis responses, two horizontal directions and vertical, on the basemat and tunnel roof to detect and define basemat/tunnel motion; and (d) measure three axis responses on basemat and soil adjacent to the experimental hall to determine soil/basemat dynamic-response characteristics.

TECHNICAL APPROACH

To achieve the above objectives, measurements were conducted under four sets of conditions).

Condition 1

Vertical acceleration at the center of the basemat was measured at 75-ft intervals, as shown in Fig. 1. The acceleration signals were double-integrated to convert them to displacement and were recorded on FM magnetic tape for later analysis. Recording commenced at approximately 3:10 PM and continued for 1.3 hr. Heavy construction activity was in progress for approximately 2/3 of the recording duration, with the site being quiet for the last 15 min. Most construction activity was west of the measurement area, and a small gasoline-powered generator was operating on the experimental hall slab near measurement locations 2-3 (see Fig. 1).

The data were reduced to yield RMS displacement as a function of time with the following bandwidths: 4-100 Hz, 10-100 Hz, 20-100 Hz, 10-100 Hz with the 28-30 Hz contribution removed, and 28-30 Hz. The 28-30 Hz displacement corresponds to the rotational speed of the gasoline generator and would not contribute to the system displacement when the APS is in operation, however it provides a good vibration source to observe basemat attenuation. In addition, rms displacements for narrow bandwidths were calculated to determine the effect of frequency on vibration propagation along the basemat/tunnel.

Condition 2

To measure the rocking response of the basemat, accelerometers were located as shown in Fig. 2 to measure vertical motion. RMS displacements as a function of time were calculated for 4-100 Hz, 10-100 Hz, and 20-100 Hz bandwidths. The site was quiet for the duration of the measurements.

Condition 3

To measure basemat and tunnel motion, two accelerometer triplets were positioned on the basemat surface and on the top of the tunnel roof, shown in Fig. 3. One triplet was centered in the tunnel, oriented in a north/east/vertical direction, and the other triplet was vertically centered above the basemat transducer, on top of the tunnel roof. RMS displacements as a function of time were calculated for 4-100 Hz, 10-100 Hz, and 20-100 Hz bandwidths. The site was quiet for the duration of the measurements.

Condition 4

One accelerometer triplet was placed on the ground and a vertically oriented accelerometer triplet was placed on the experimental hall floor at locations shown in Fig. 4. Basemat motion was measured with the same accelerometer triplet used for Condition 3 basemat measurements. The latter two accelerometers measured the response of the basemat/experimental hall to ground vibration. RMS displacements as a function of time were calculated for 4-100 Hz, 10-100 Hz, and 20-100 Hz bandwidths. The site was quiet for the duration of the measurements.

DISCUSSION

Condition 1

Basemat-displacement-response measurements were made from 3:12 PM to 4:30 PM, a period that included times of heavy construction activities. Typical displacement power spectra for periods of heavy construction and with the site quiet are shown in Figs. 5 and 6, respectively. Response peaks appear at approximately 7, 14, and 28 Hz in Fig. 5. Typically, the only response peak in the majority of the power spectra at periods of heavy construction is that for 28 Hz, which is associated with the portable gasoline generator and equipment it powers. Only the low-level integrator noise is observed on the power spectra measured during the period when the site was quiet.

Displacement response (4-100 Hz) as a function of time for locations 1-7 is shown in Figs. 7-13. The construction periods are clearly evident with amplitude levels exceeding 300 nm. Amplitude levels of approximately 40 nm are observed during periods when the site is quiet, which is consistent with the measurements described in Ref. 1. The integrator noise is included in the measurements, thus allowing conservatism. Quiet-period amplitudes at locations 6 and 7 are lower than those of the other locations, due primarily to the characteristics of their associated electronics; their noise floor is below that of the other modules. Generally,

construction activity is located close to location 1. Basemat amplitudes typically decrease with distance from location 1, giving an indication of the attenuation characteristics. This will be elaborated later.

Displacement response (10-100 Hz) as a function of time for locations 1-7 is shown in Figs. 14-20. Again, the periods of heavy construction activity are obvious. The measured amplitudes with the site quiet are approximately 10 nm, a considerable reduction from the 40 nm noted above. This is due to exclusion of the integrator noise. Basemat amplitudes also decrease with distance from location 1.

Displacement response (20-100 Hz) as a function of time for locations 1-7 is shown in Figs. 21-27. Although the trends are similar to those for the 4-100 Hz and 10-100 Hz data, there is still a large-amplitude response during periods of heavy construction. This indicates that an excitation source with a frequency of greater than 20 Hz is present. The source is the portable gasoline generator and associated equipment. The generator rotates at approximately 1740 r/min, which corresponds to 29 Hz. Displacement response for a 28-30 Hz frequency band is shown in Figs. 28-34. Although the generator is small (about 8-10 hp) and is mounted on vibration dampers, it is responsible for a large portion of the basemat displacement. This is a good example of the care that must be exercised in the choice and placement of vibrating equipment on the storage ring basemat/experimental hall.

The displacement response (10-100 Hz) with the 28-30 Hz band digitally filtered is shown in Figs. 35-41. Overall, the amplitude relating to the heavy construction period is significantly reduced, with a general decrease in amplitude with distance from location 1.

Because the basemat exhibits attenuation characteristics, the measurement data were manipulated to determine the effect of frequency. A displacement power spectrum corresponding to a measurement time of 3:20:48 PM was digitally filtered using 2 Hz bandwidths at center frequencies of 8, 12, 19, 29, 39, 49, and 59 Hz. The results are plotted in Fig. 42, normalized to location-1 amplitude, as a function of distance from location 1. Generally, the higher frequencies tend to attenuate more rapidly than the lower frequencies. A general equation for surface wave attenuation is:

$$\left(\frac{W}{W_1}\right) = \left(\frac{R_1}{R}\right)^{0.5} e^{-\alpha(R-R_1)} \quad (1)$$

where W and W_1 are amplitudes at respective distances R and R_1 from the source, and α is an exponent relating to material/soil damping. α can be calculated from

the data used in Fig. 42; its value is typically negative, thus indicating an attenuation lower than that of a pure geometrically associated attenuation.

Condition 2

The vibration measurements were conducted from 4:46 PM to 5:09 PM with the site quiet. Displacement response (4-100 Hz) for locations 1-2, 3-5, and 6-7 are shown in Figs. 43, 44, and 45 respectively. If the basemat was rocking about its center, the amplitudes at locations 3 and 4 would be greater than that at location 4 (Fig. 44). Because all amplitudes are approximately equal, we can assume that with the ambient ground excitation at the time of the measurements, the basemat does not rock. The reduced amplitude at locations 6 and 7 (Fig. 45) is attributed to the previously mentioned noise of the measurement system integrator.

The same general comments are applicable to the displacement response (10-100 Hz), Figs. 46-48, and the displacement response (20-100 Hz), Figs. 49-51.

Condition 3

Vibration measurements were conducted from approximately 7:08 PM to 7:22 PM with the site quiet. Figs. 52 and 53 show the 4-100 Hz displacement response of the basemat and roof, respectively, in the horizontal and vertical directions. The reduced amplitude of the basemat vertical displacement (Fig. 53) is attributed to the previously mentioned noise of the measurement system integrator. A comparison of displacement response in the north, east, and vertical directions is presented in Figs. 54, 55, and 56, respectively. No unusual response was observed on any of the plots. However with the site quiet, no sufficiently large excitation source was present to dynamically excite the basemat tunnel; the tunnel's behavior may vary considerably, depending on excitation level, frequency content, and location.

The same general comments are applicable to the displacement response (10-100 Hz), Figs. 57-61, and the displacement response (20-100 Hz), Figs. 62-66.

Condition 4

Vibration measurements were conducted from approximately 7:35 PM to 7:48 PM with the site quiet. Figs. 67 and 68 show the 4-100 Hz displacement response of the soil and basemat, respectively. Figs. 69, 70, and 71 compare the displacement response of the soil and basemat in the north, east, and vertical directions. The "filtering" ability of the basemat to horizontal soil vibration is again seen in Figs. 69 and 70.

The same general comments are applicable to the displacement response (10-100 Hz), Figs. 72-76, and the displacement response (20-100 Hz), Figs. 77-81.

General Comments

No specific frequency-response peaks were observed on the basemat/tunnel system, thus indicating that no high magnification factor exists in the soil/tunnel system.

While no attenuation was observed in the vertical direction, the soil/tunnel system exhibited attenuation in the horizontal direction.

When excitation sources are located on the basemat/tunnel or experimental hall, attenuation with distance was observed, but the measured rate of attenuation with distance was lower than would be expected for geometric attenuation alone. However, attenuation increased at higher frequencies. A vibration source on the basemat/tunnel or experimental hall could be expected to propagate to a considerable distance.

No rocking or rotational response modes of the basemat/tunnel system were observed, but considering the low level of site noise excitation during the measurements, these modes may still exist.

REFERENCES

1. J. A. Jendrzejczyk, Z. Nagy, and R. K. Smith, "Ambient Ground Motion Measurements at the 7 GeV Site at Argonne National Laboratory over Extended Timer Periods," LS-136 (Dec. 1988).
2. J. A. Jendrzejczyk, M. W. Wambsganss, and R. K. Smith, "Vibration Response of the APS Linac Floor Slab to Ambient Ground Motion," APS/IN/VIB/92-1 (Nov. 1991).
3. J. A. Jendrzejczyk, M. W. Wambsganss, and R. K. Smith, "Dynamic Response of the APS Storage Ring Basemat: Preliminary Measurements," APS/IN/VIB/92-5 (June 1992).

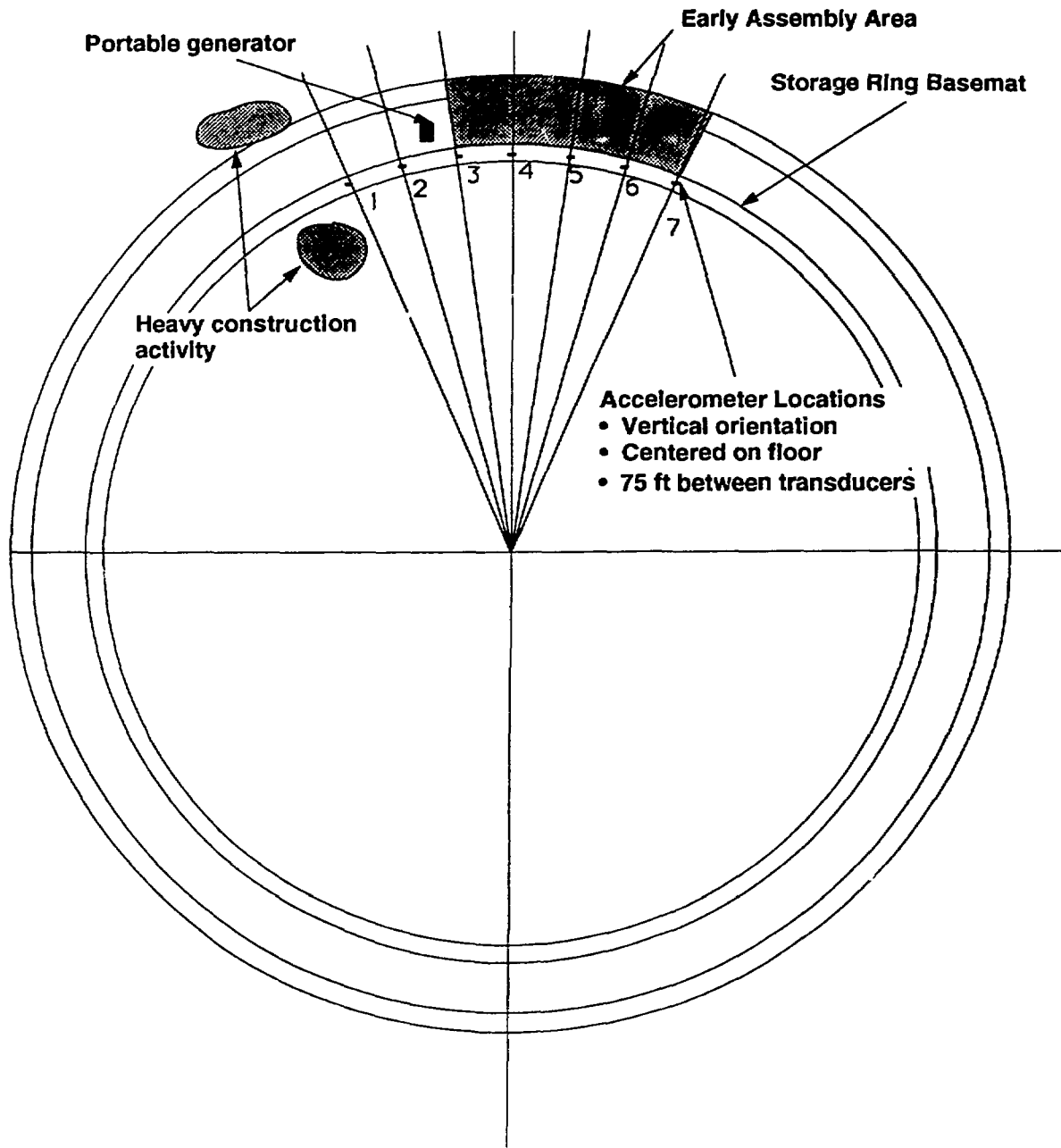
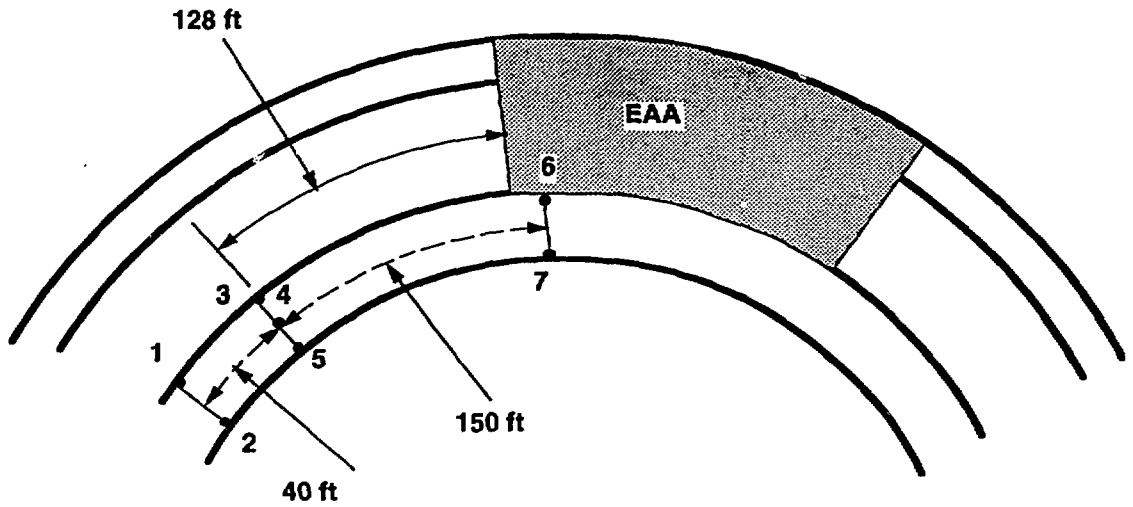
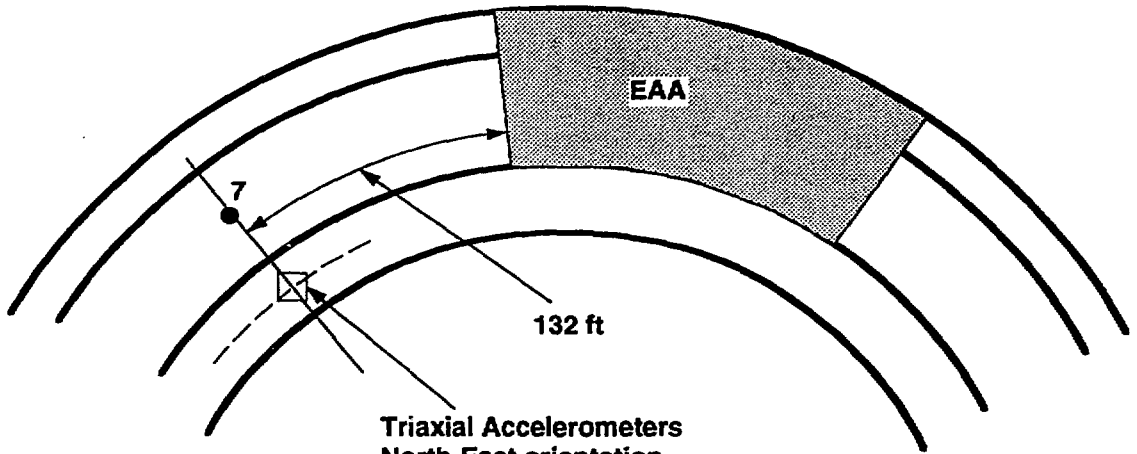


Fig. 1. Accelerometer (PCB-393C) locations for Condition 1



Note: All accelerometers oriented vertically

Fig. 2. Accelerometer locations for Condition 2



**Triaxial Accelerometers
North-East orientation**

On Basemat:

Acc #1=North

Acc #2=East

Acc #3=Vertical

On Storage Ring Roof:

Acc #4=North

Acc #5=East

Acc #6=Vertical

Fig. 3. Accelerometer locations for Condition 3

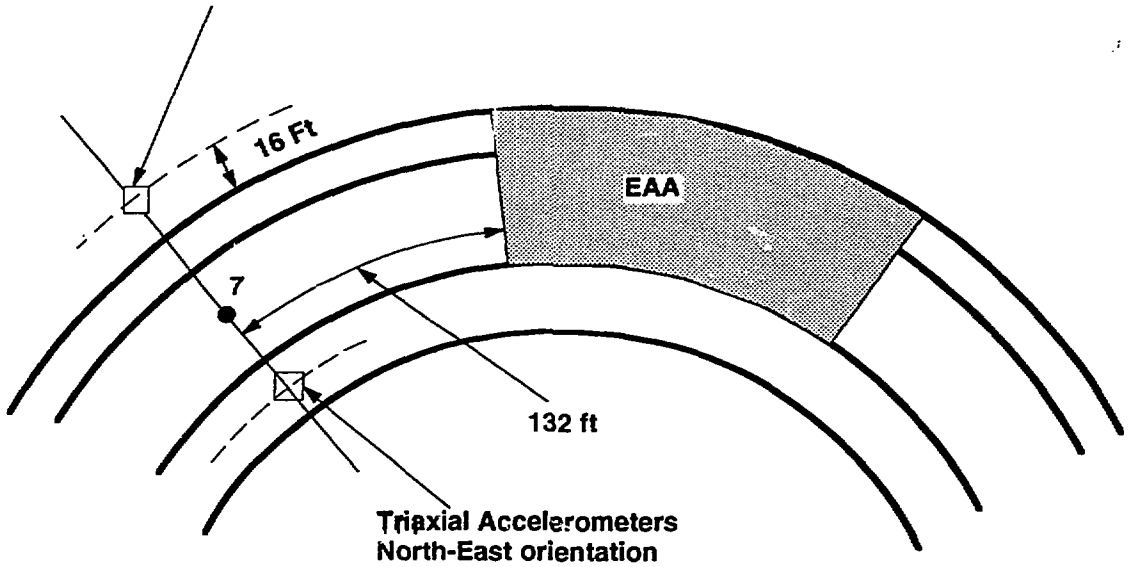
**Triaxial Accelerometers
North-East orientation**

On Soil:

Acc #4=North

Acc #5=East

Acc #6=Vertical



On Basemat:

Acc #1=North

Acc #2=East

Acc #3=Vertical

Fig. 4. Accelerometer locations for Condition 4

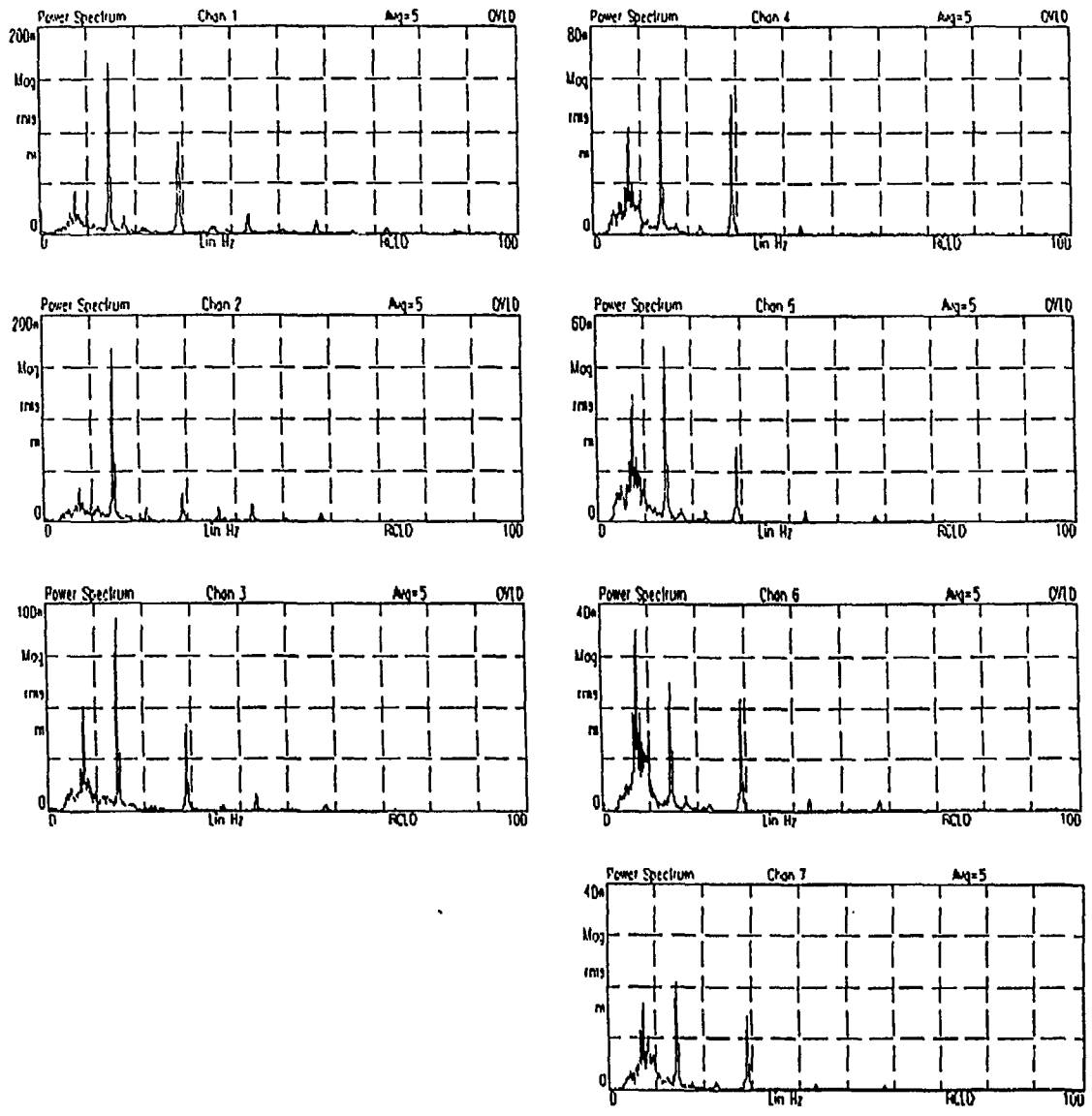


Fig. 5. Power spectrum for Condition 1, 3:30 PM, heavy construction. Note: Channel number = location number.

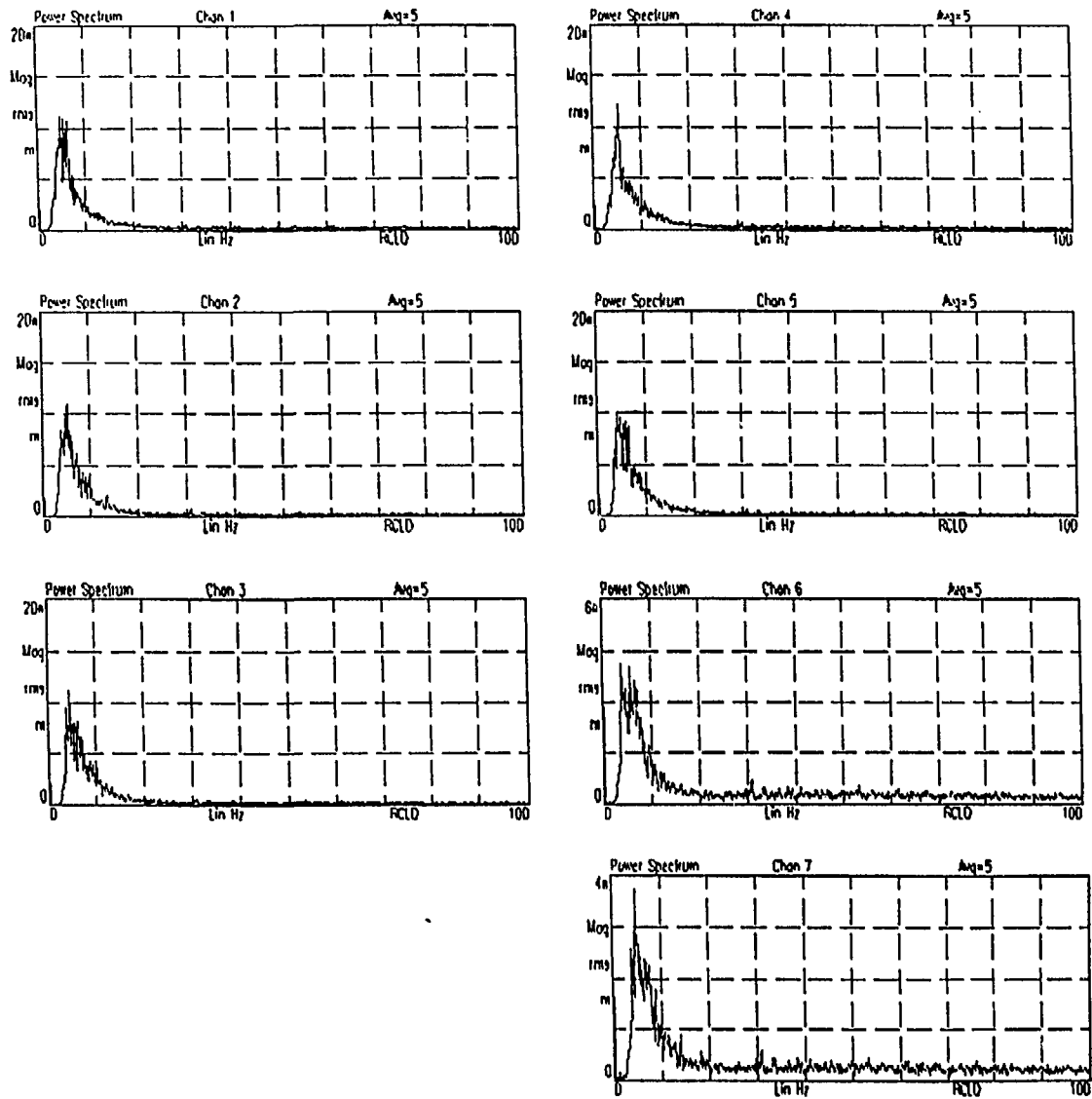


Fig. 6. Power spectrum for Condition 1, 4:22 PM, site quiet. Note: Channel number = location number.

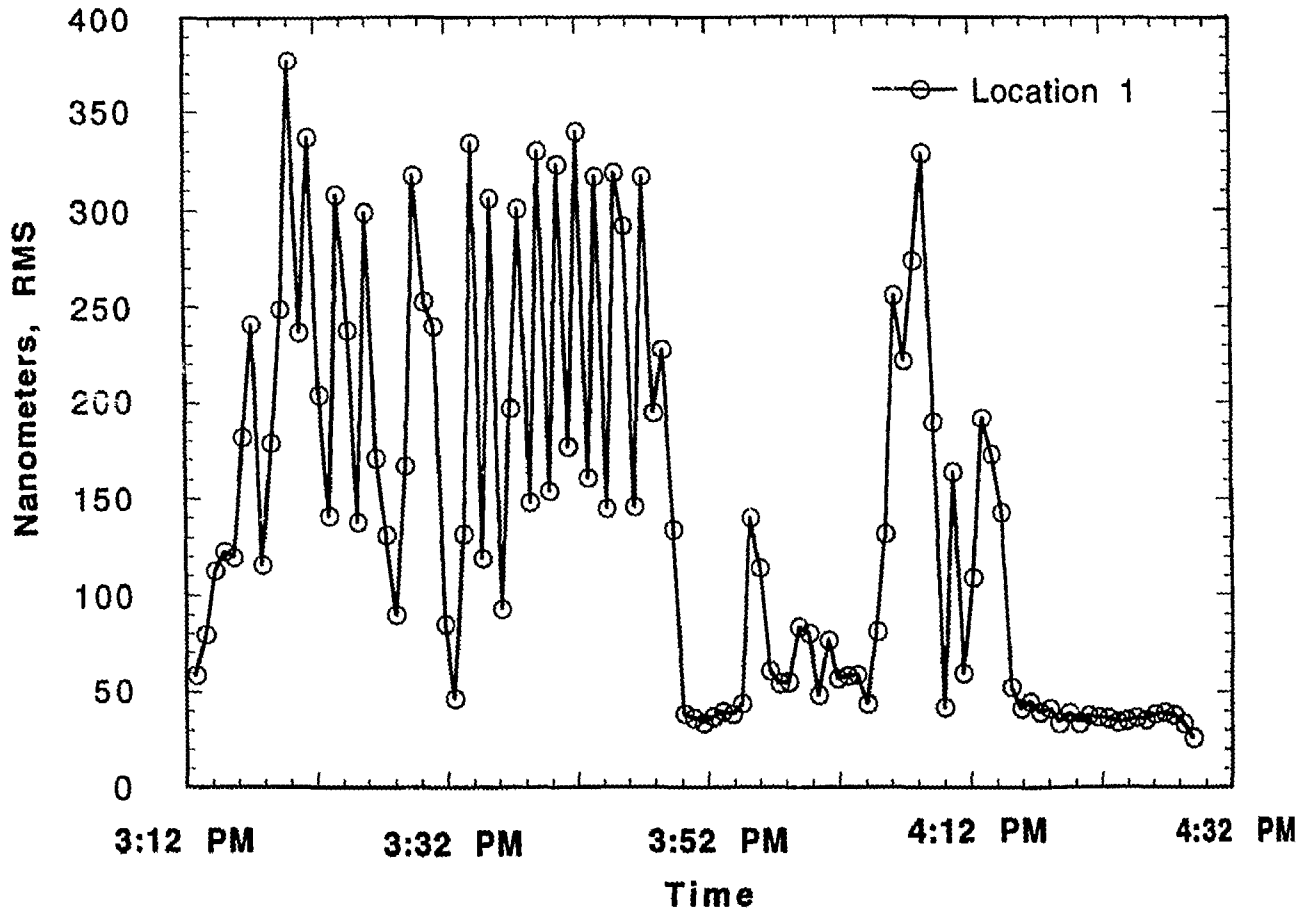


Fig. 7. Displacement response, Condition 1, at location 1, 4-100 Hz

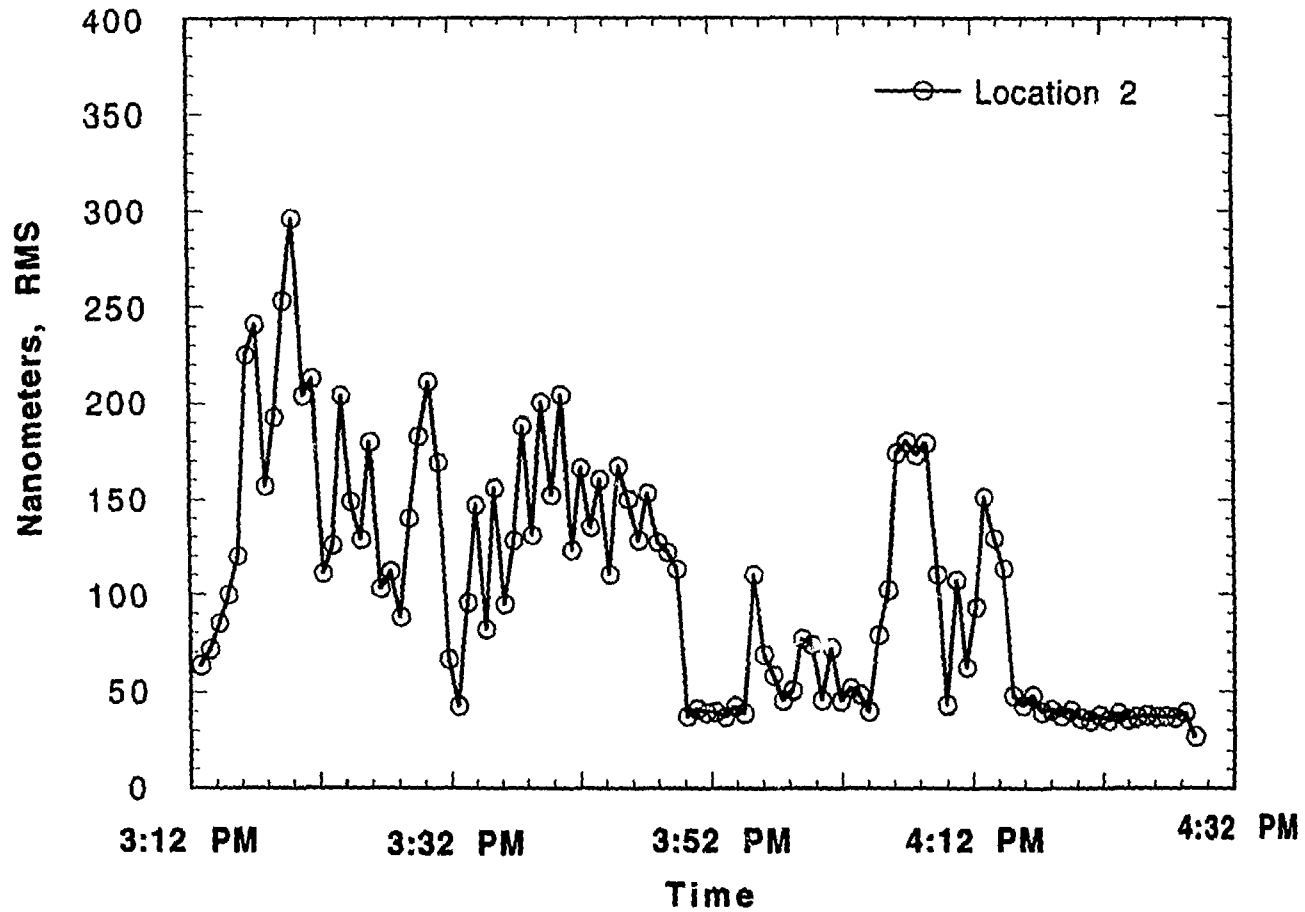


Fig. 8. Displacement response, Condition 1, at location 2, 4-100 Hz

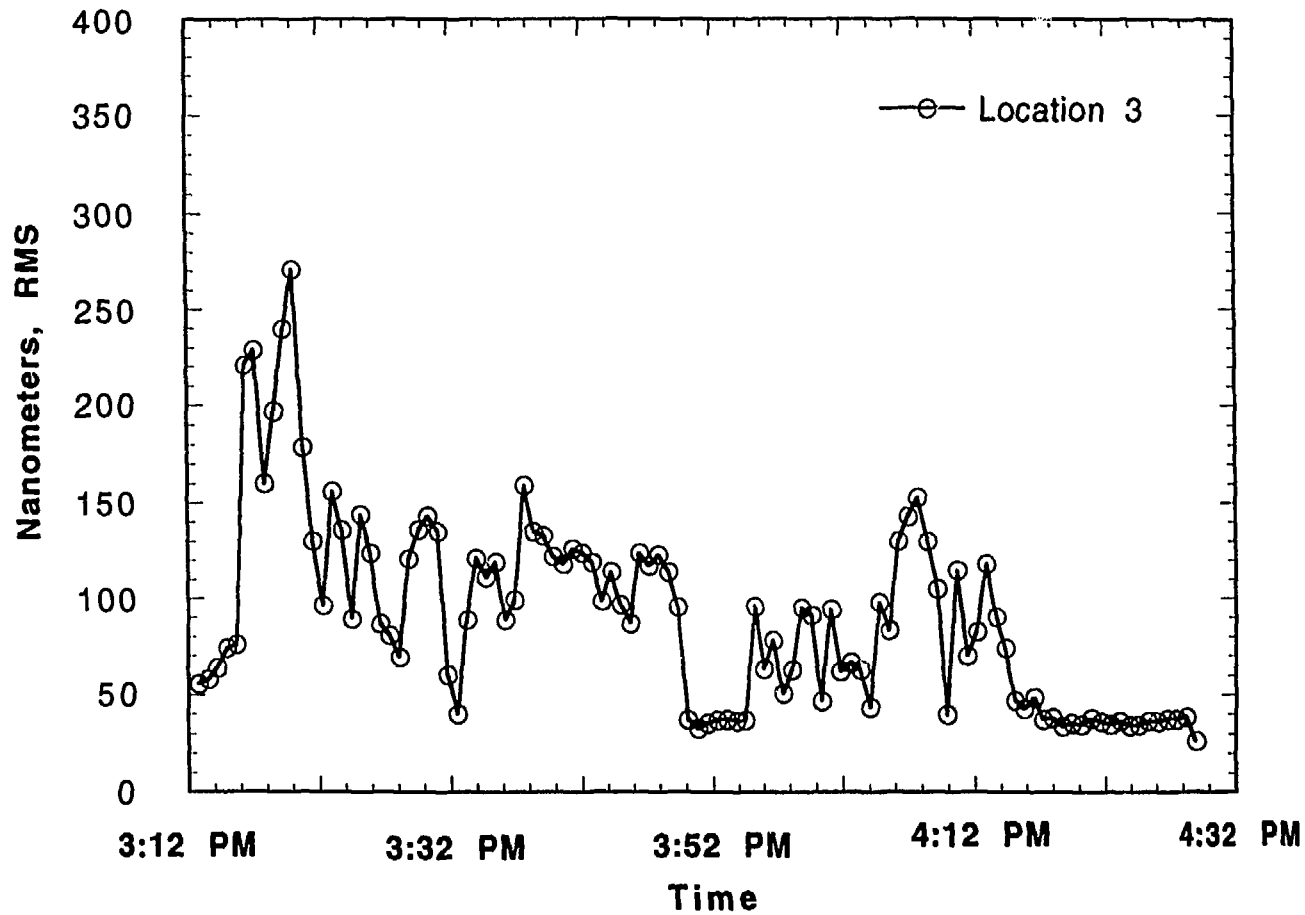


Fig. 9. Displacement response, Condition 1, at location 3, 4-100 Hz

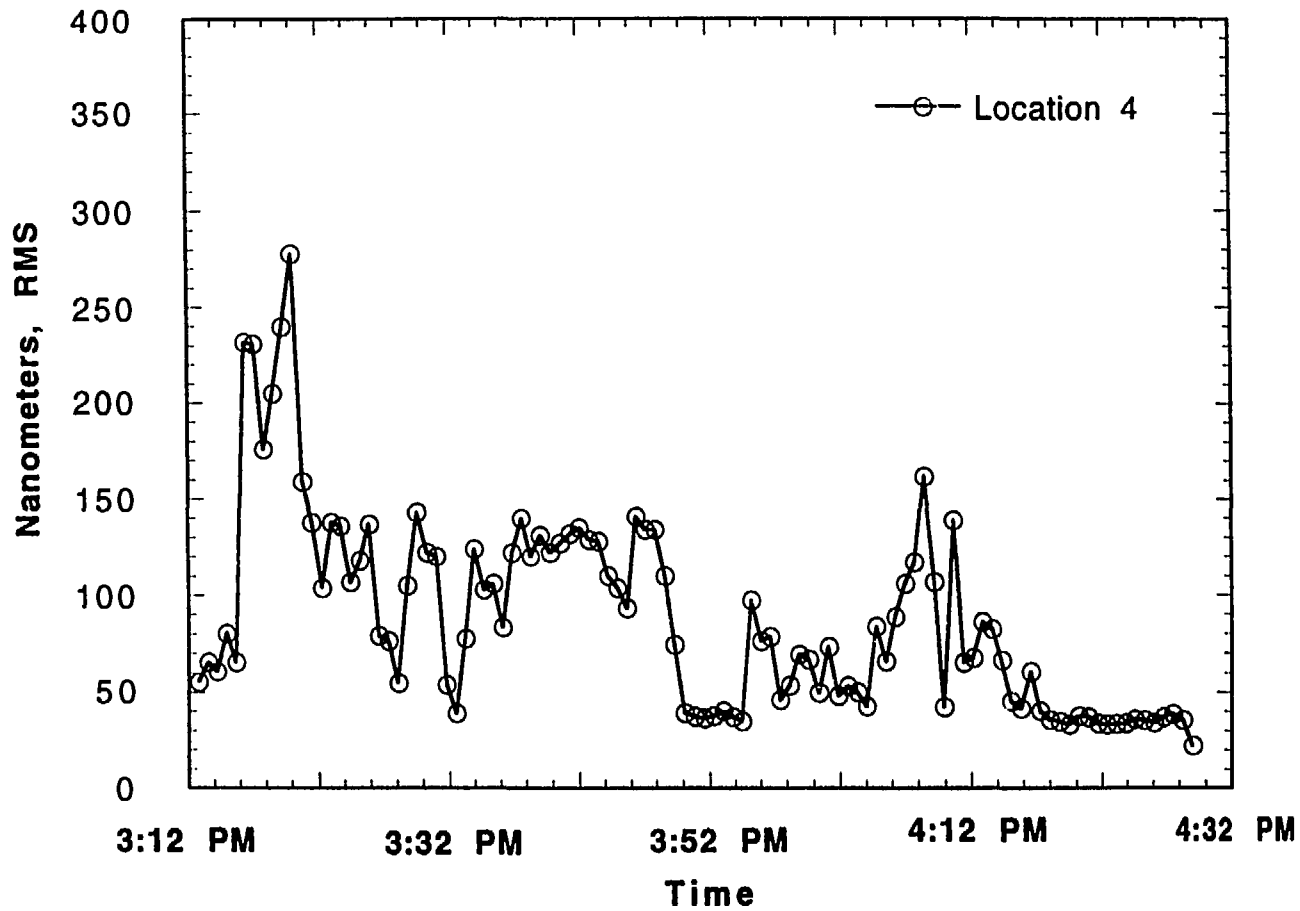


Fig. 10. Displacement response, Condition 1, at location 4, 4-100 Hz

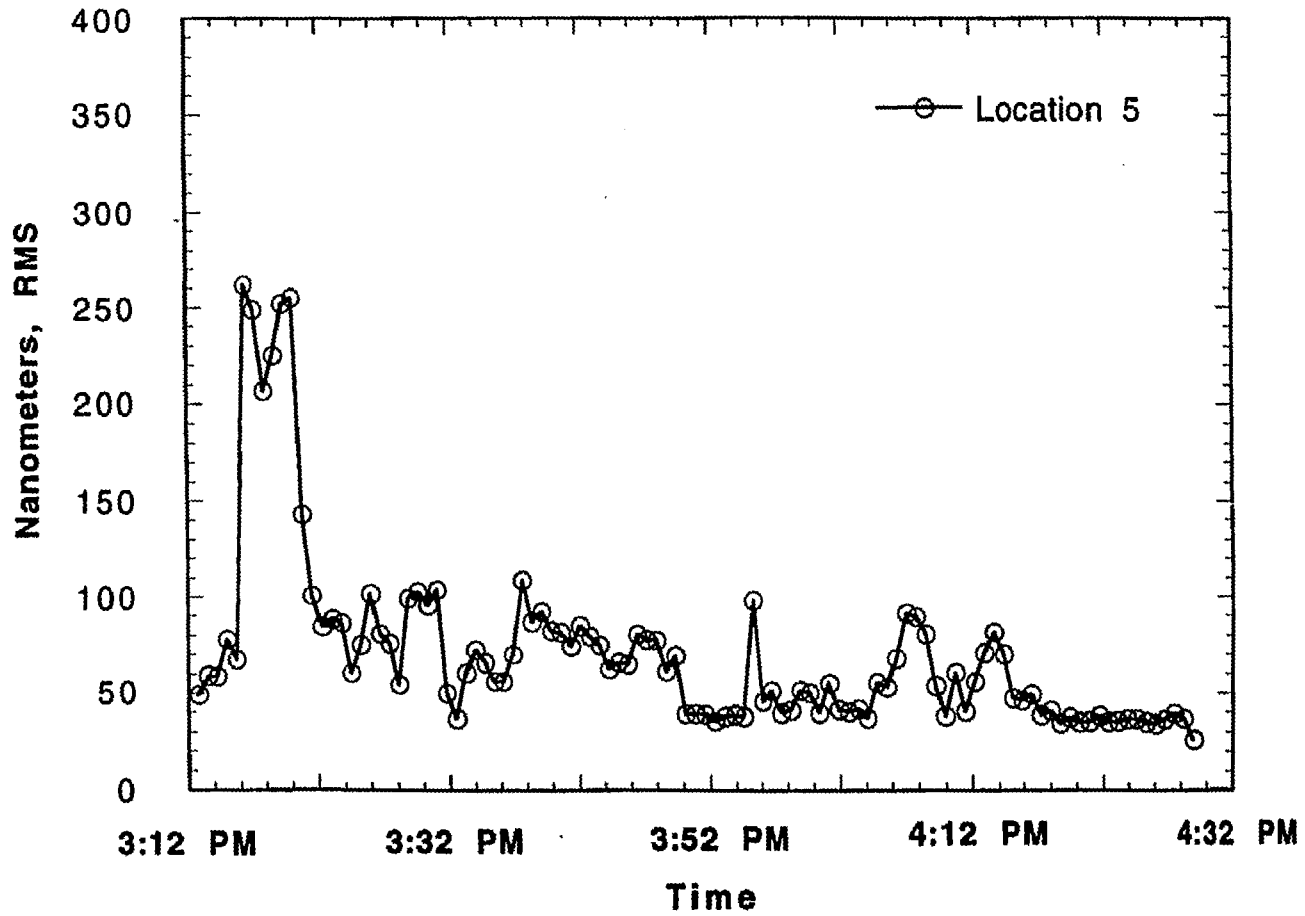


Fig. 11. Displacement response, Condition 1, at location 5, 4-100 Hz

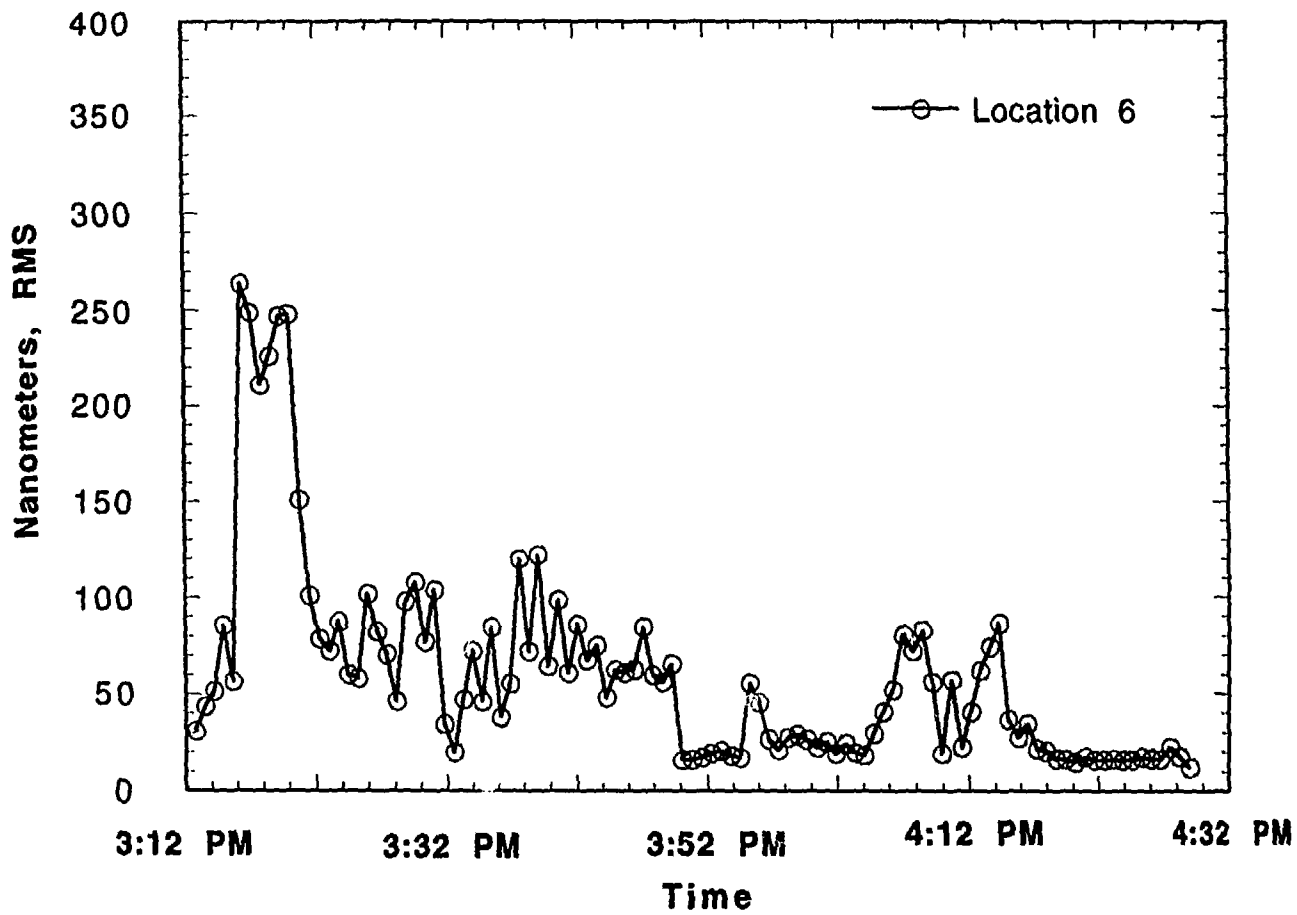


Fig. 12. Displacement response, Condition 1, at location 6, 4-100 Hz

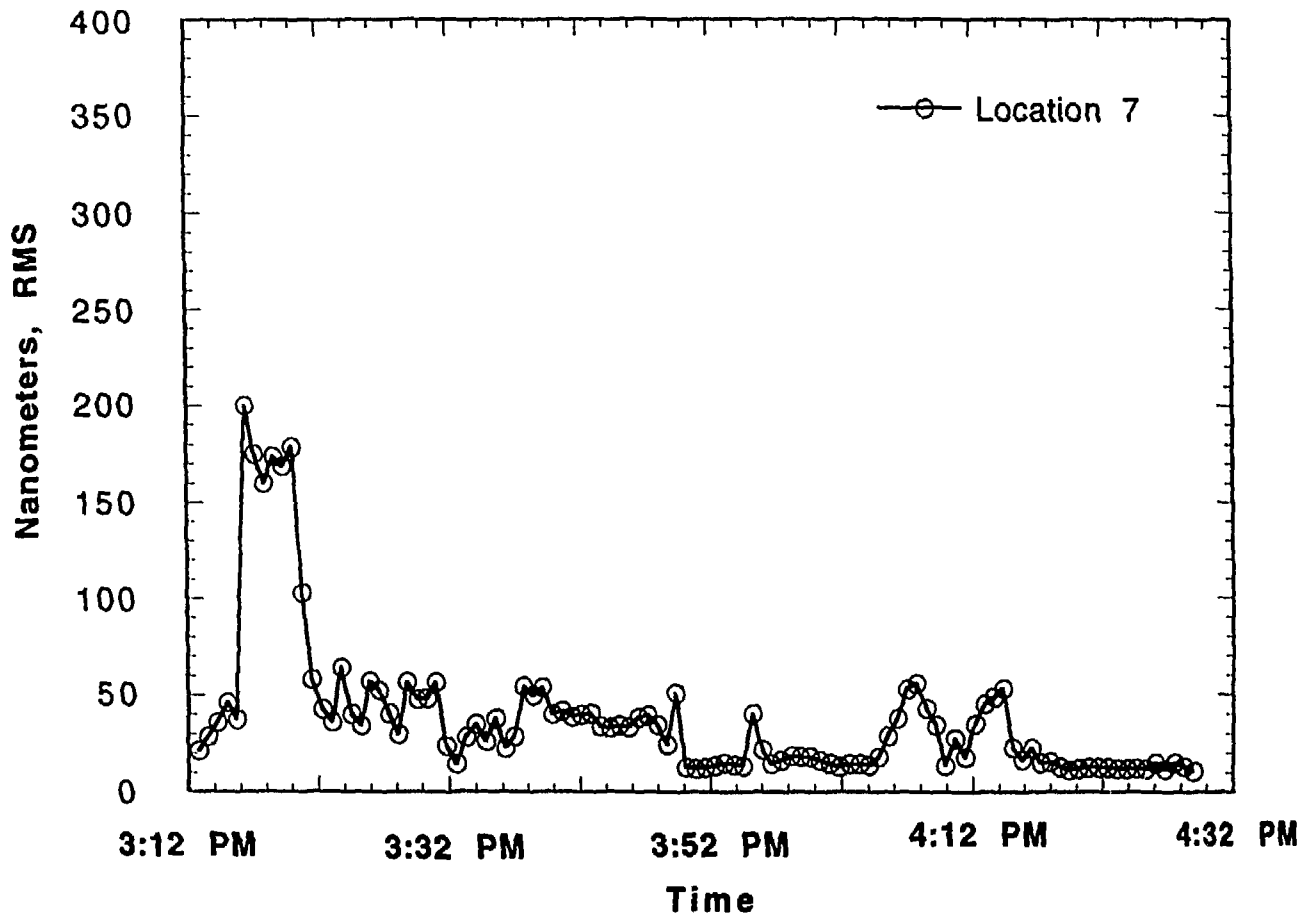


Fig. 13. Displacement response, Condition 1, at location 7, 4-100 Hz

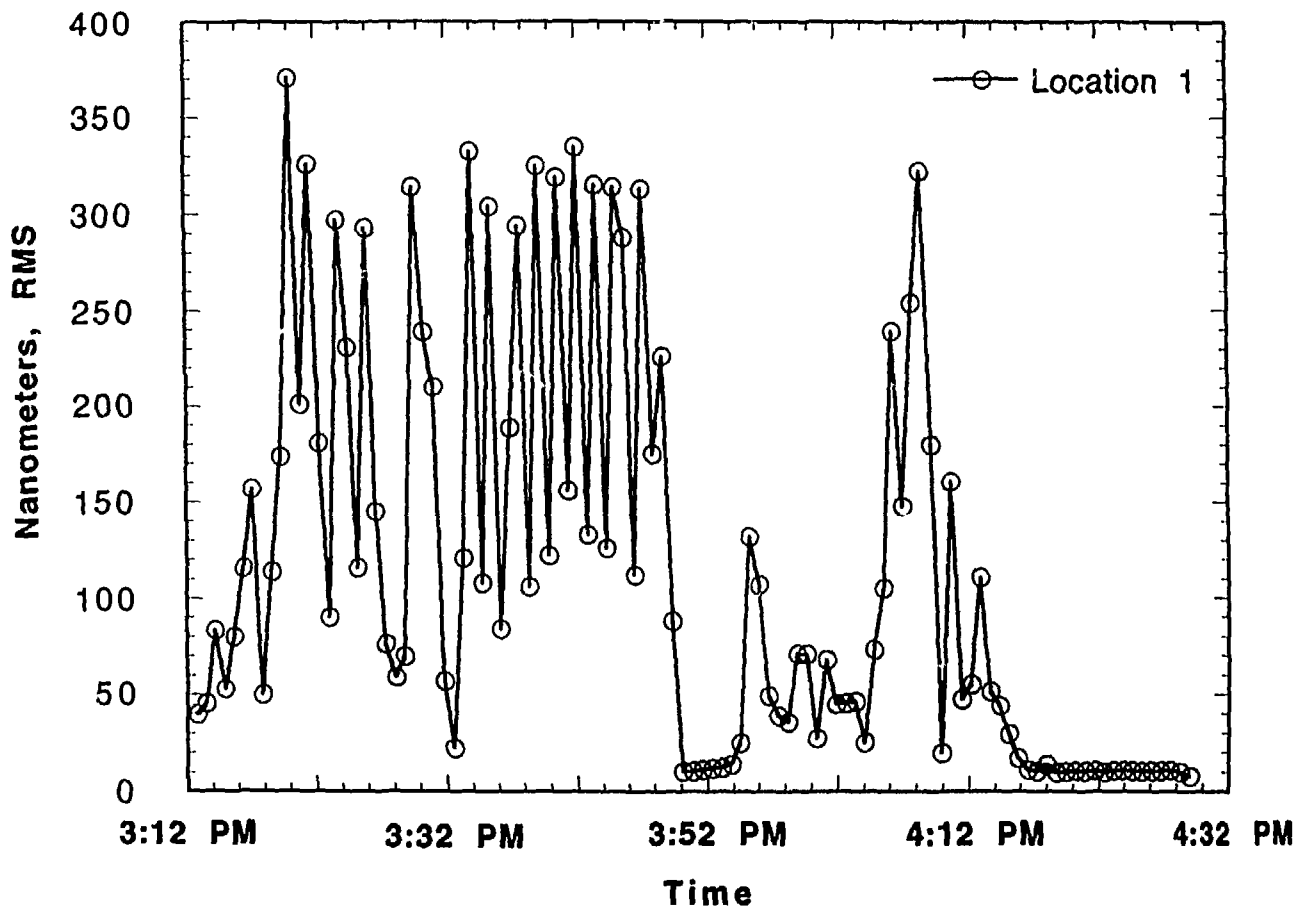


Fig. 14. Displacement response, Condition 1, at location 1, 10-100 Hz

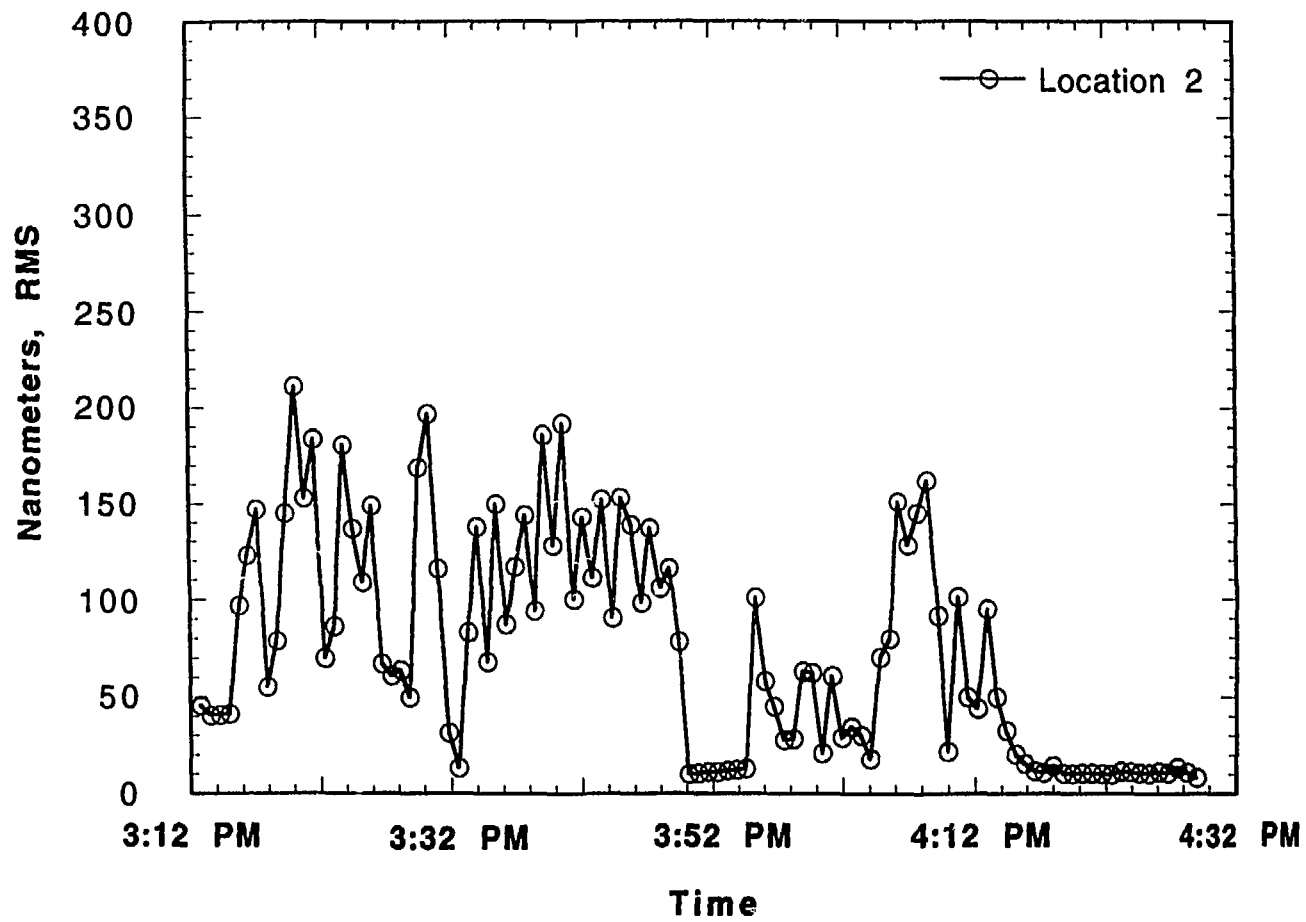


Fig. 15. Displacement response, Condition 1, at location 2, 10-100 Hz

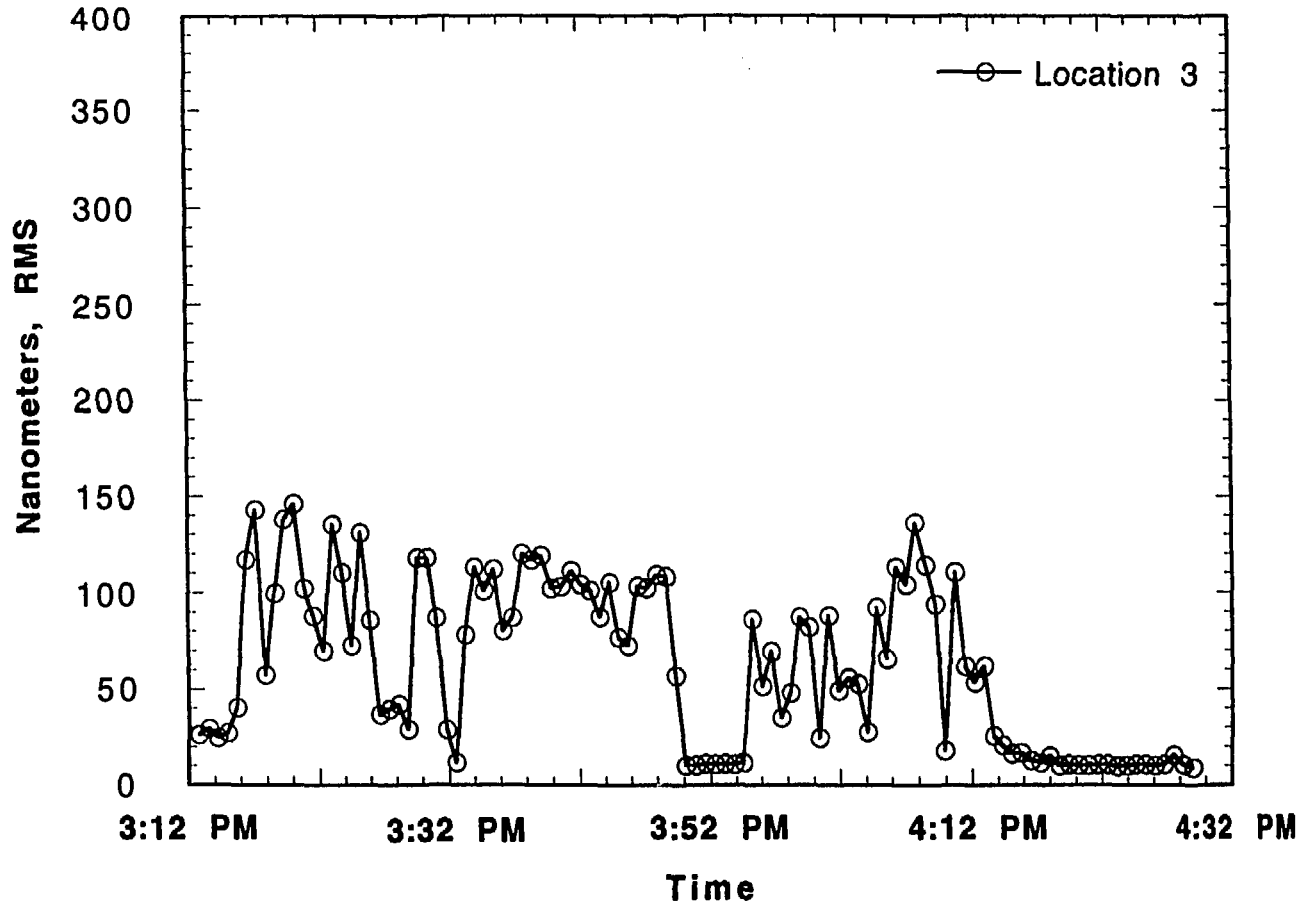


Fig. 16. Displacement response, Condition 1, at location 3, 10-100 Hz

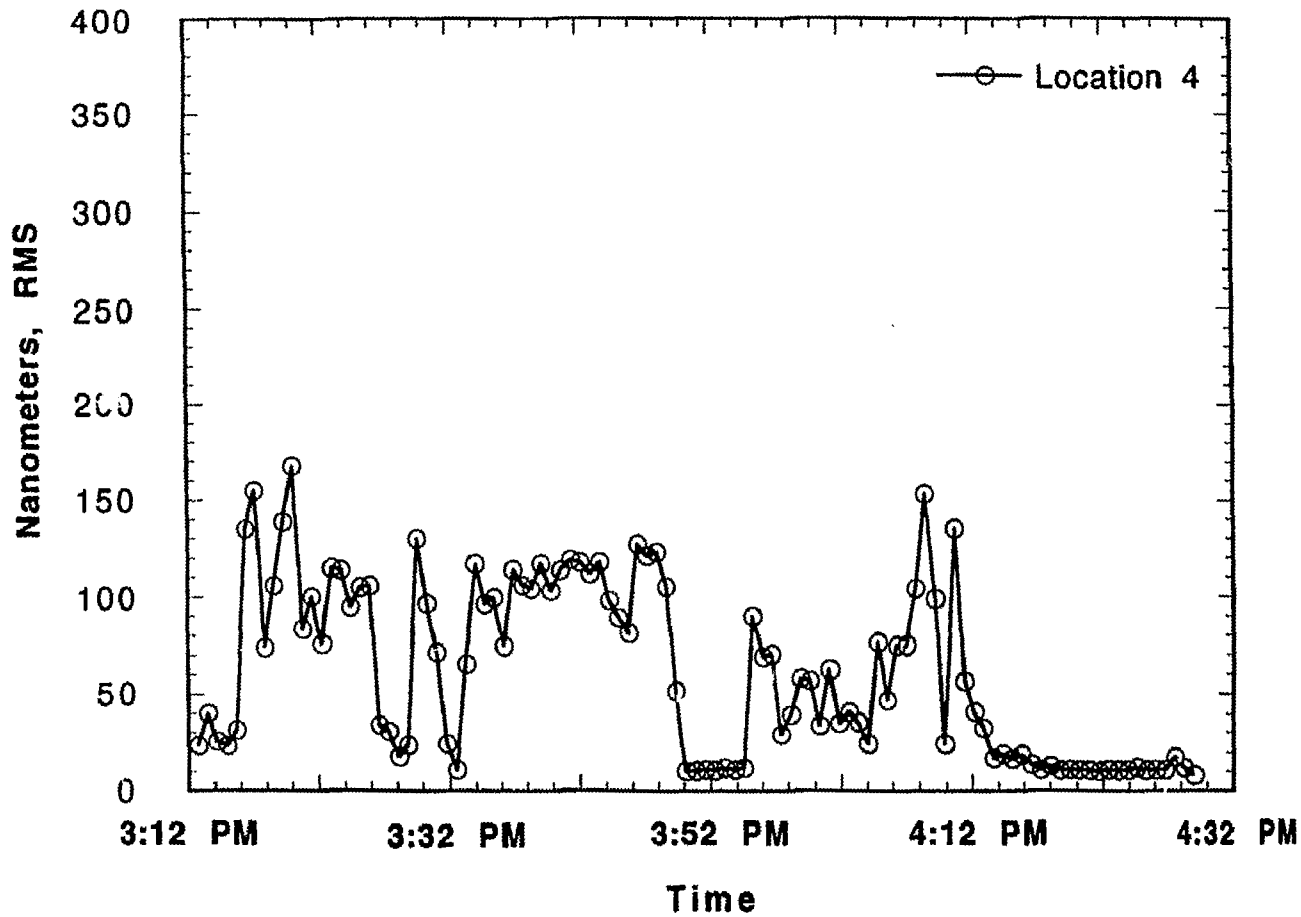


Fig. 17. Displacement response, Condition 1, at location 4, 10-100 Hz

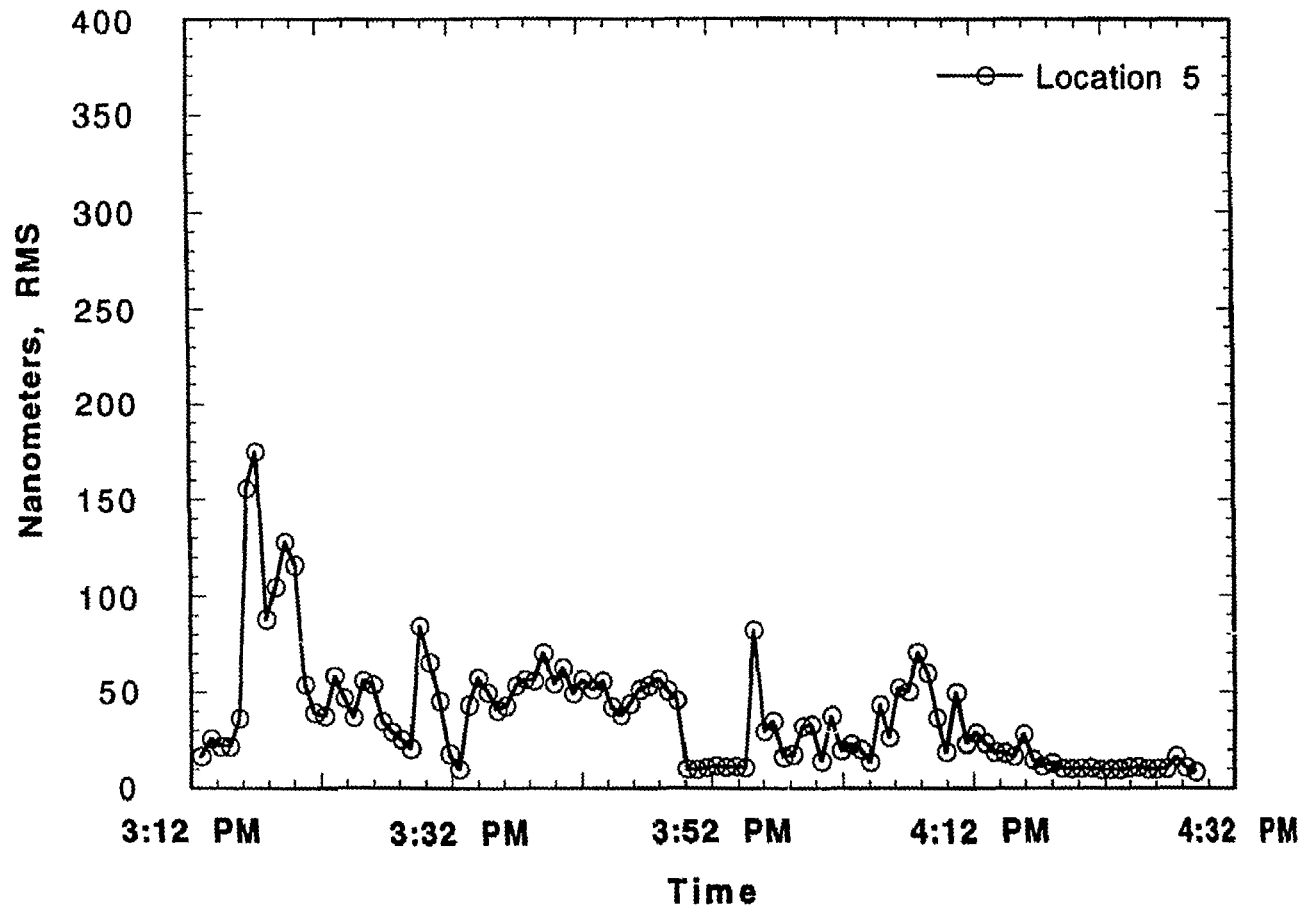


Fig. 18. Displacement response, Condition 1, at location 5, 10-100 Hz

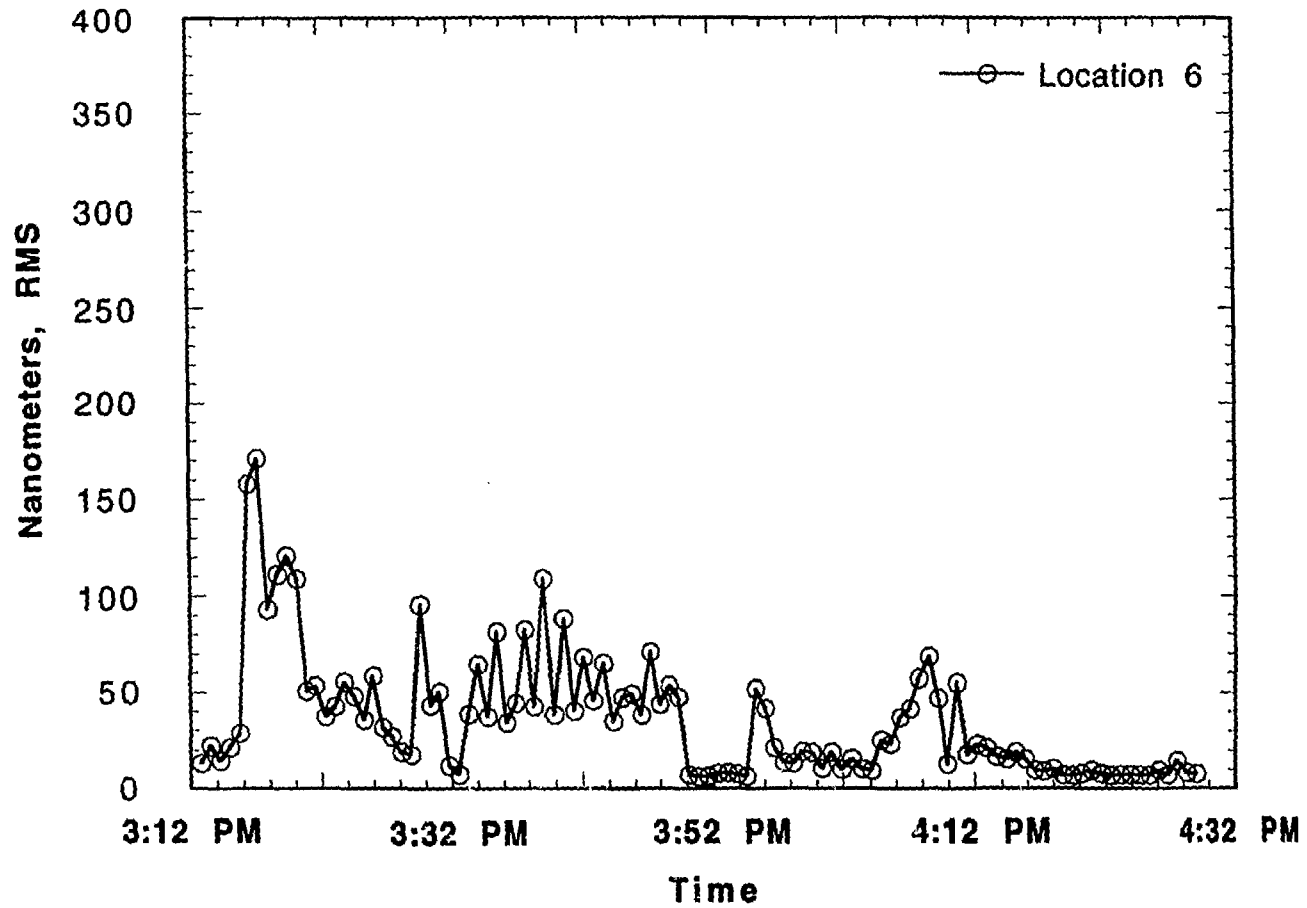


Fig. 19. Displacement response, Condition 1, at location 6, 10-100 Hz

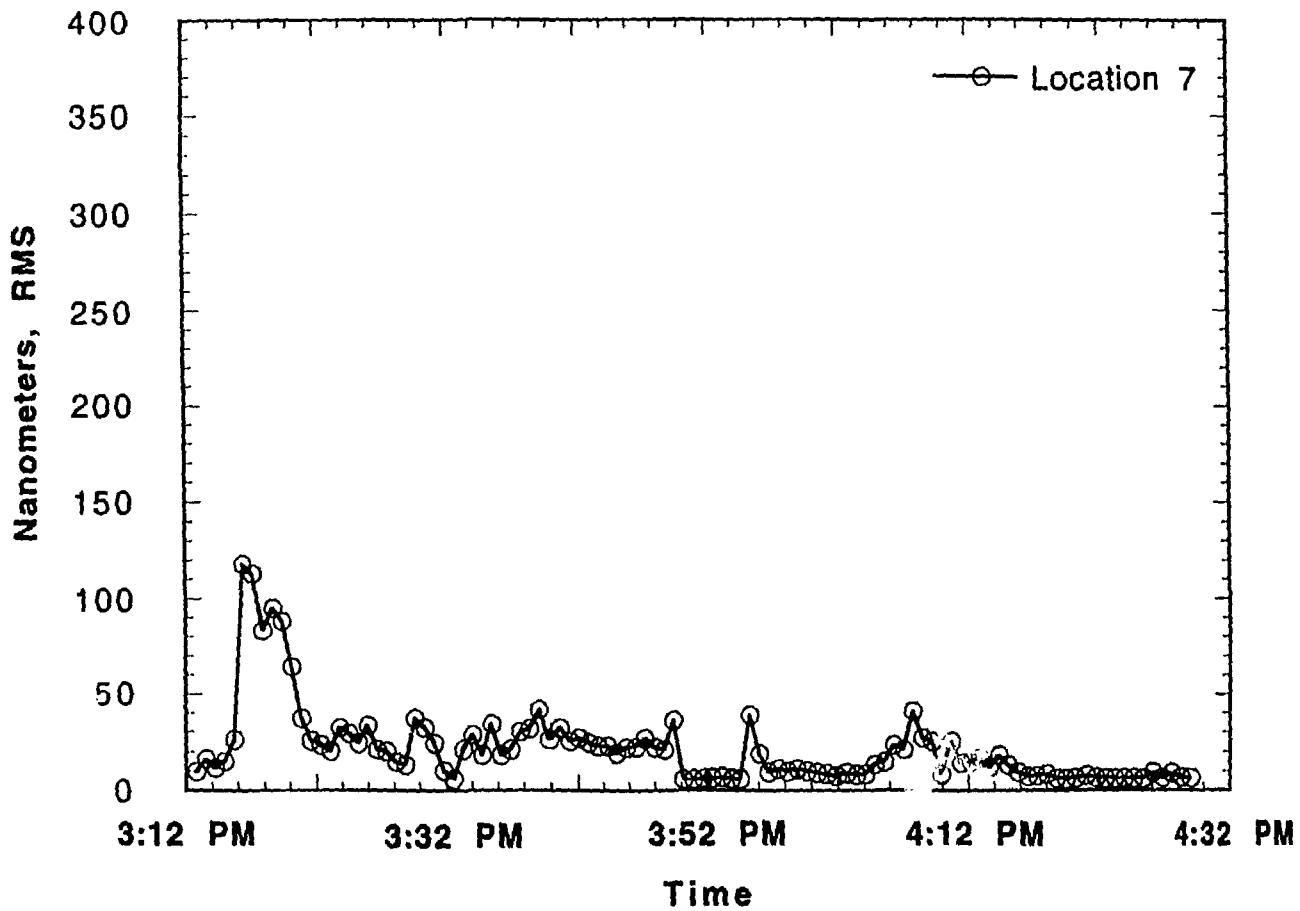


Fig. 20. Displacement response, Condition 1, at location 7, 10-100 Hz

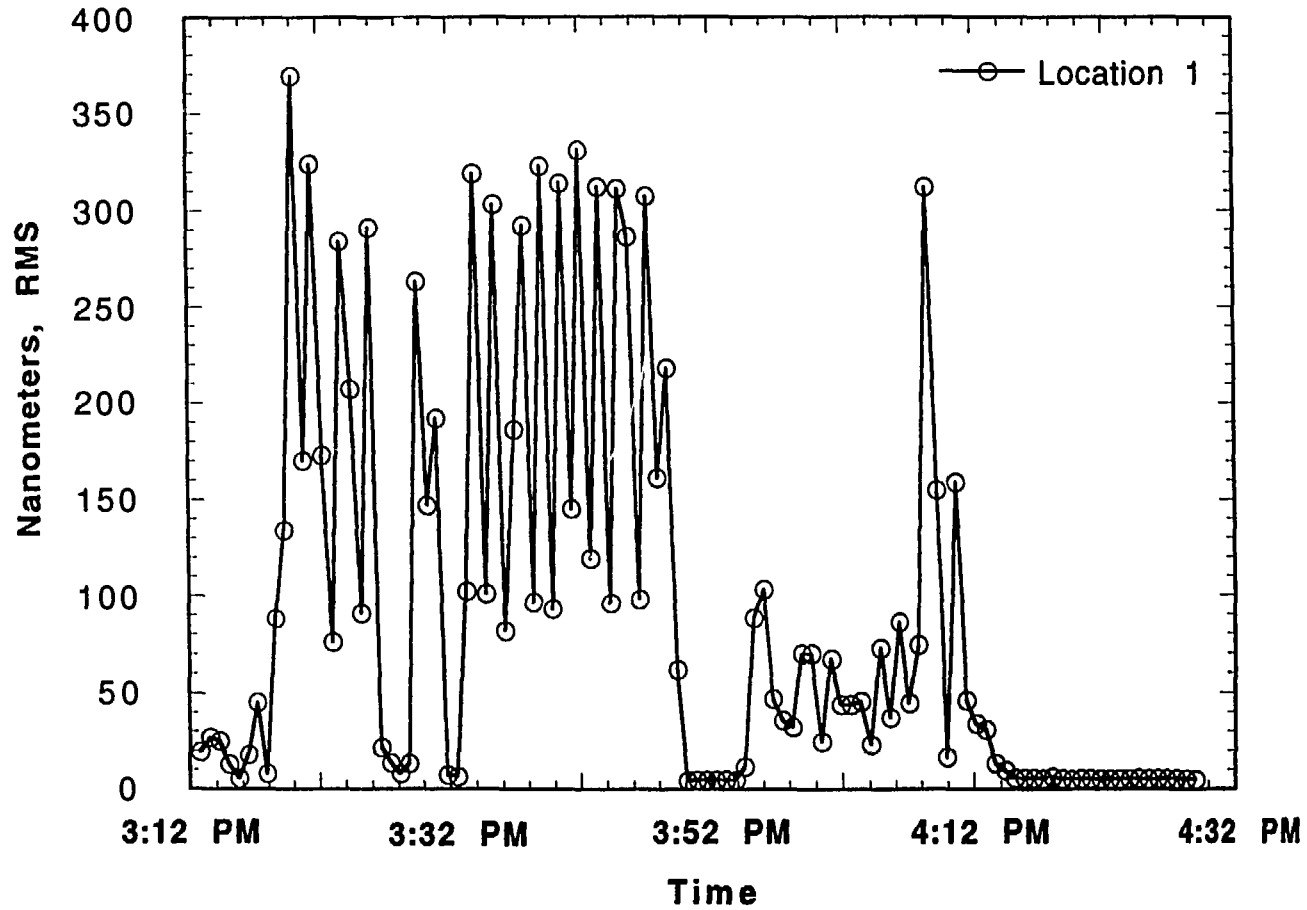


Fig. 21. Displacement response, Condition 1, at location 1, 20-100 Hz

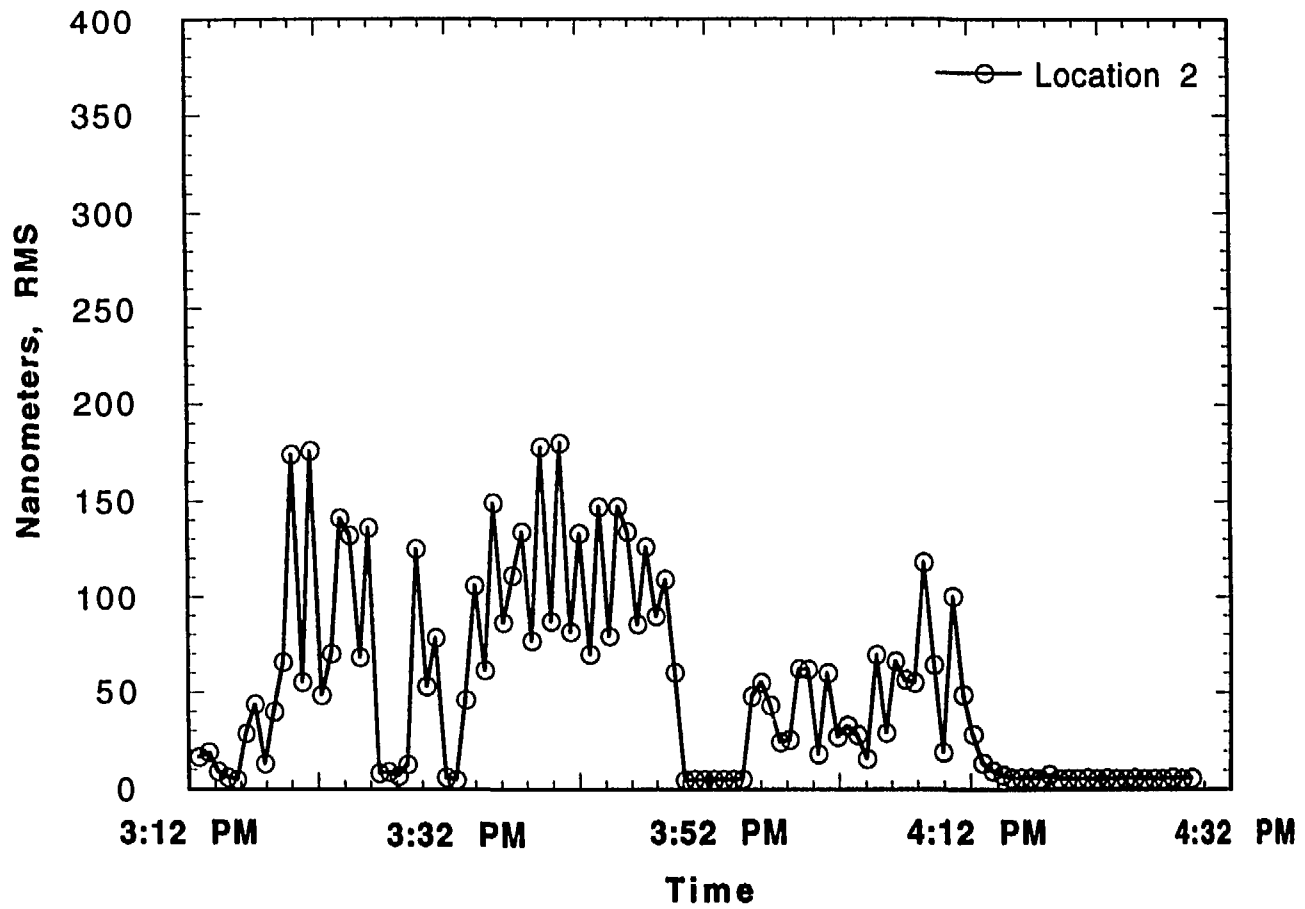


Fig. 22. Displacement response, Condition 1, at location 2, 20-100 Hz

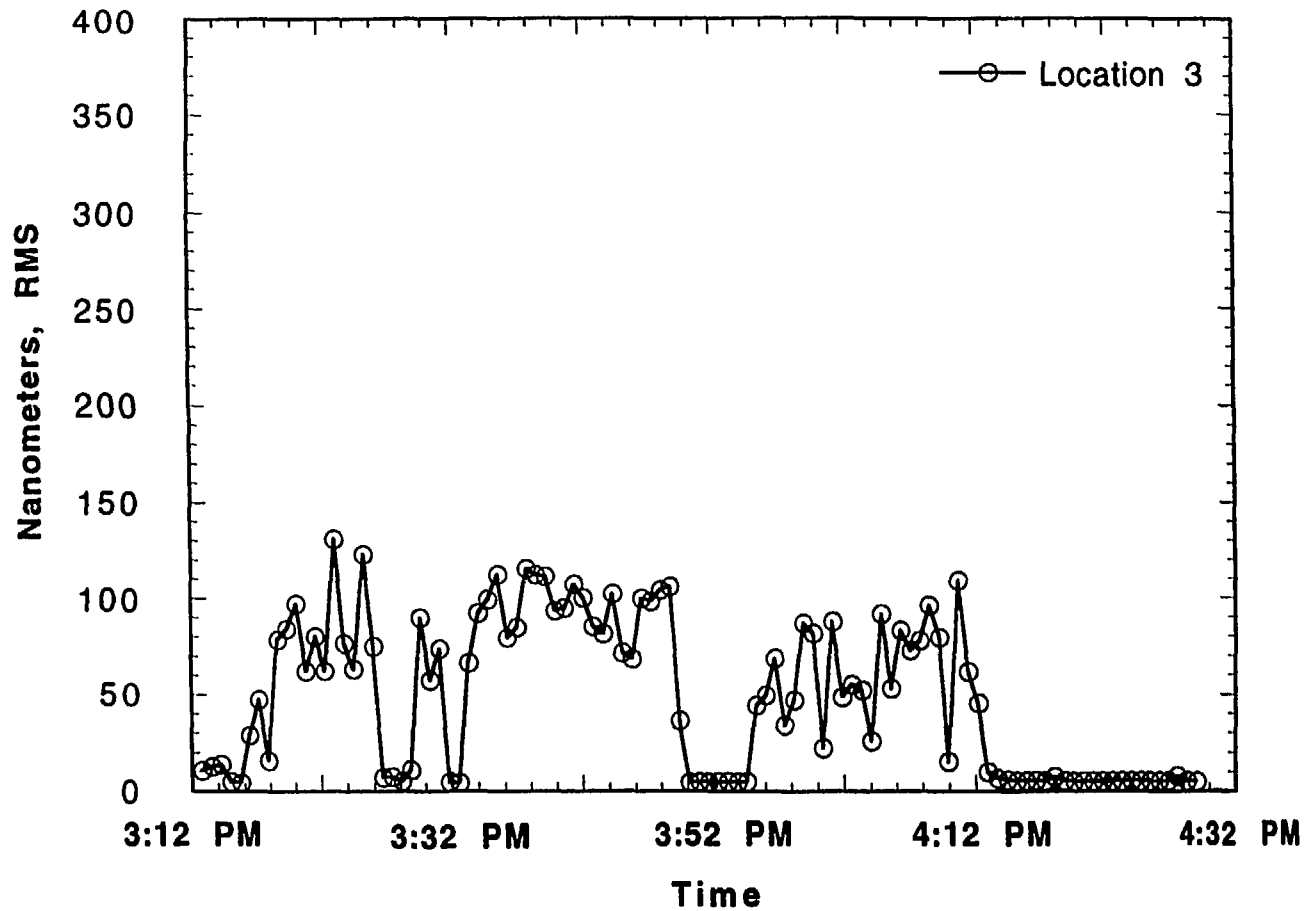


Fig. 23. Displacement response, Condition 1, at location 3, 20-100 Hz

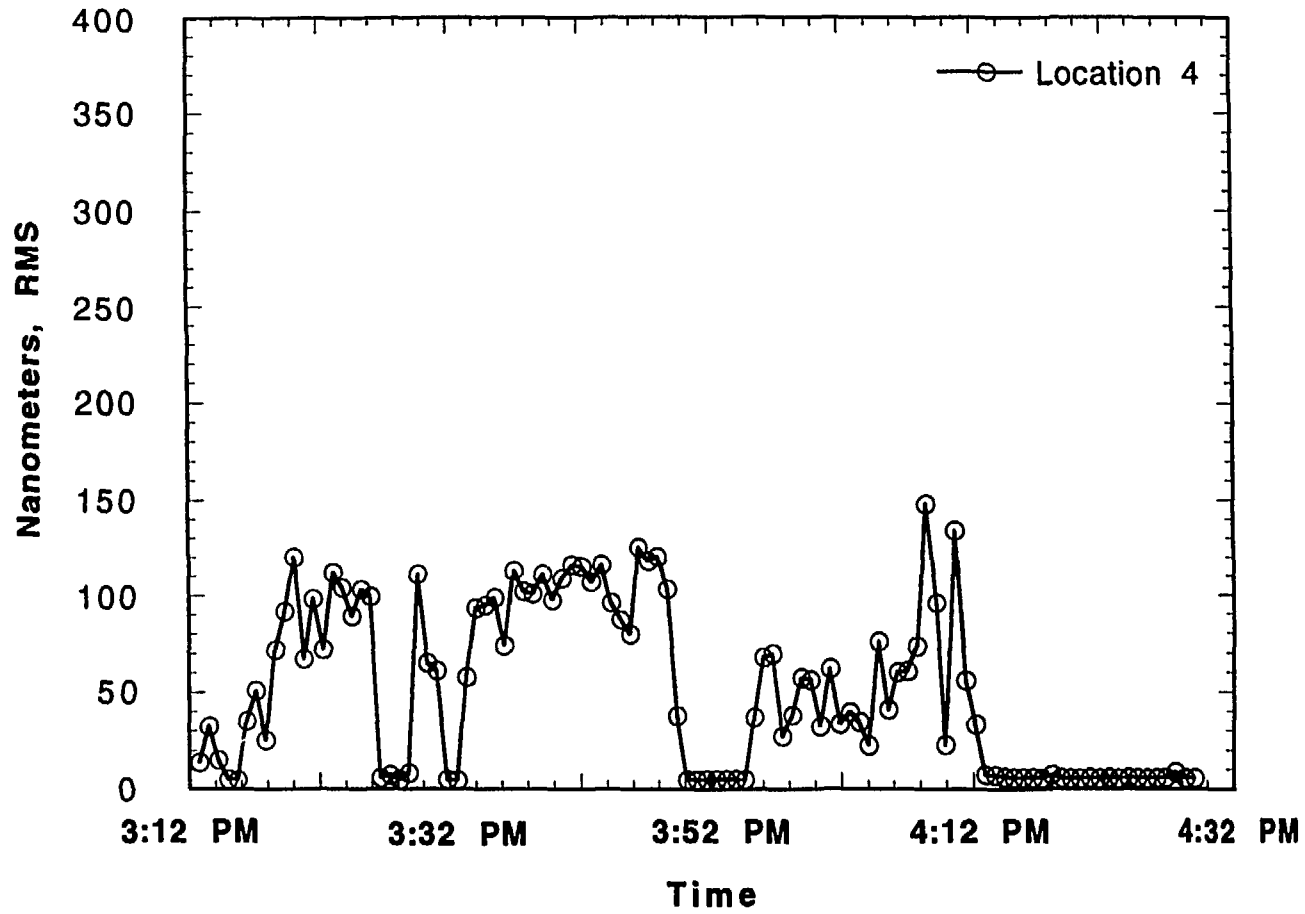


Fig. 24. Displacement response, Condition 1, at location 4, 20-100 Hz

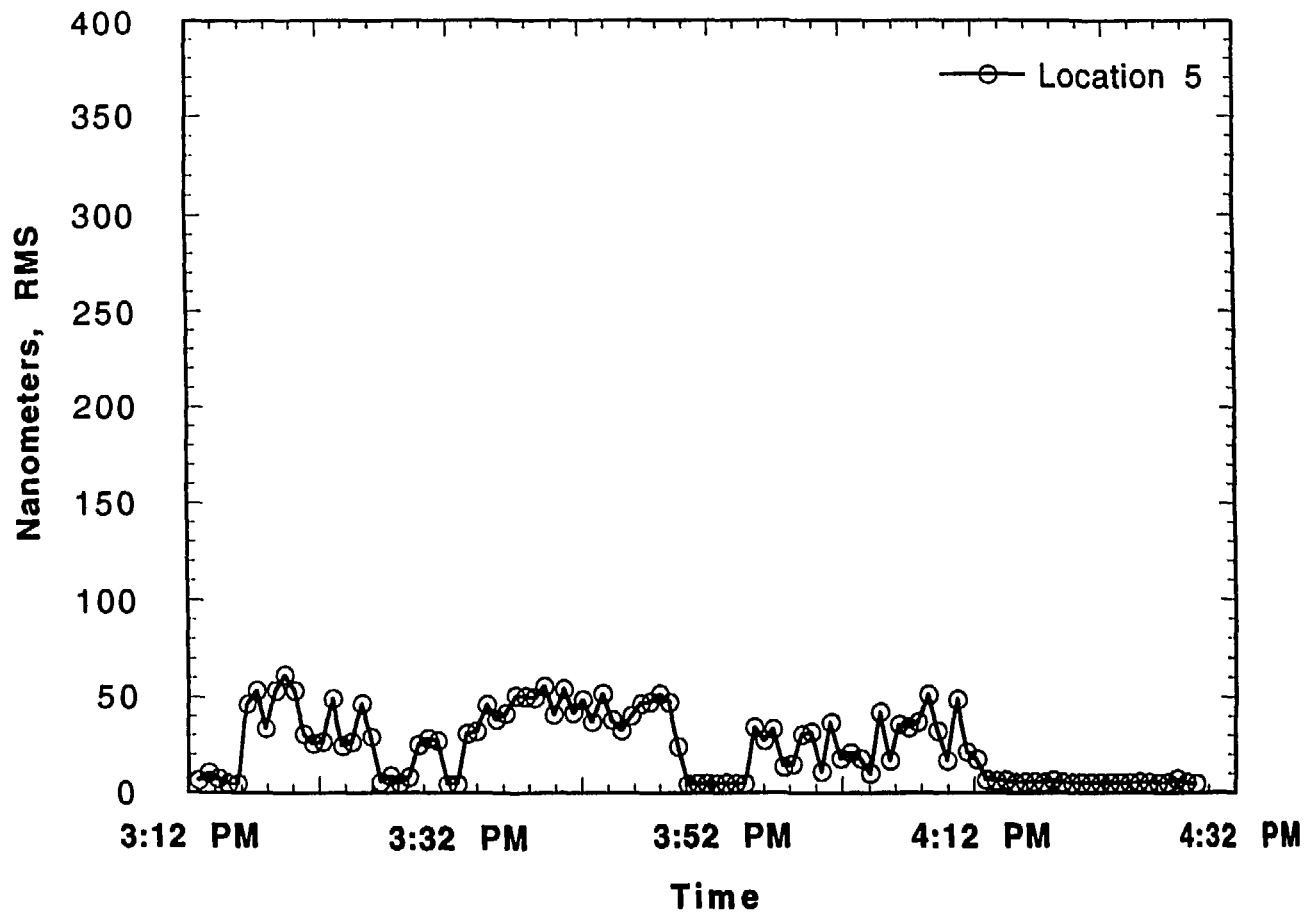


Fig. 25. Displacement response, Condition 1, at location 5, 20-100 Hz

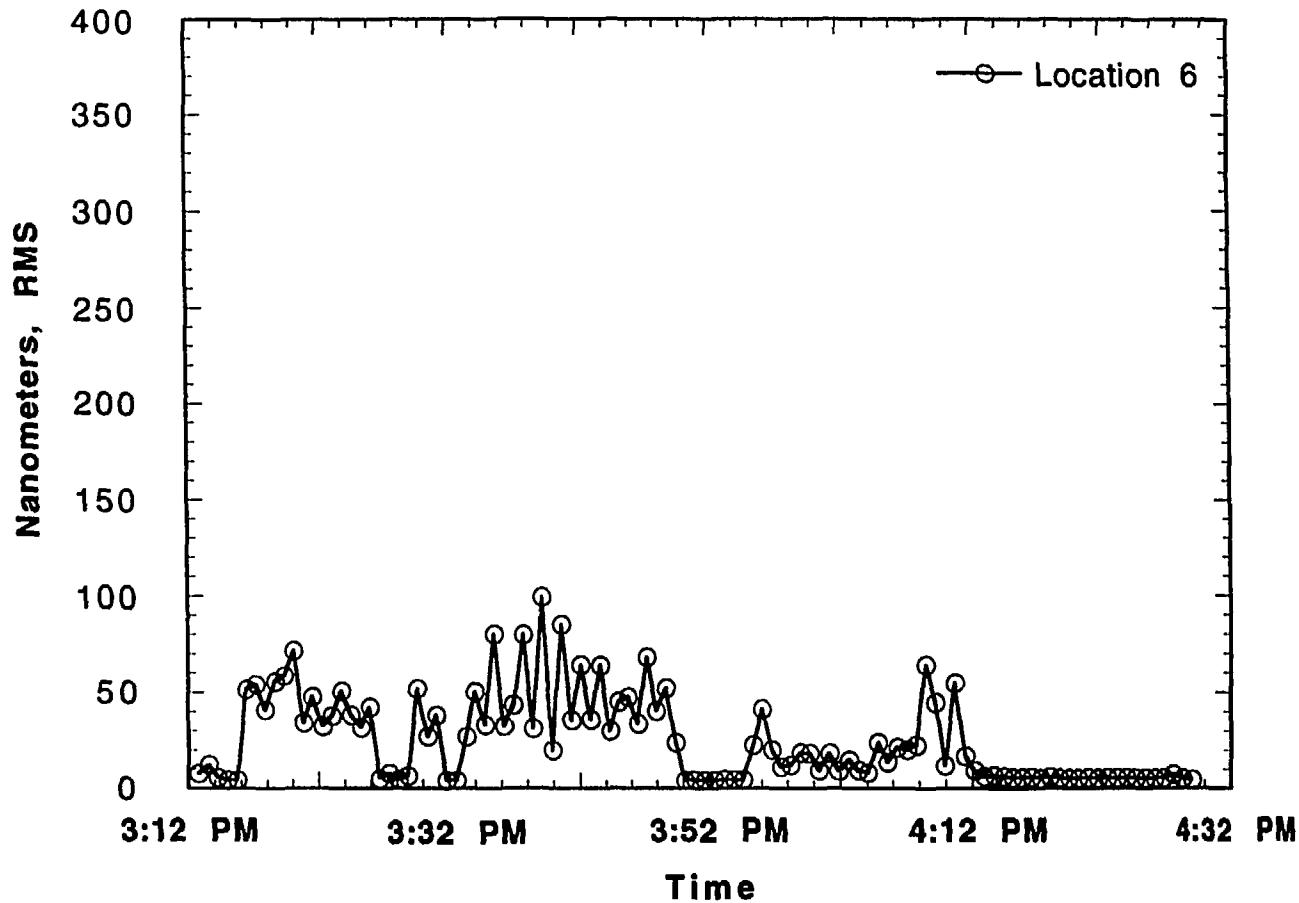


Fig. 26. Displacement response, Condition 1, at location 6, 20-100 Hz

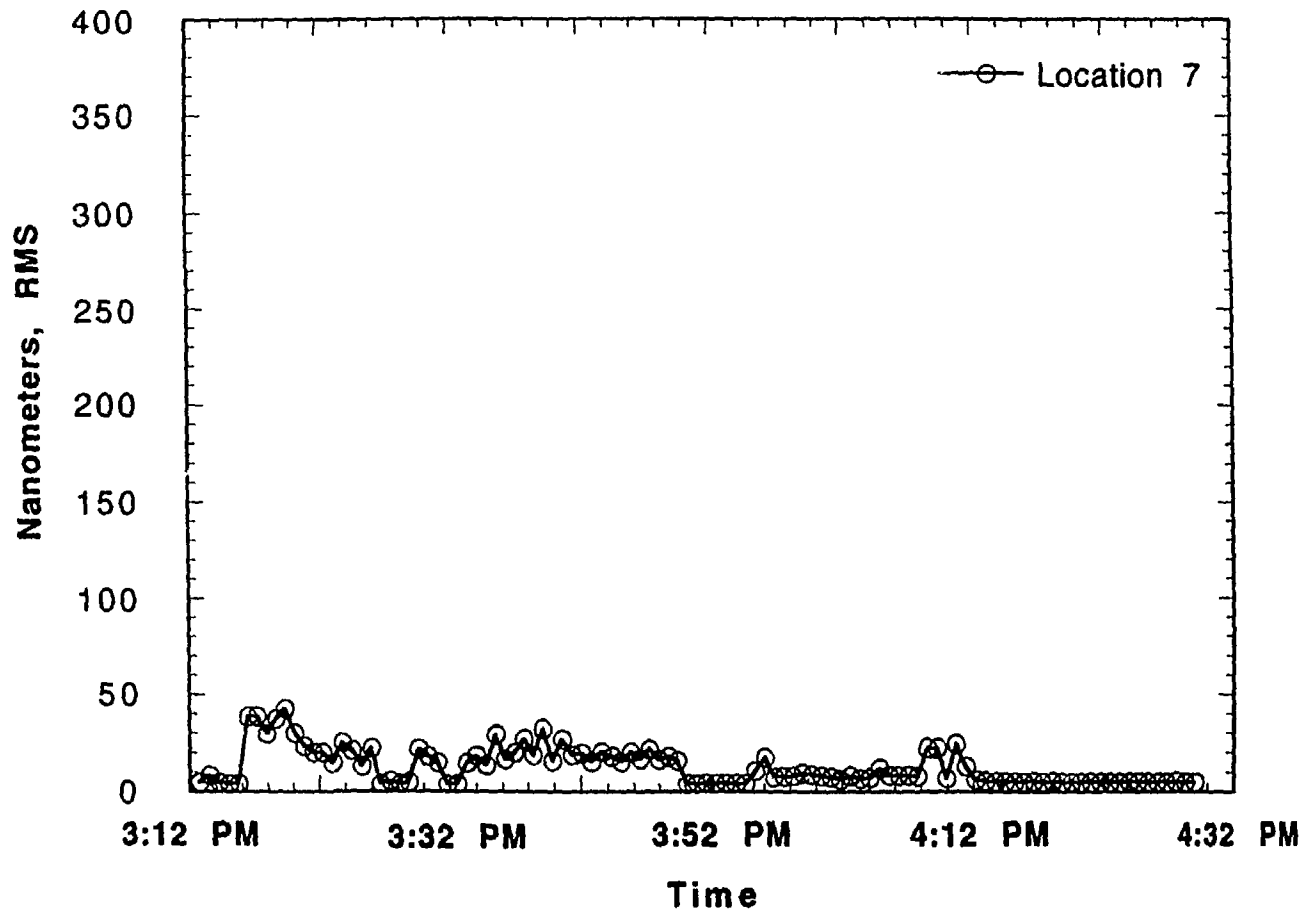


Fig. 27. Displacement response, Condition 1, at location 7, 20-100 Hz

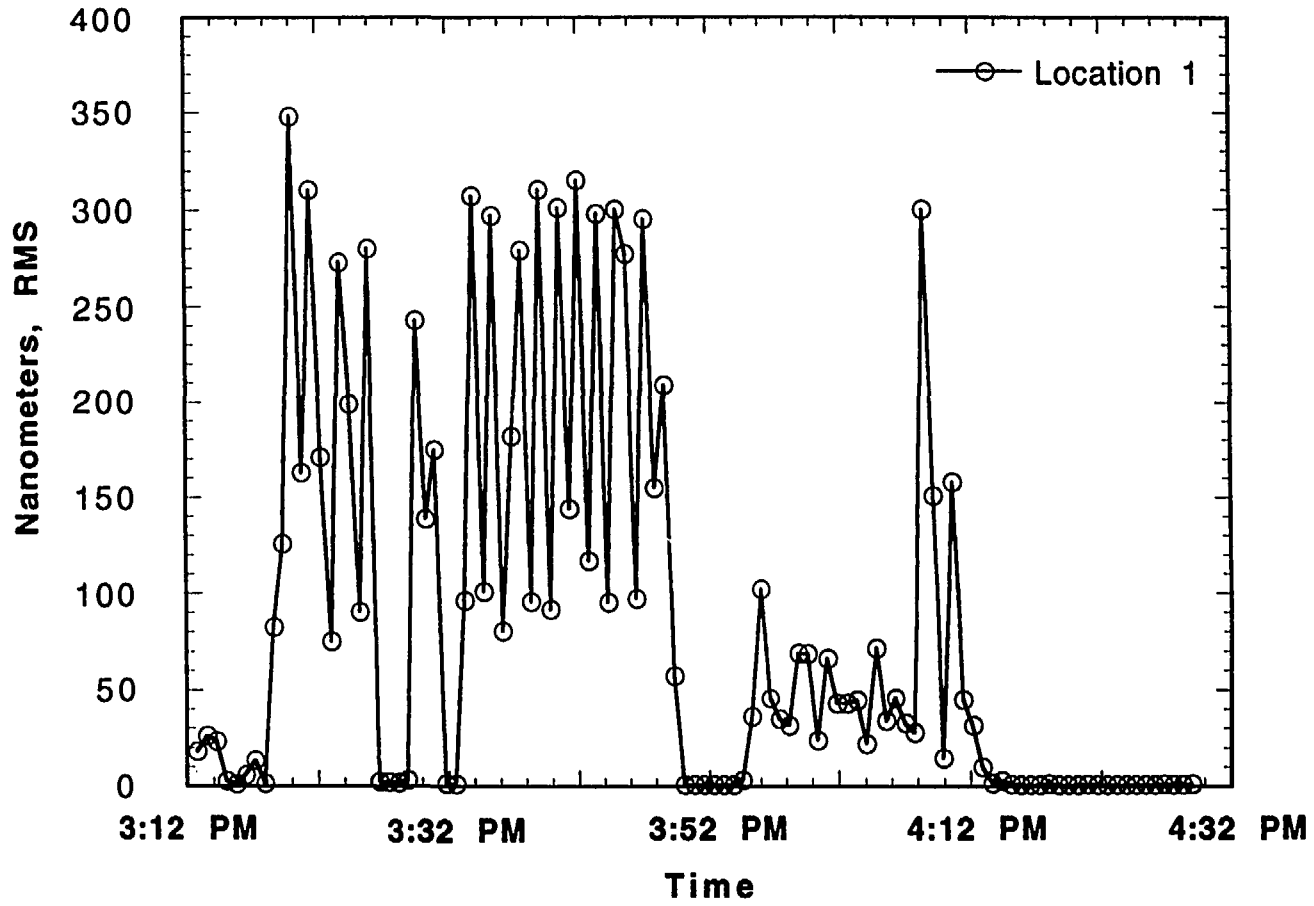


Fig. 28. Displacement response, Condition 1, at location 1, 20-100 Hz

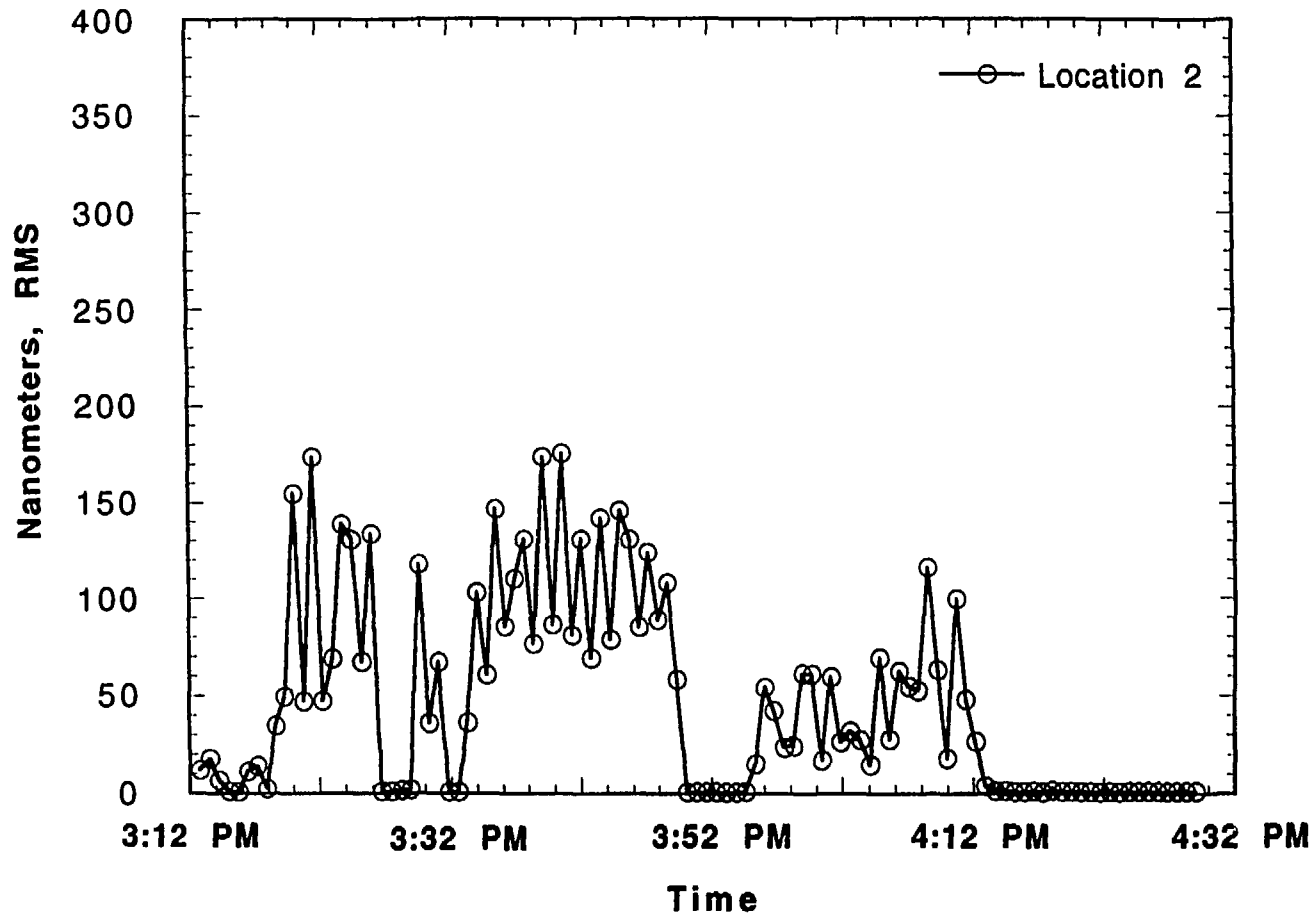


Fig. 29. Displacement response, Condition 1, at location 2, 28-30 Hz

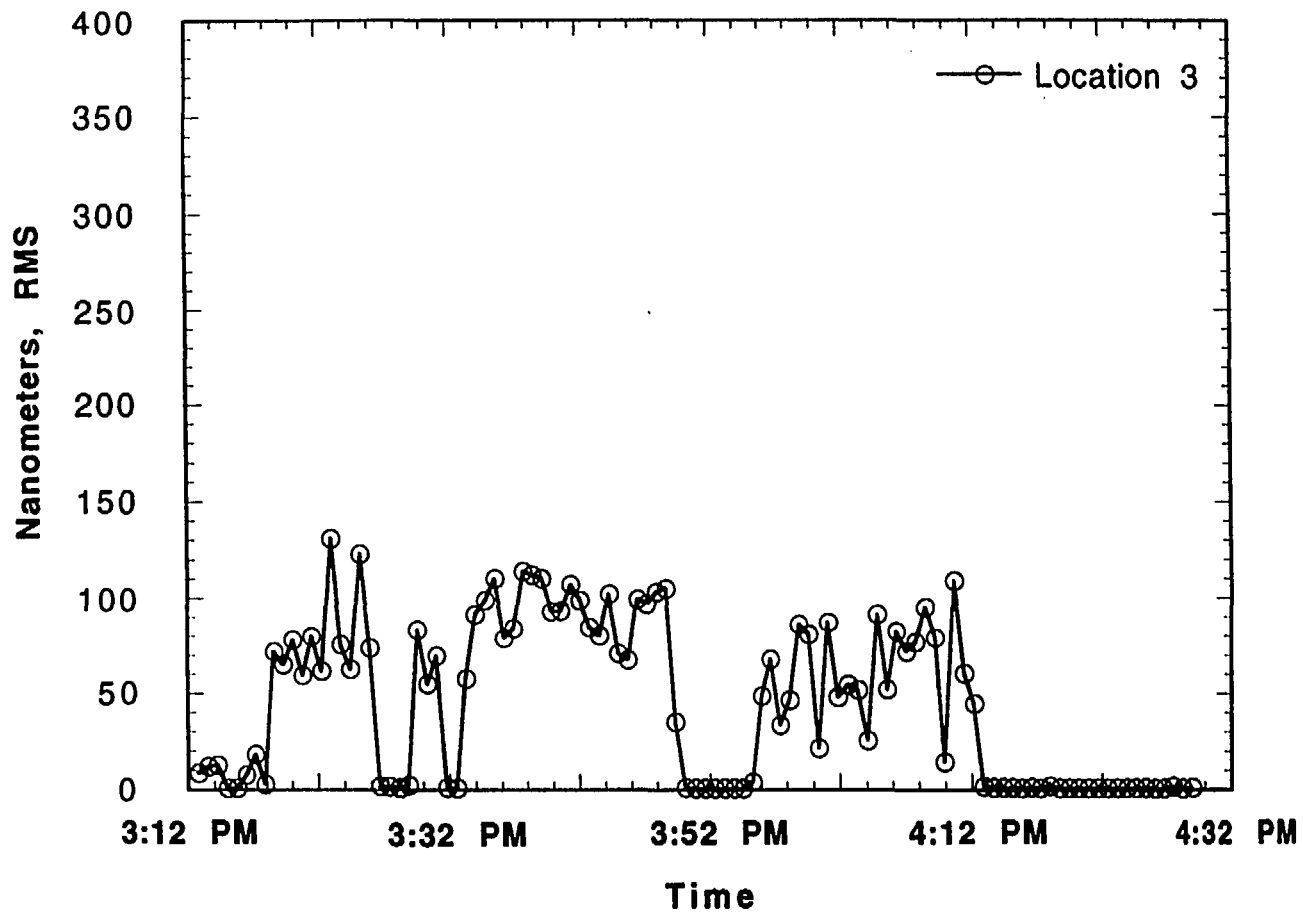


Fig. 30. Displacement response, Condition 1, at location 3, 28-30 Hz

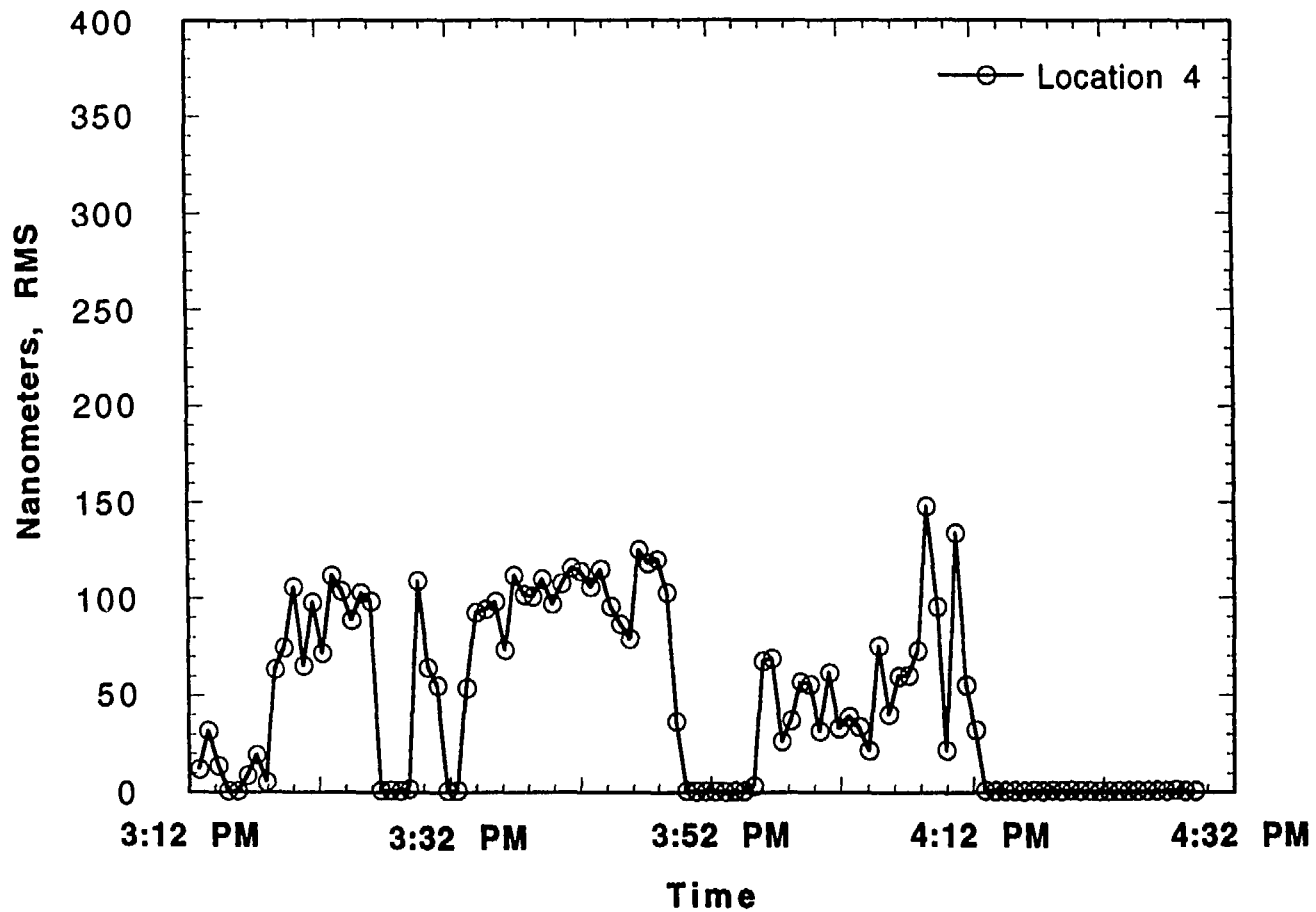


Fig. 31. Displacement response, Condition 1, at location 4, 28-30 Hz

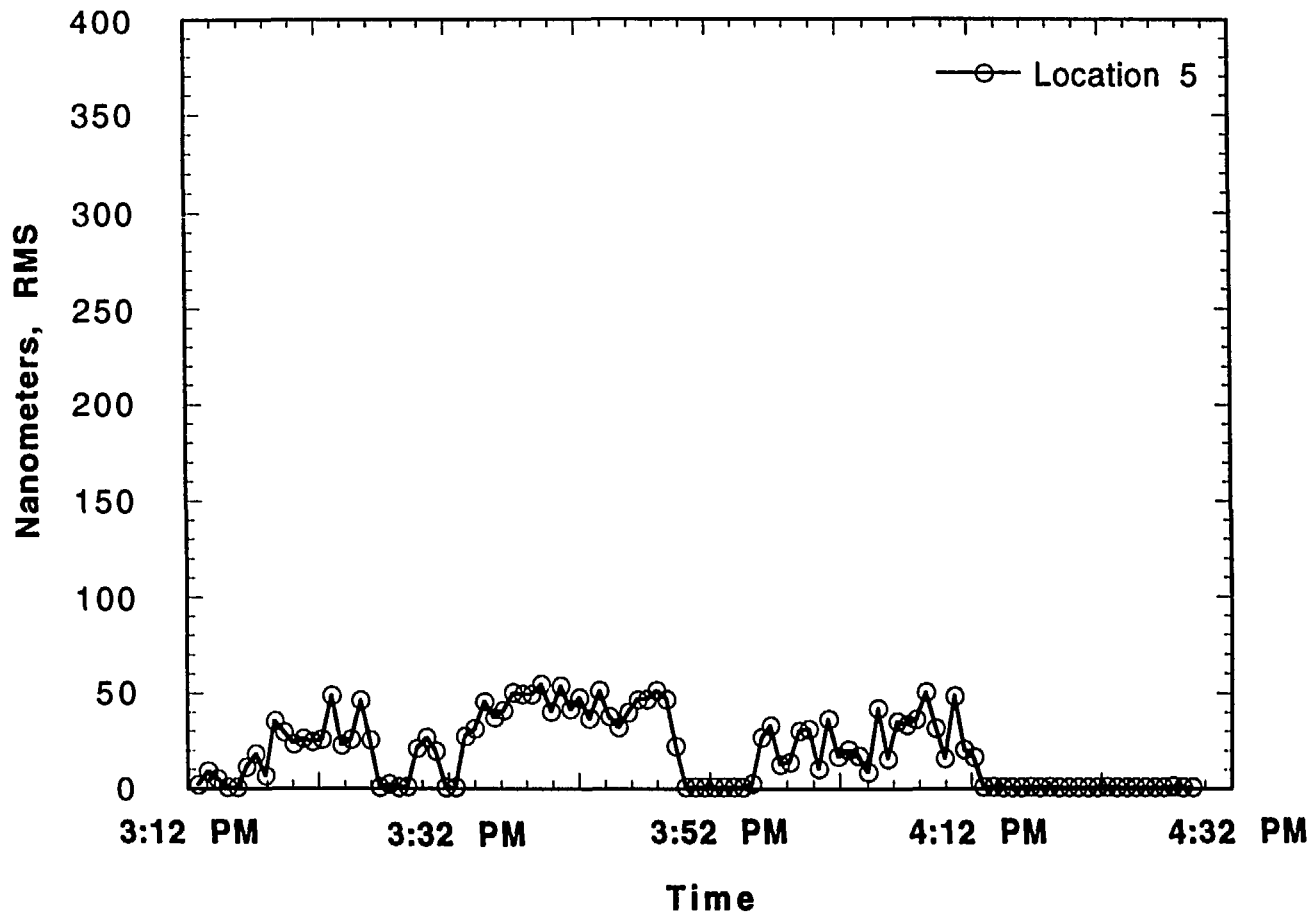


Fig. 32. Displacement response, Condition 1, at location 5, 28-30 Hz

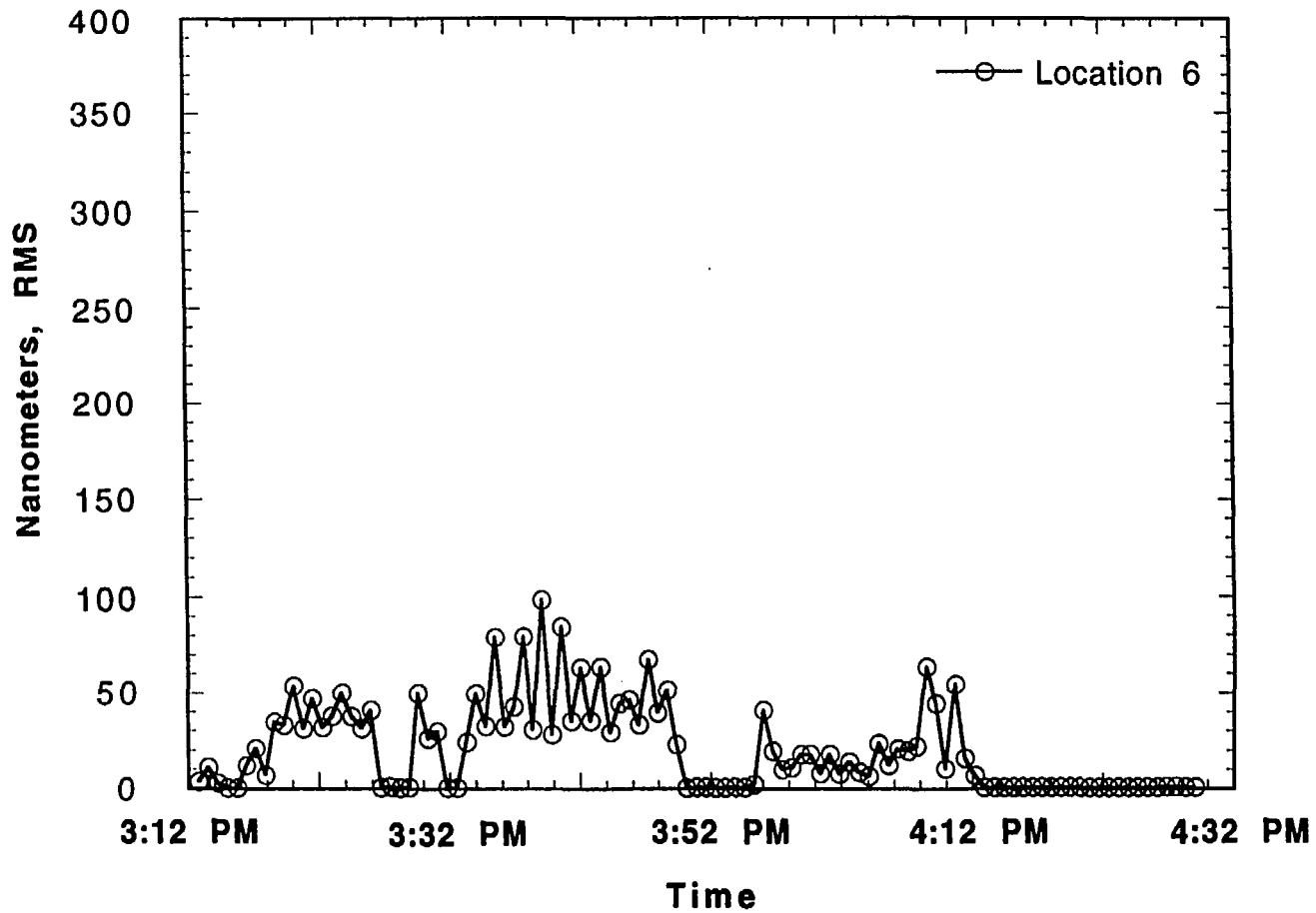


Fig. 33. Displacement response, Condition 1, at location 6, 28-30 Hz

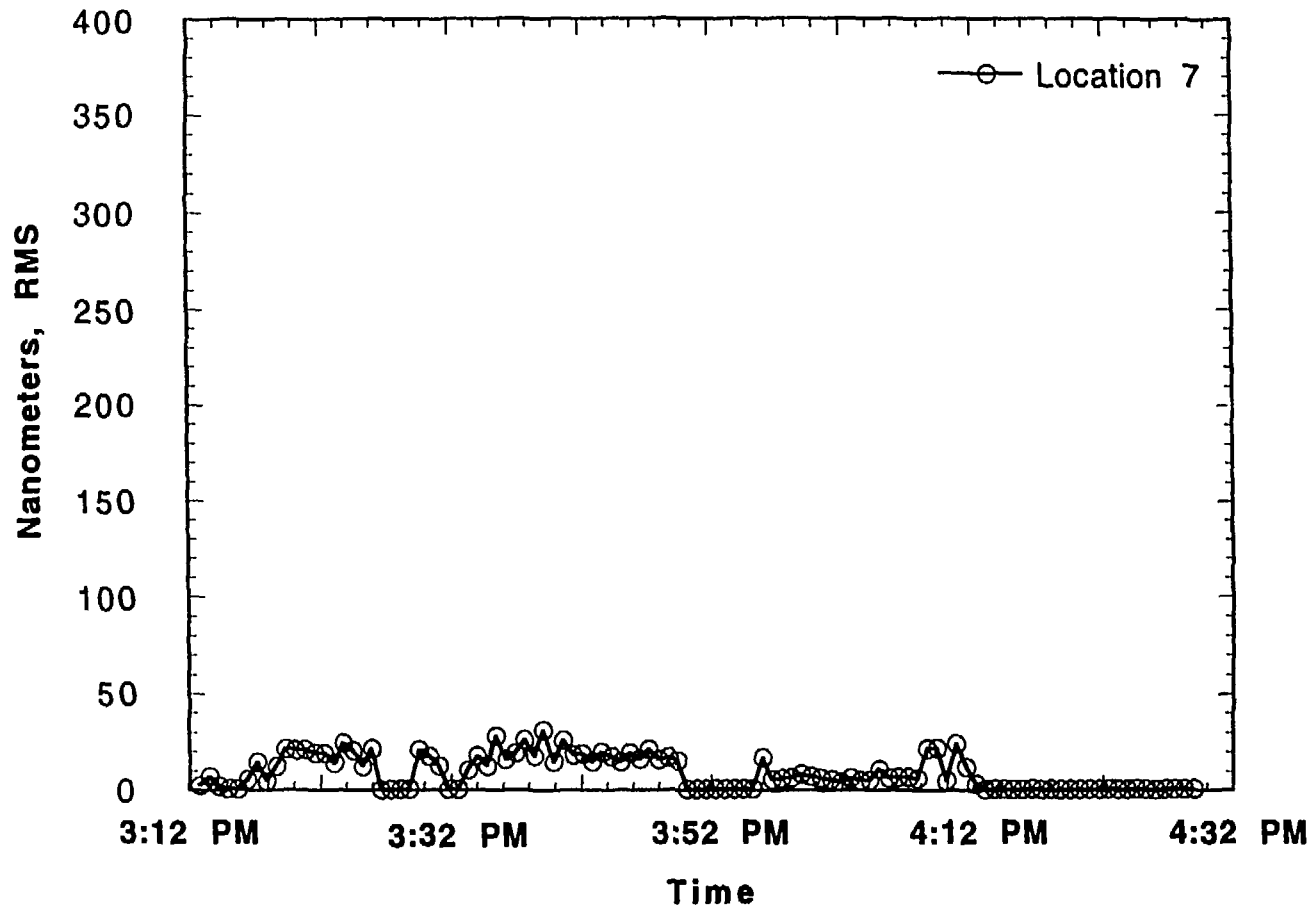


Fig. 34. Displacement response, Condition 1, at location 7, 28-30 Hz

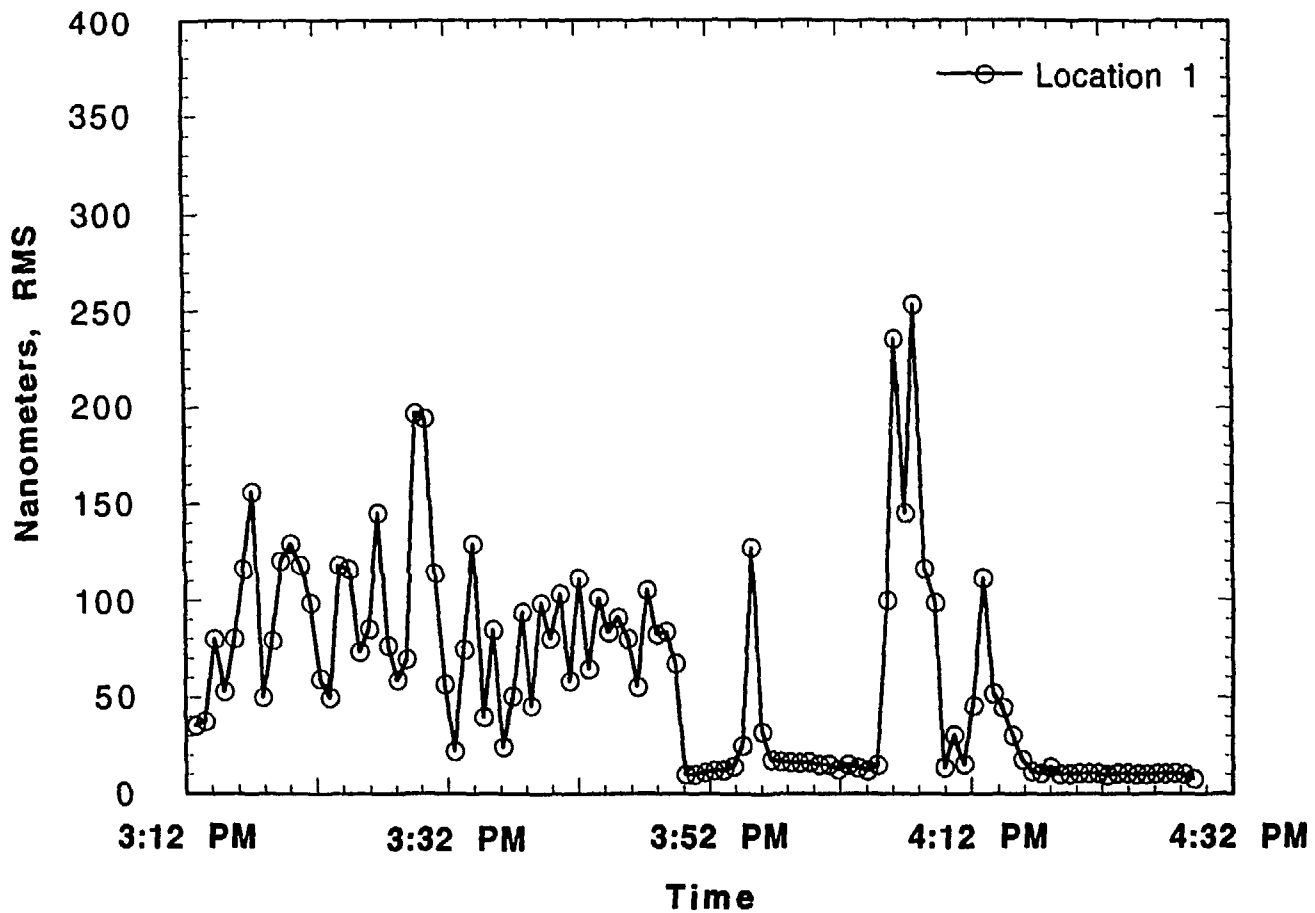


Fig. 35. Displacement response, Condition 1, at location 1, 10-100 Hz (28-30 Hz removed)

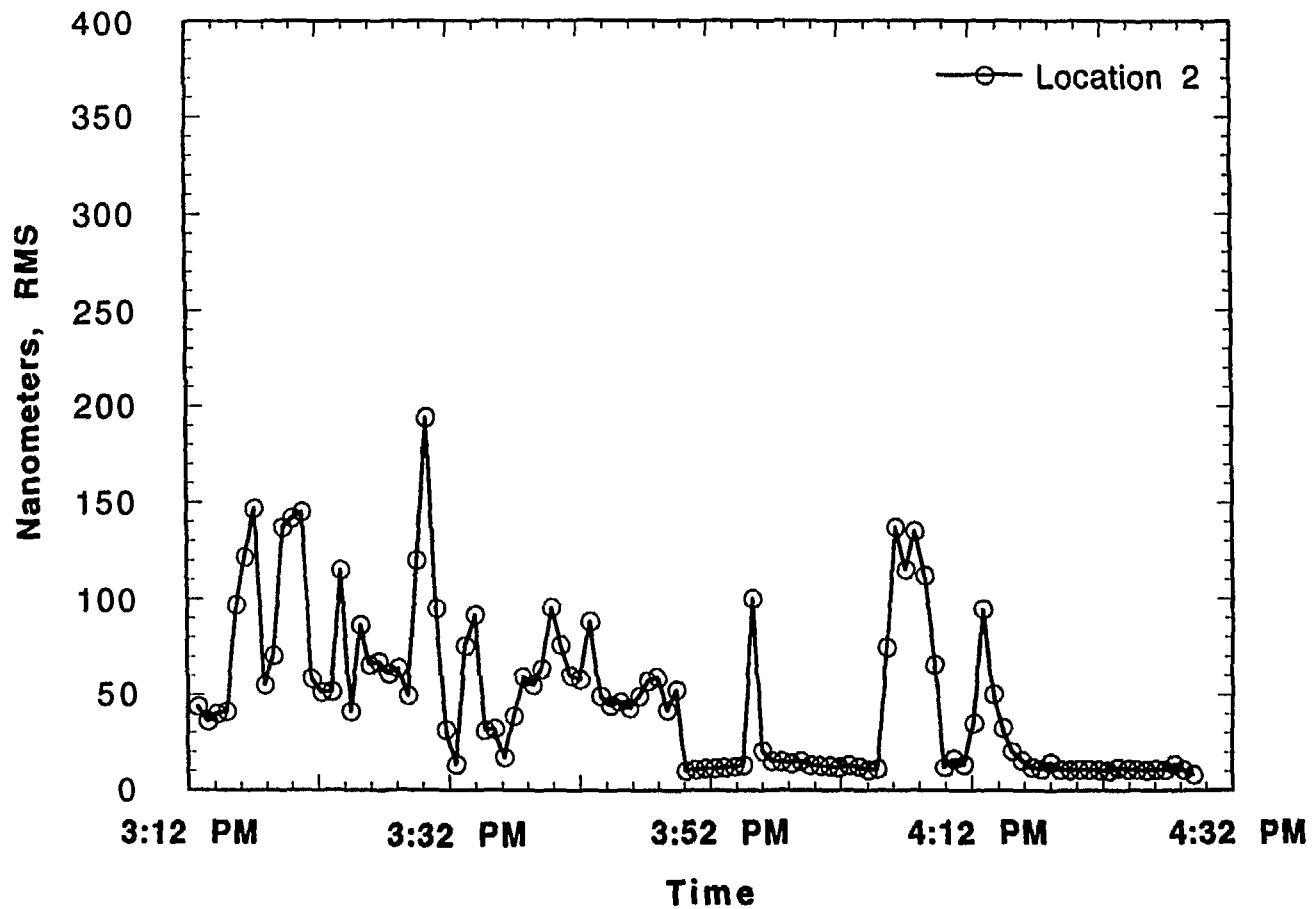


Fig. 36. Displacement response, Condition 1, at location 2, 10-100 Hz (28-30 Hz removed)

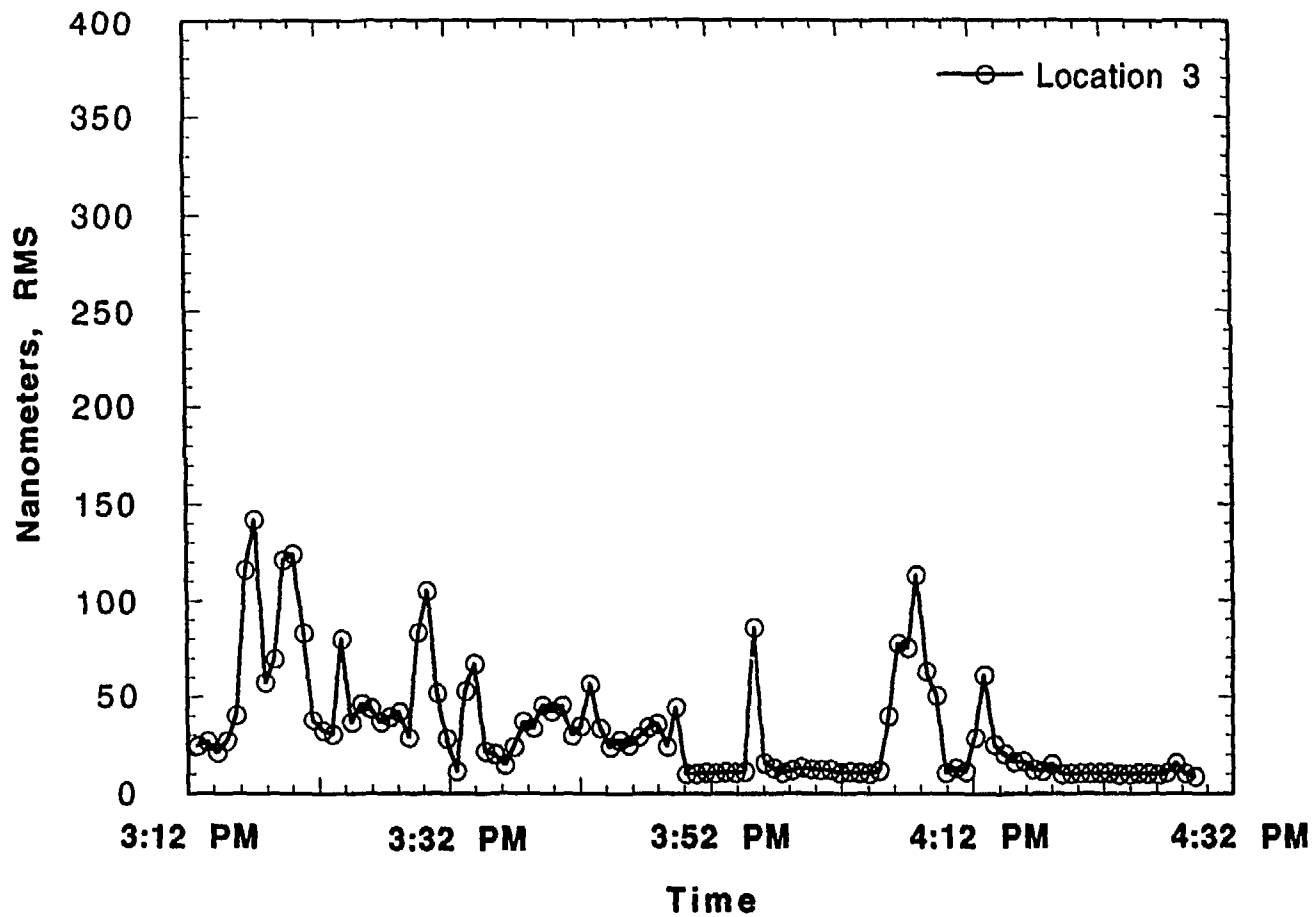


Fig. 37. Displacement response, Condition 1, at location 3, 10-100 Hz (28-30 Hz removed)

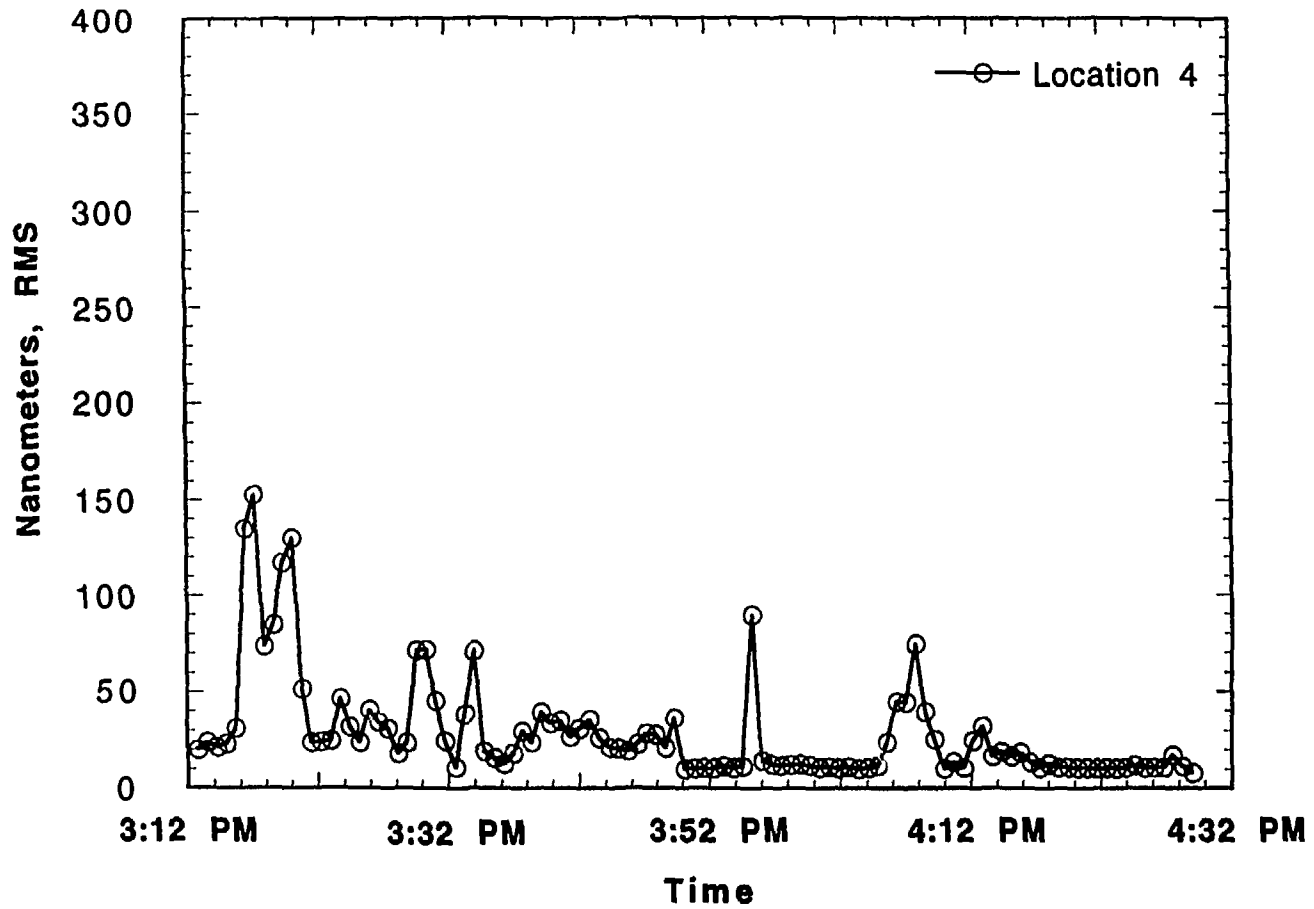


Fig. 38. Displacement response, Condition 1, at location 4, 10-100 Hz (28-30 Hz removed)

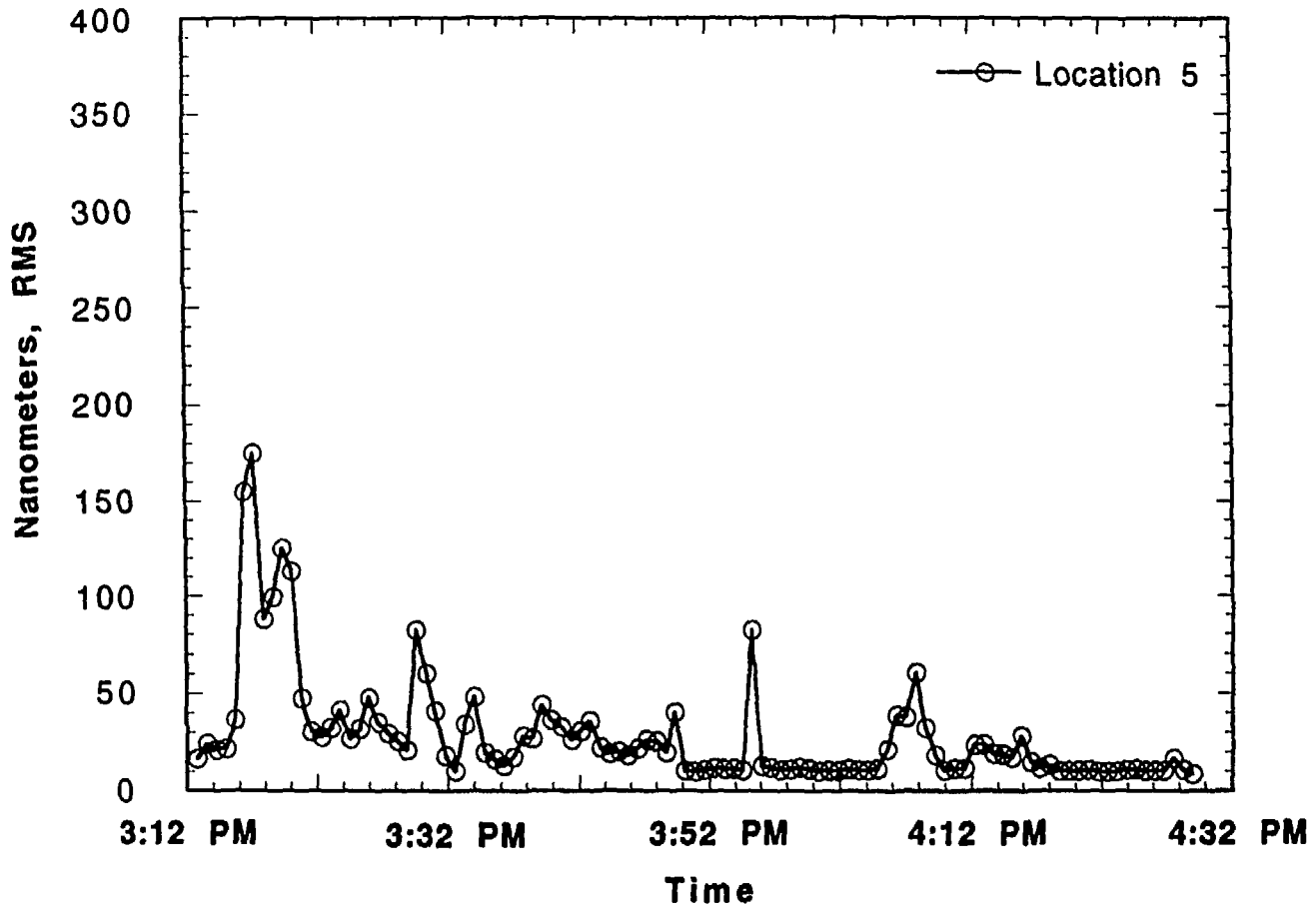


Fig. 39. Displacement response, Condition 1, at location 5, 10-100 Hz (28-30 Hz removed)

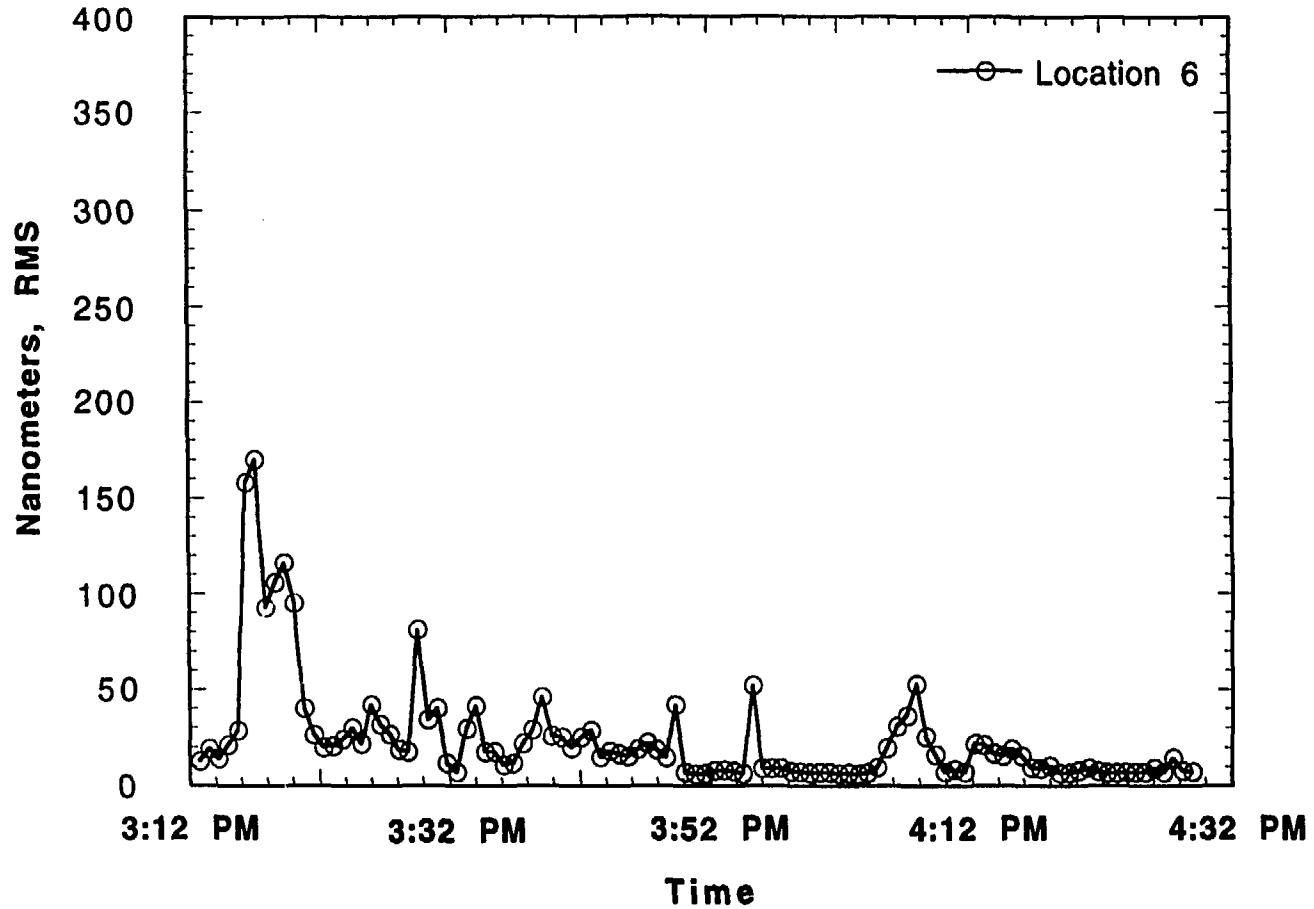


Fig. 40. Displacement response, Condition 1, at location 6, 10-100 Hz (28-30 Hz removed)

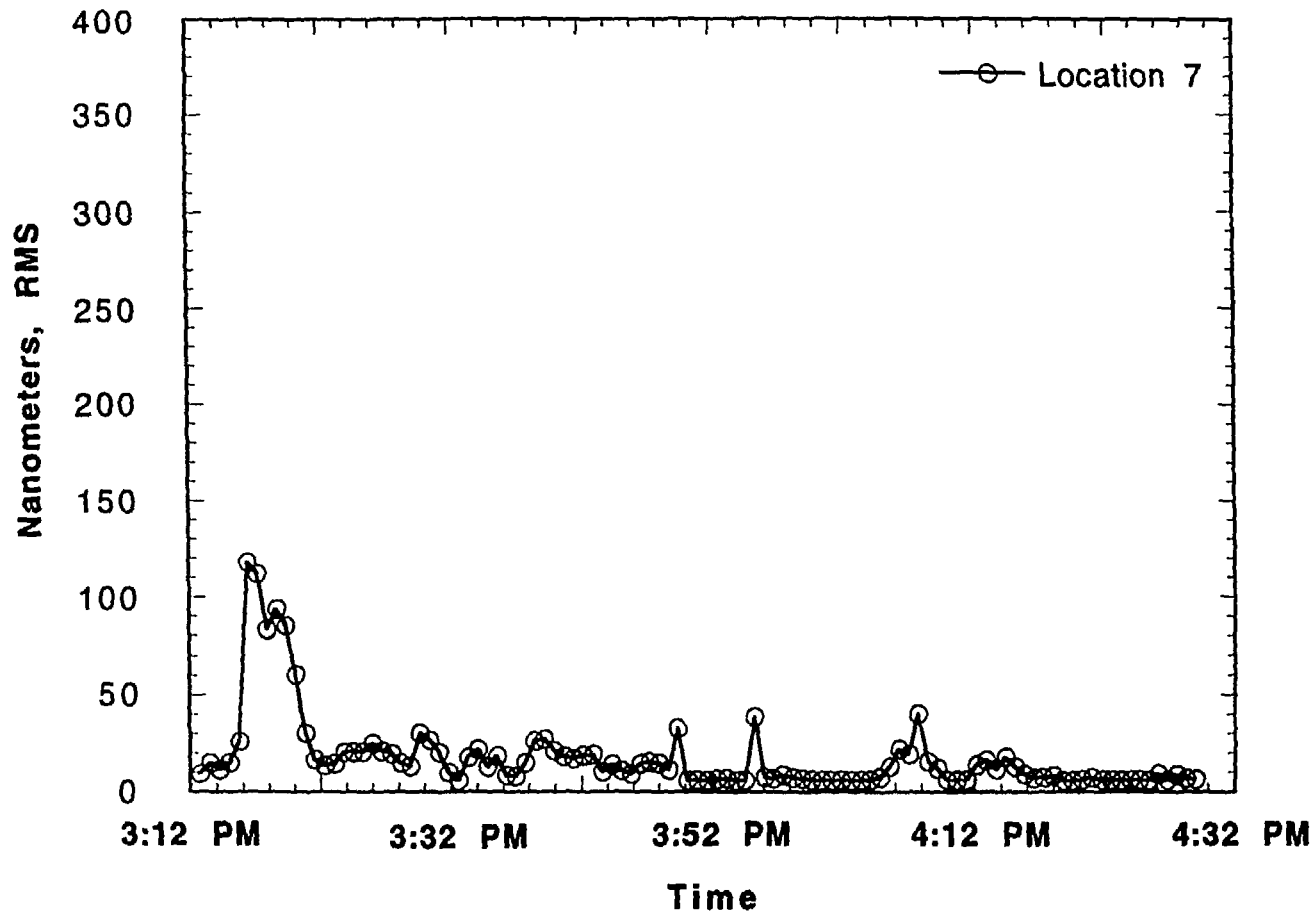


Fig. 41. Displacement response, Condition 1, at location 7, 10-100 Hz (28-30 Hz removed)

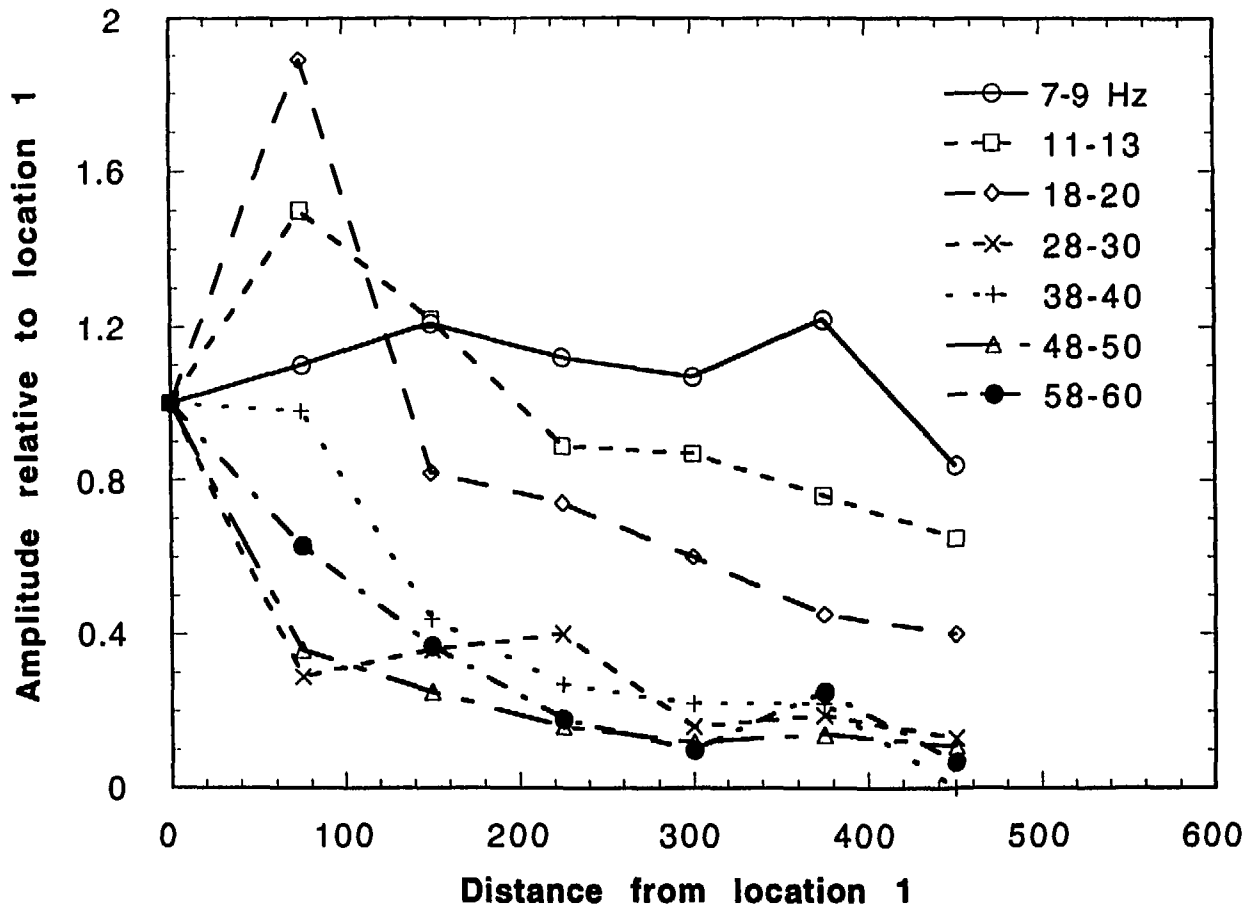


Fig. 42. Normalized amplitude as a function of distance for various frequencies

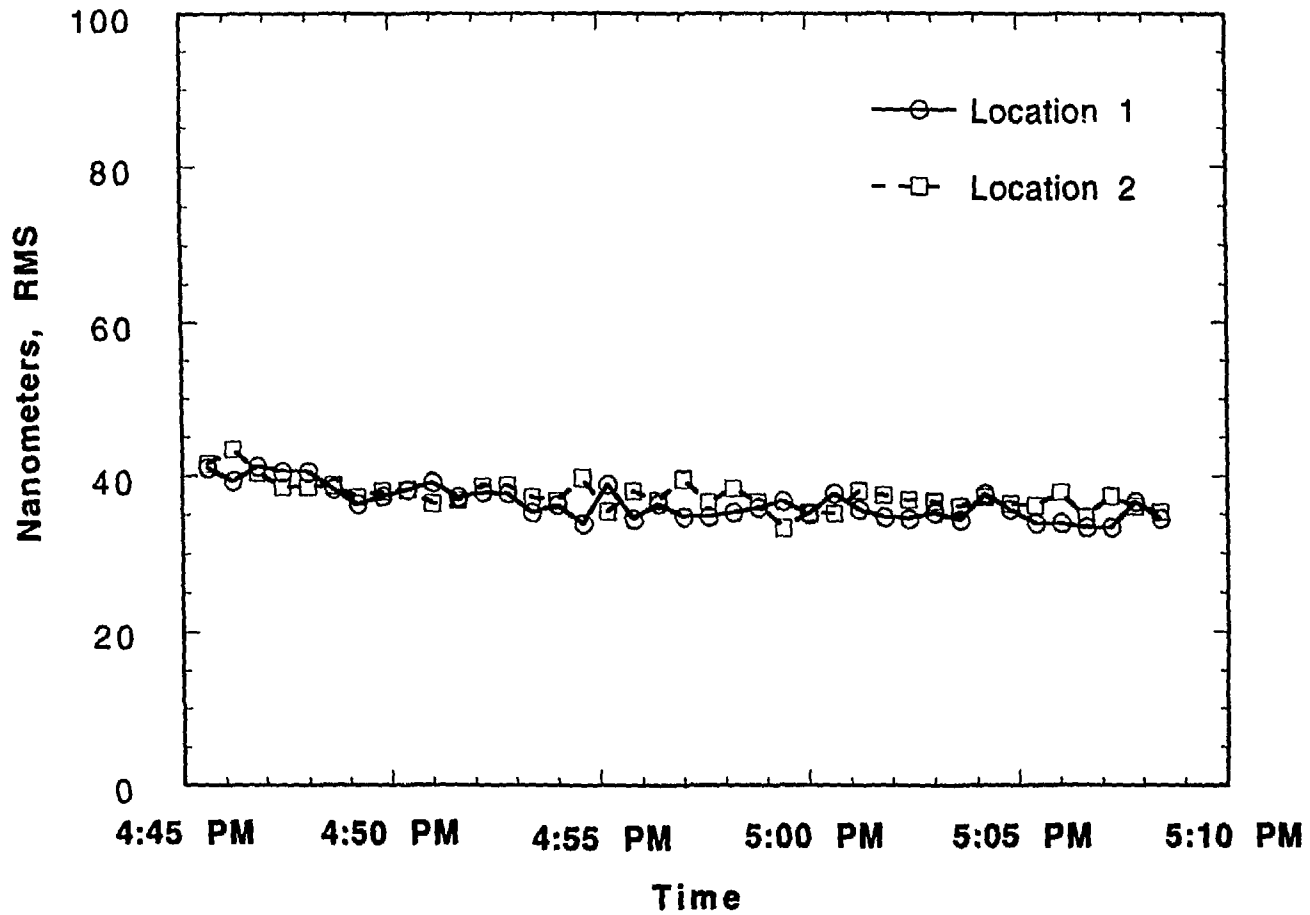


Fig. 43. Displacement response, Condition 2, at locations 1 and 2, 4-100 Hz

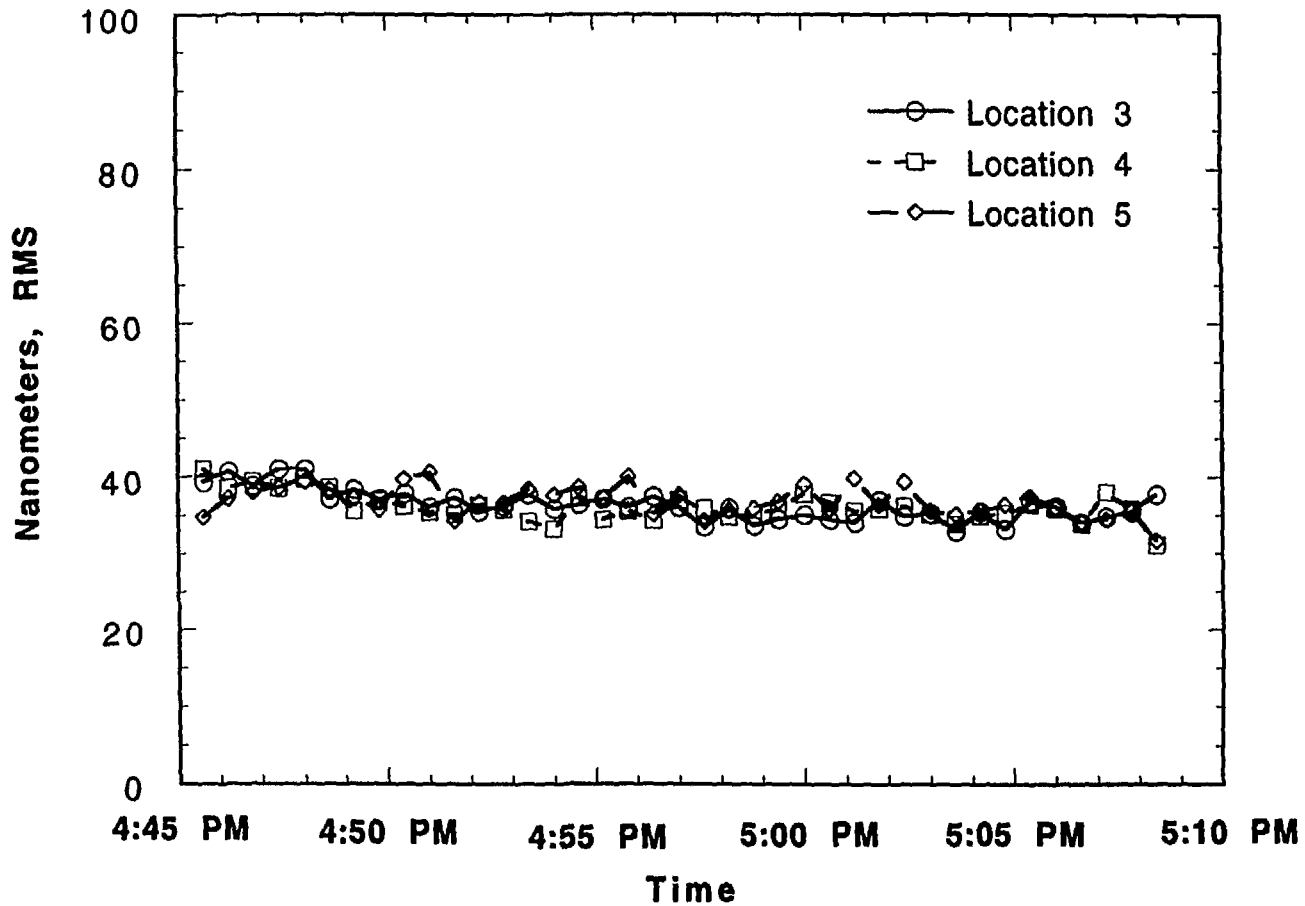


Fig. 44. Displacement response, Condition 2, at locations 3, 4, and 5, 4-100 Hz

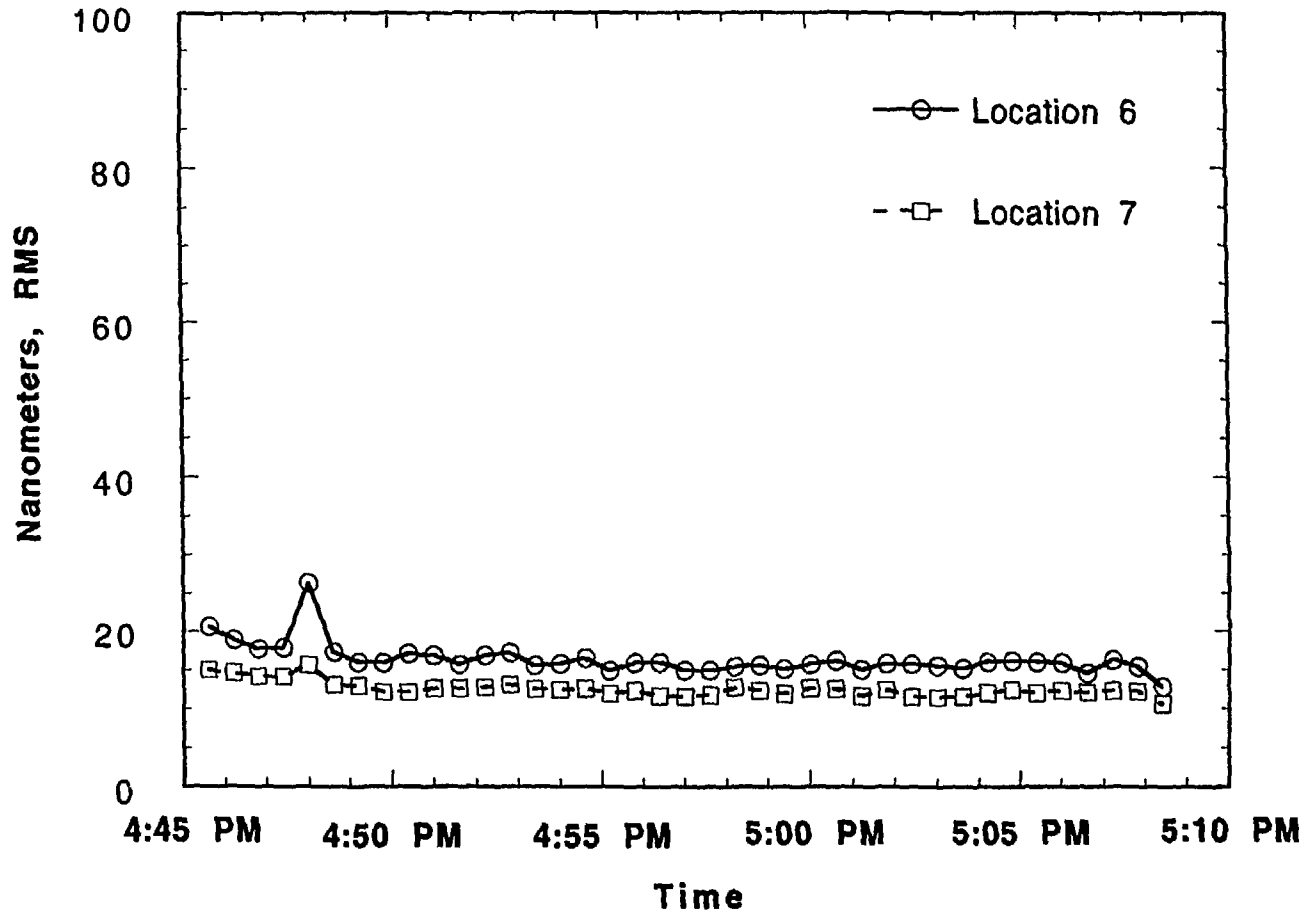


Fig. 45. Displacement response, Condition 2, at locations 6 and 7, 4-100 Hz

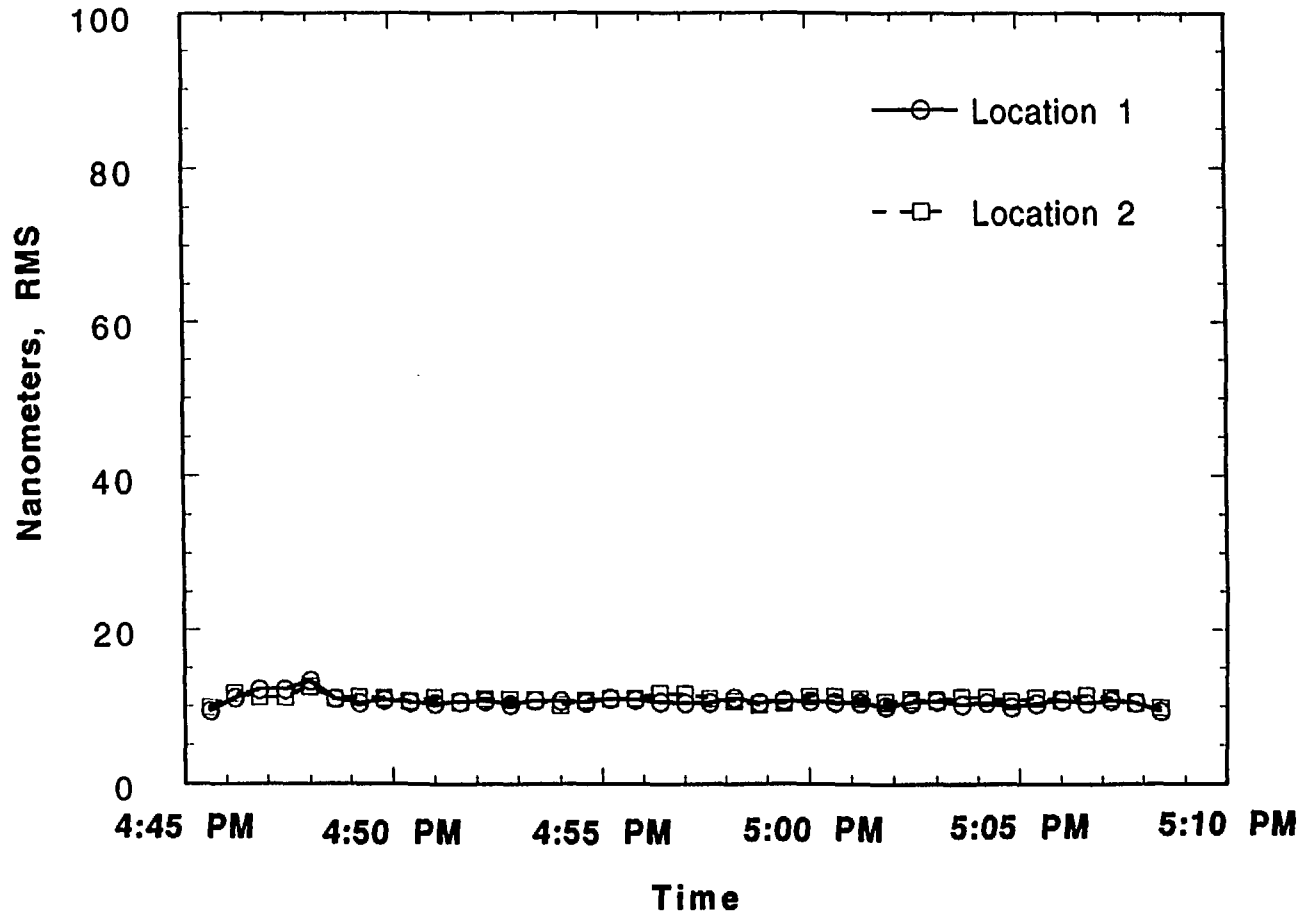


Fig. 46. Displacement response, Condition 2, at locations 1 and 2, 10-100 Hz

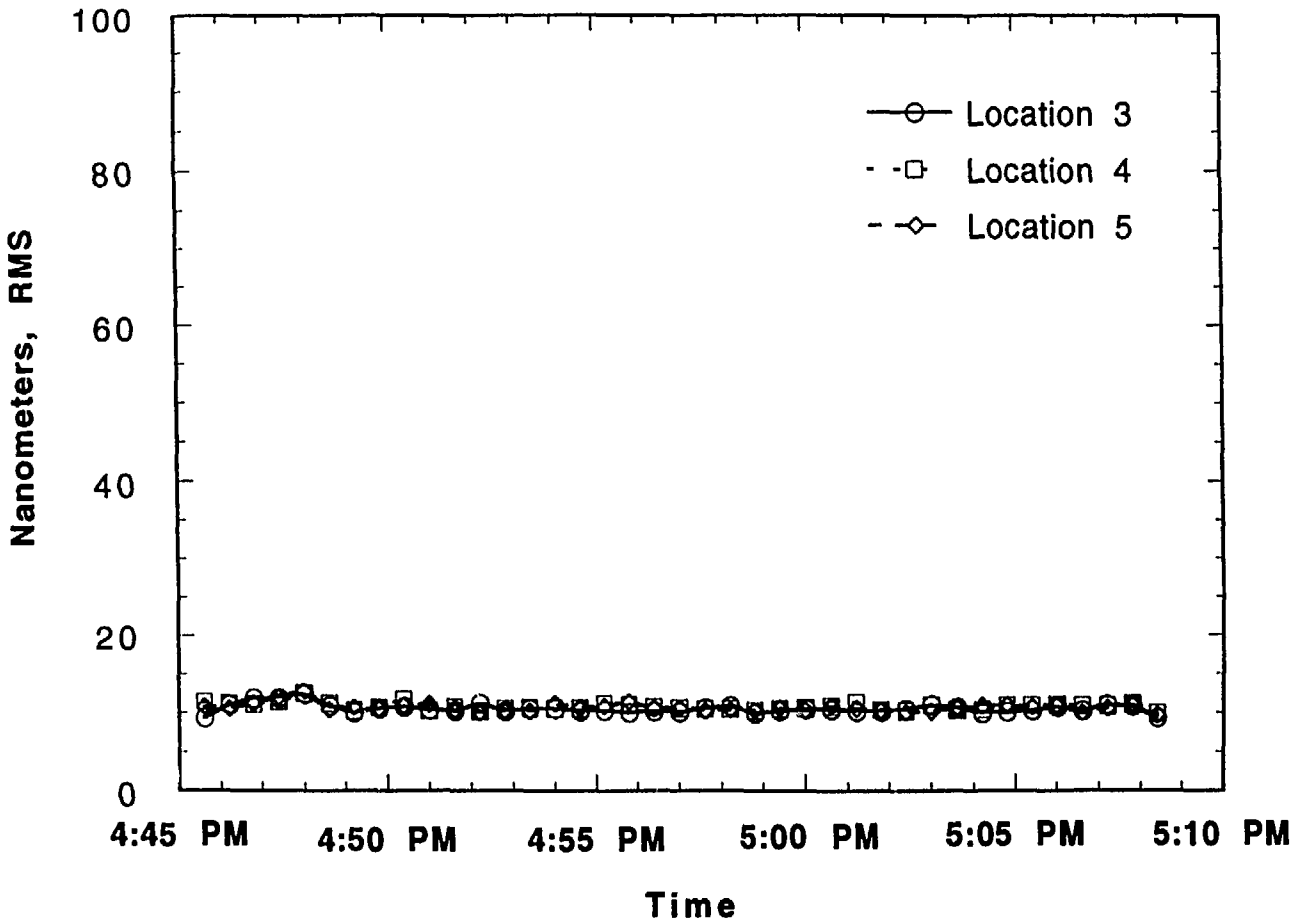


Fig. 47. Displacement response, Condition 2, at locations 3, 4, and 5, 10-100 Hz

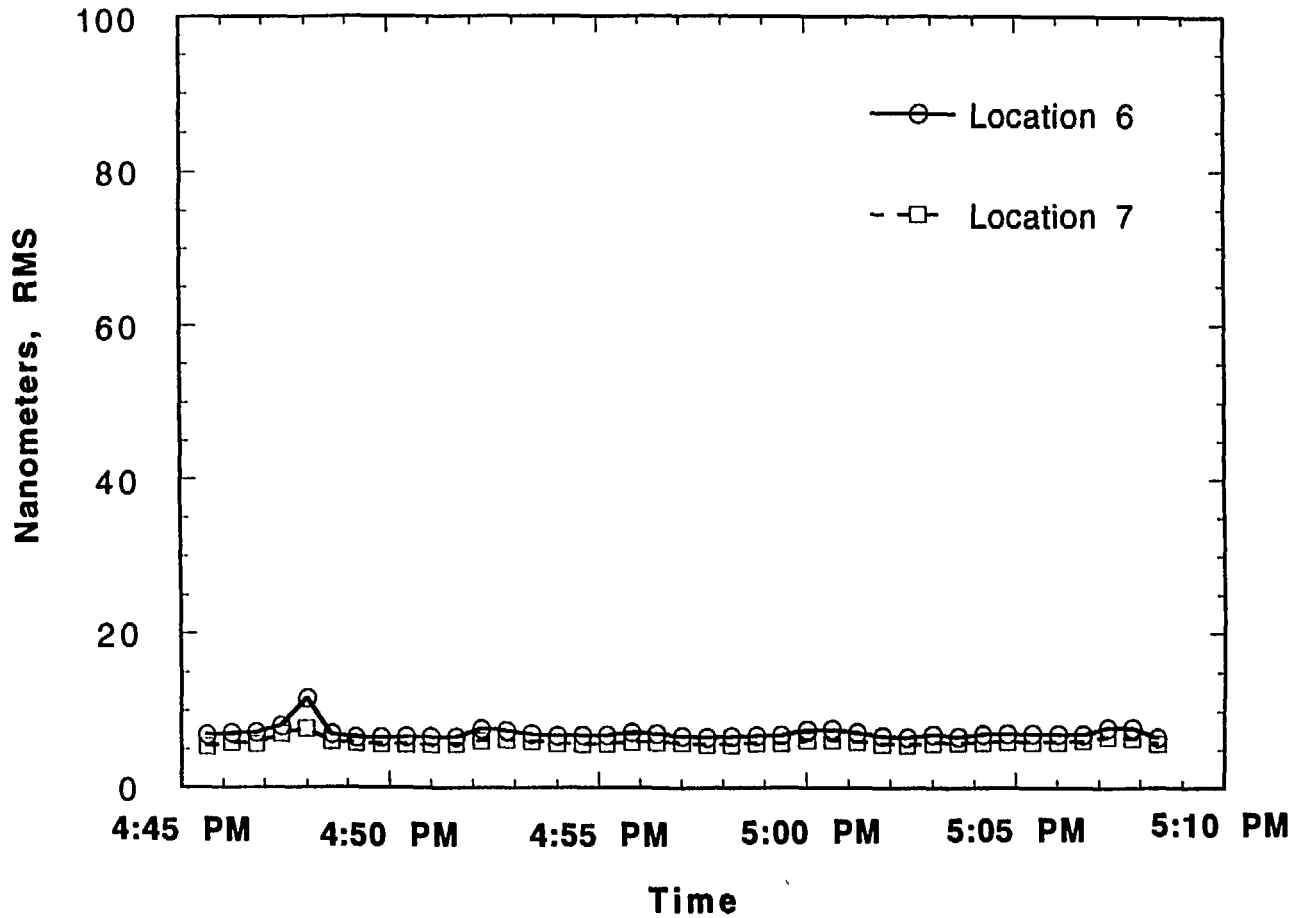


Fig. 48. Displacement response, Condition 2, at locations 6 and 7, 10-100 Hz

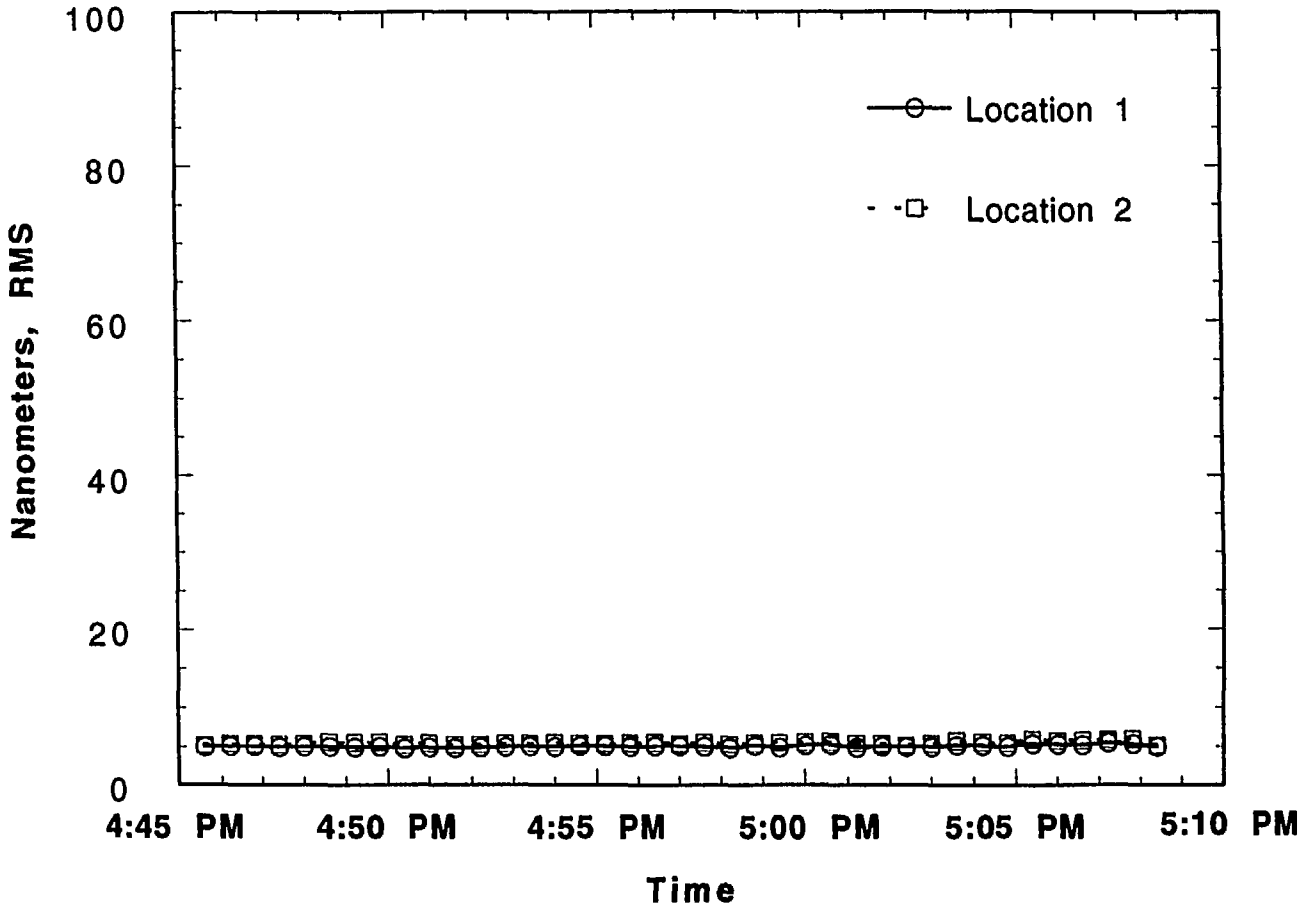


Fig. 49. Displacement response, Condition 2, at locations 1 and 2, 20-100 Hz

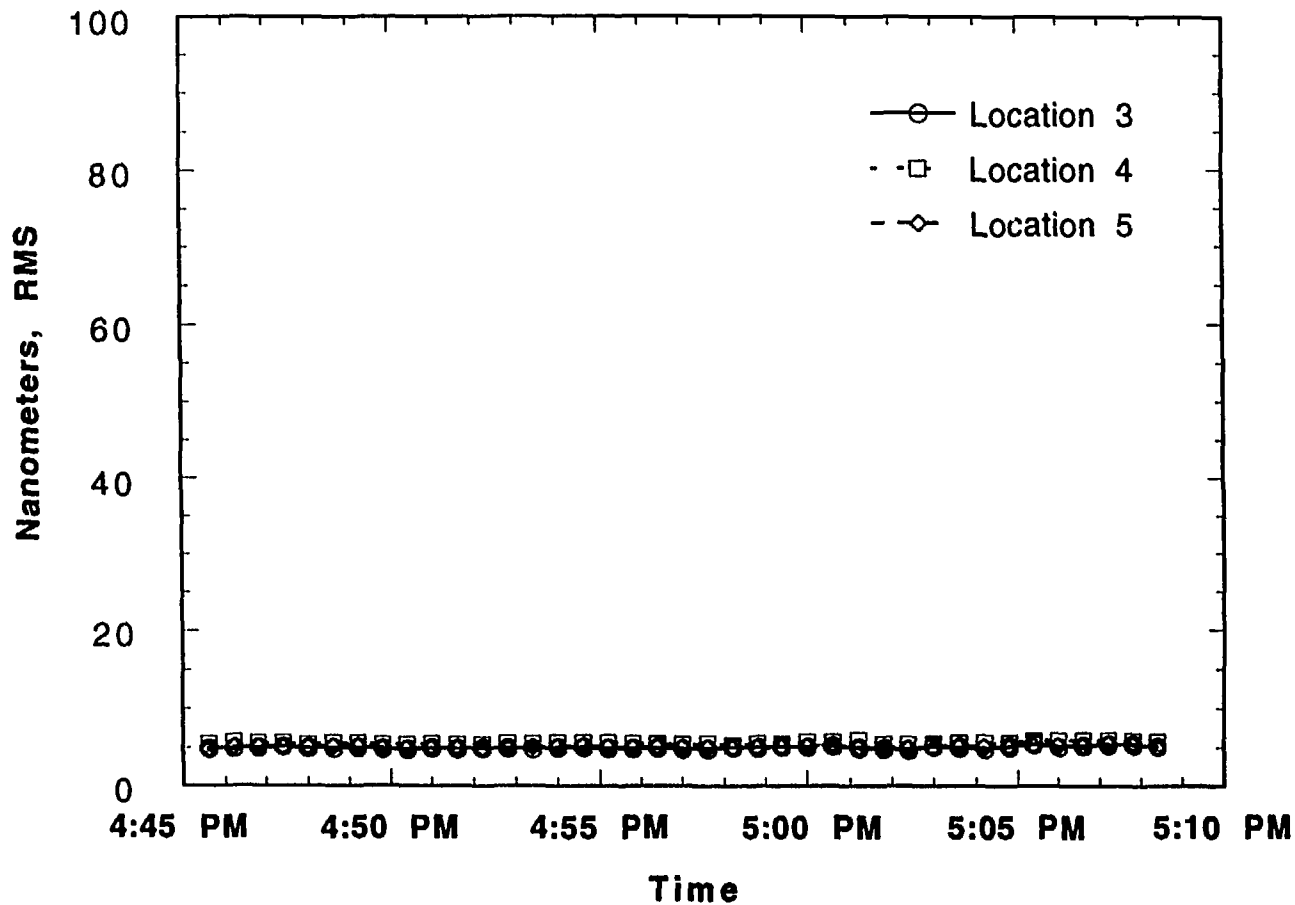


Fig. 50. Displacement response, Condition 2, at locations 3, 4, and 5, 20-100 Hz

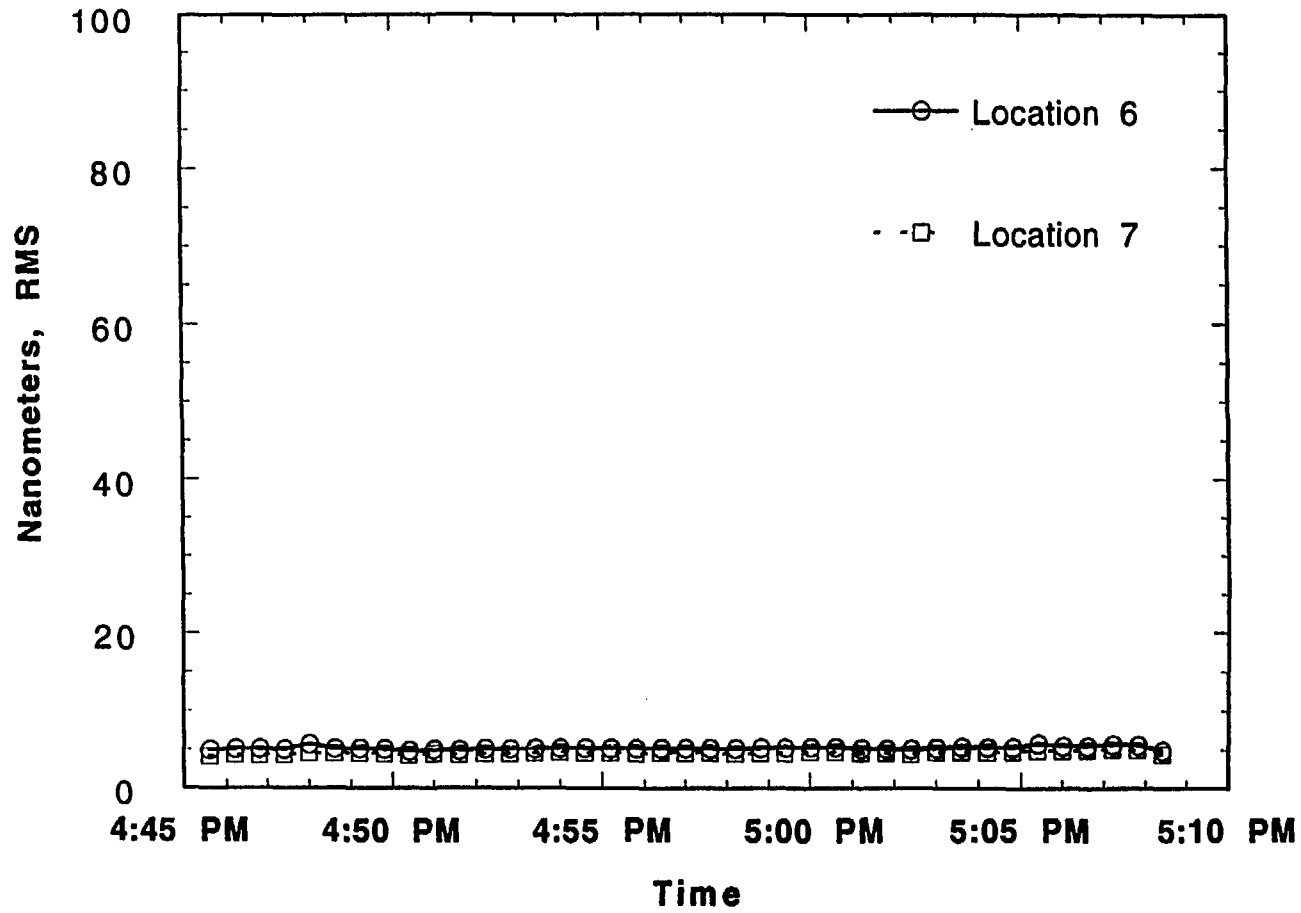


Fig. 51. Displacement response, Condition 2, at locations 6 and 7, 20-100 Hz

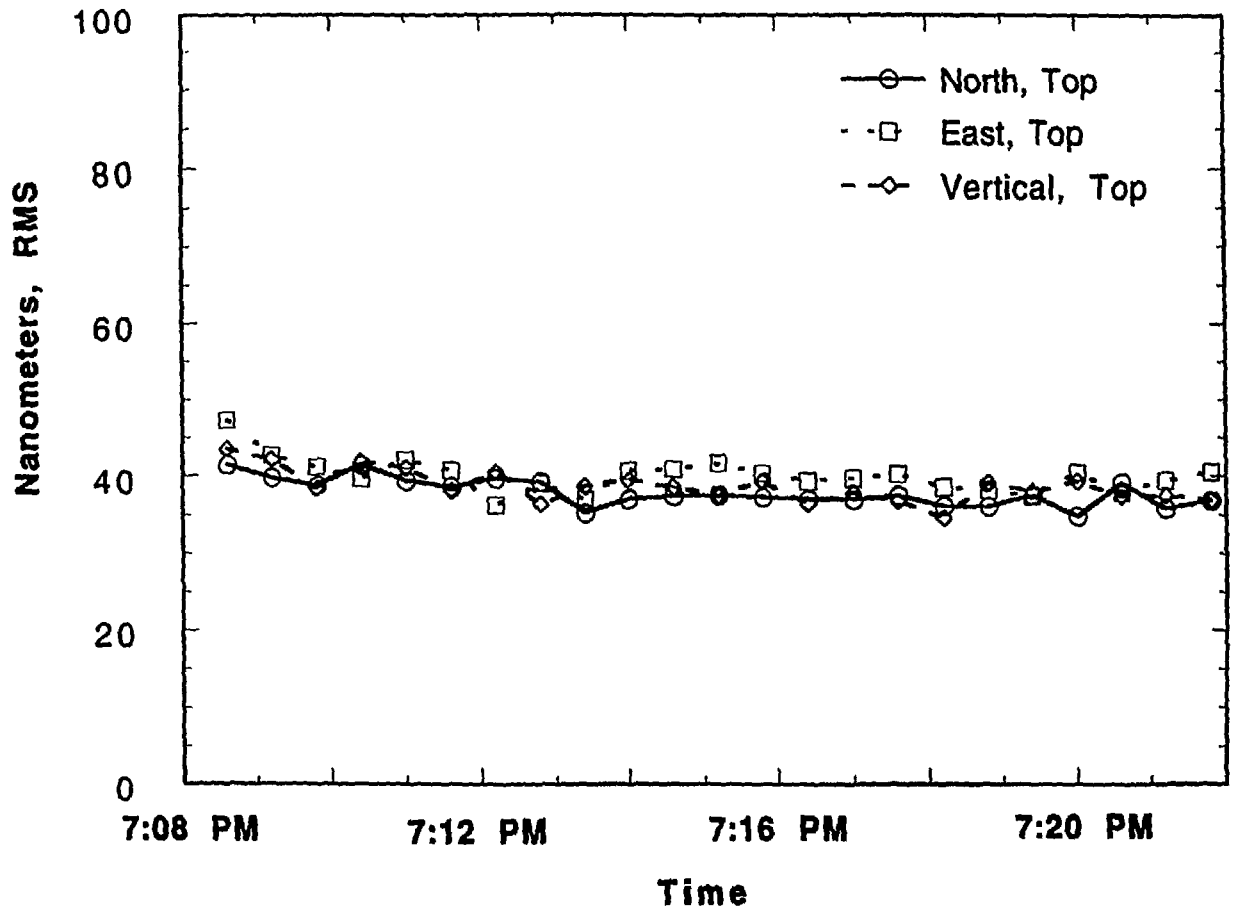


Fig. 52. Displacement response, Condition 3, on roof, 4-100 Hz

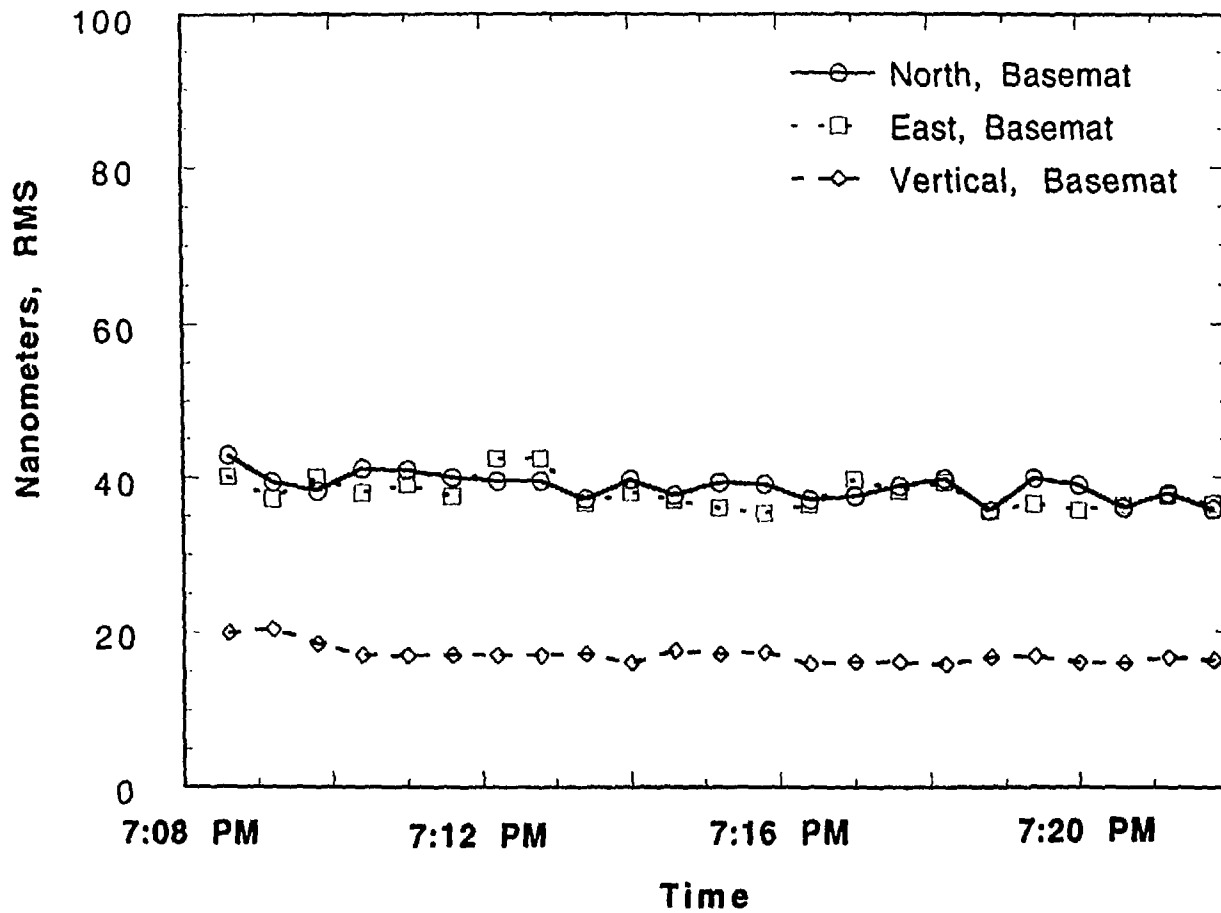


Fig. 53. Displacement response, Condition 3, on basemat, 4-100 Hz

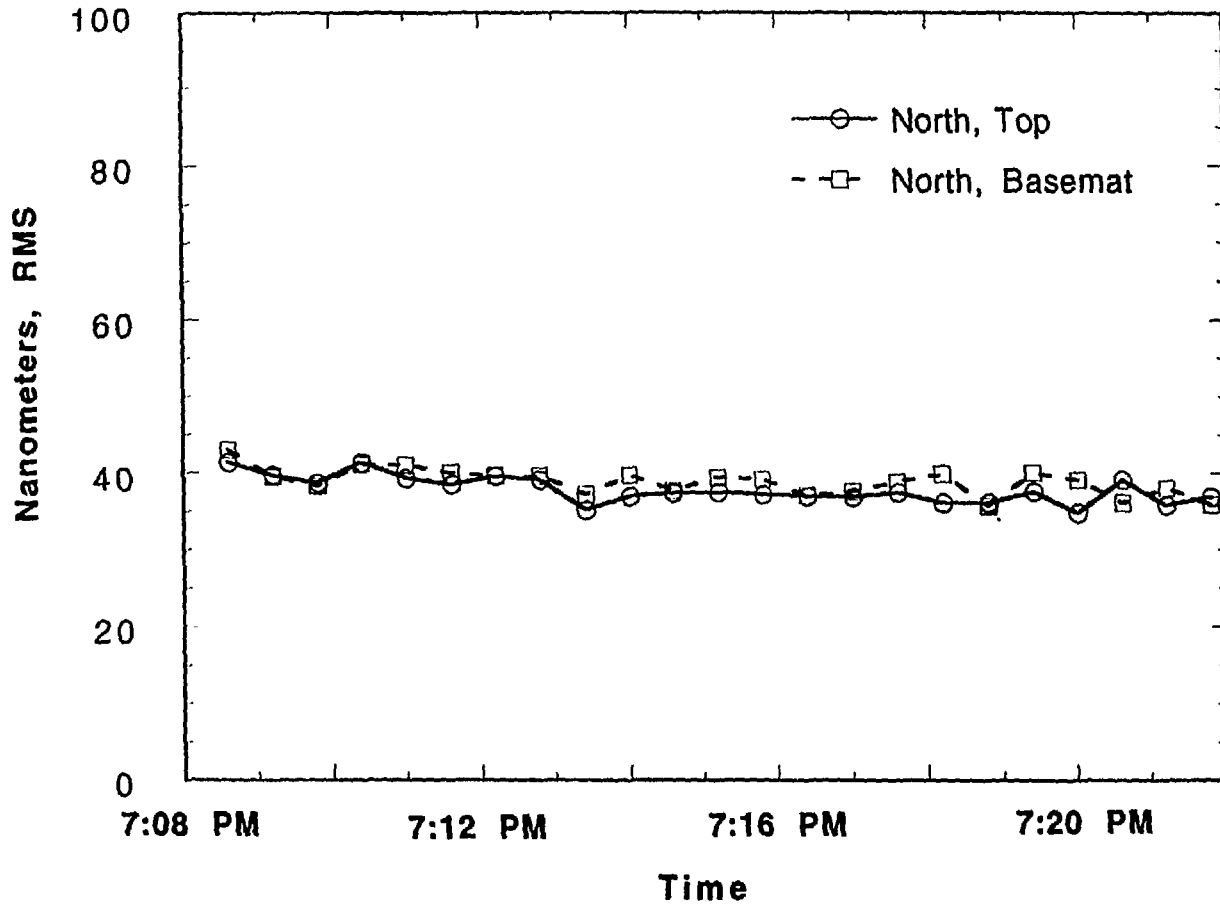


Fig. 54. Comparison of displacements, north roof to north basemat, 4-100 Hz

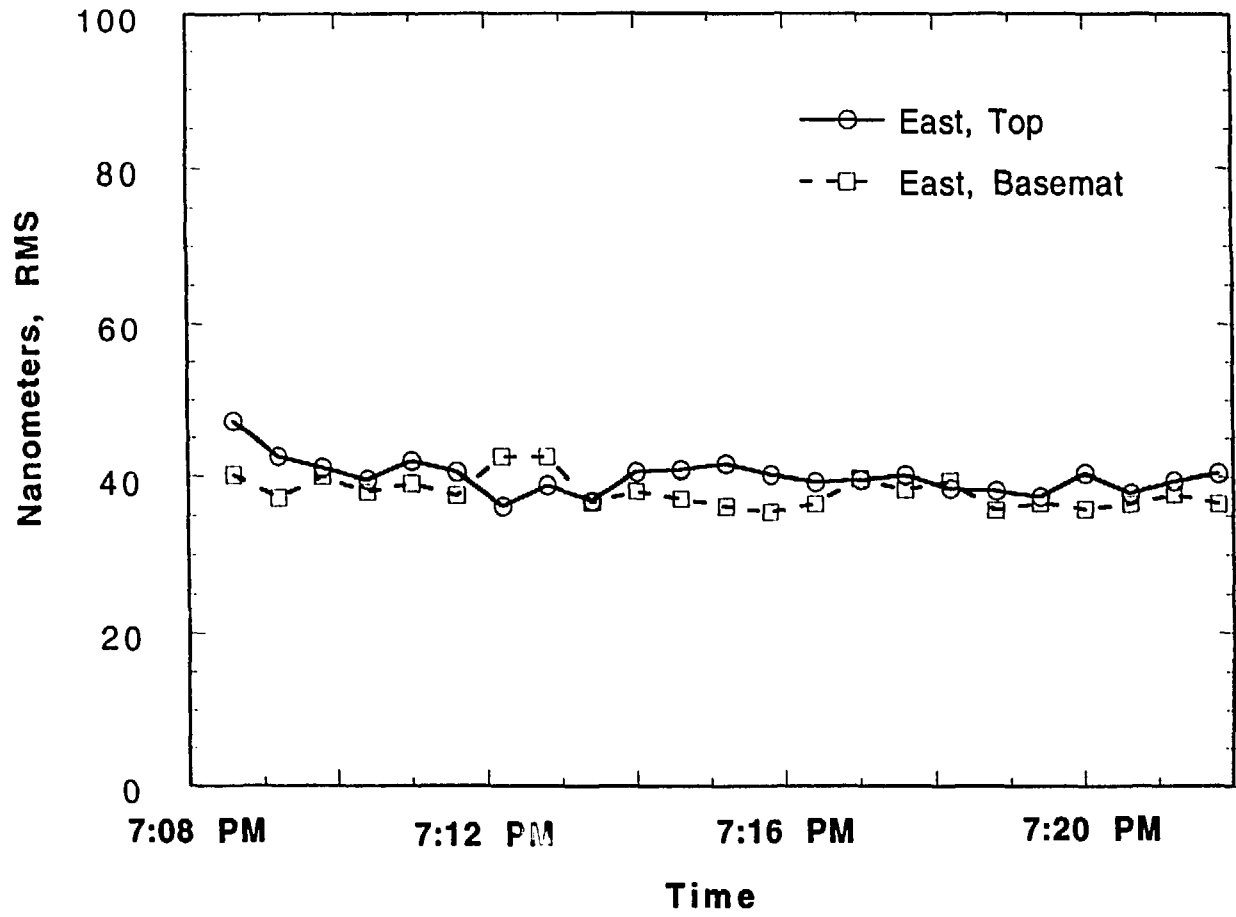


Fig. 55. Comparison of displacements, east roof to east basemat, 4-100 Hz

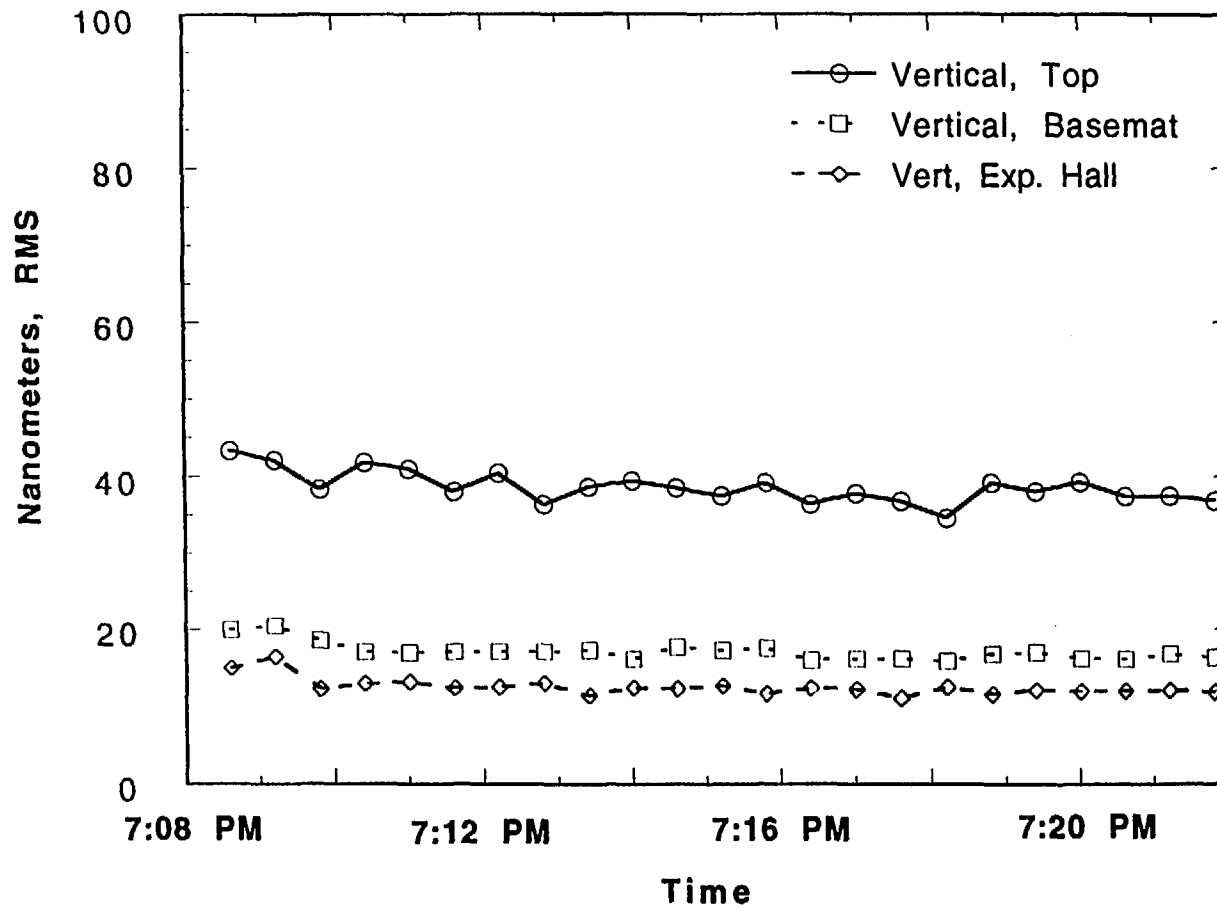


Fig. 56. Vertical displacements, Condition 3, 4-100 Hz

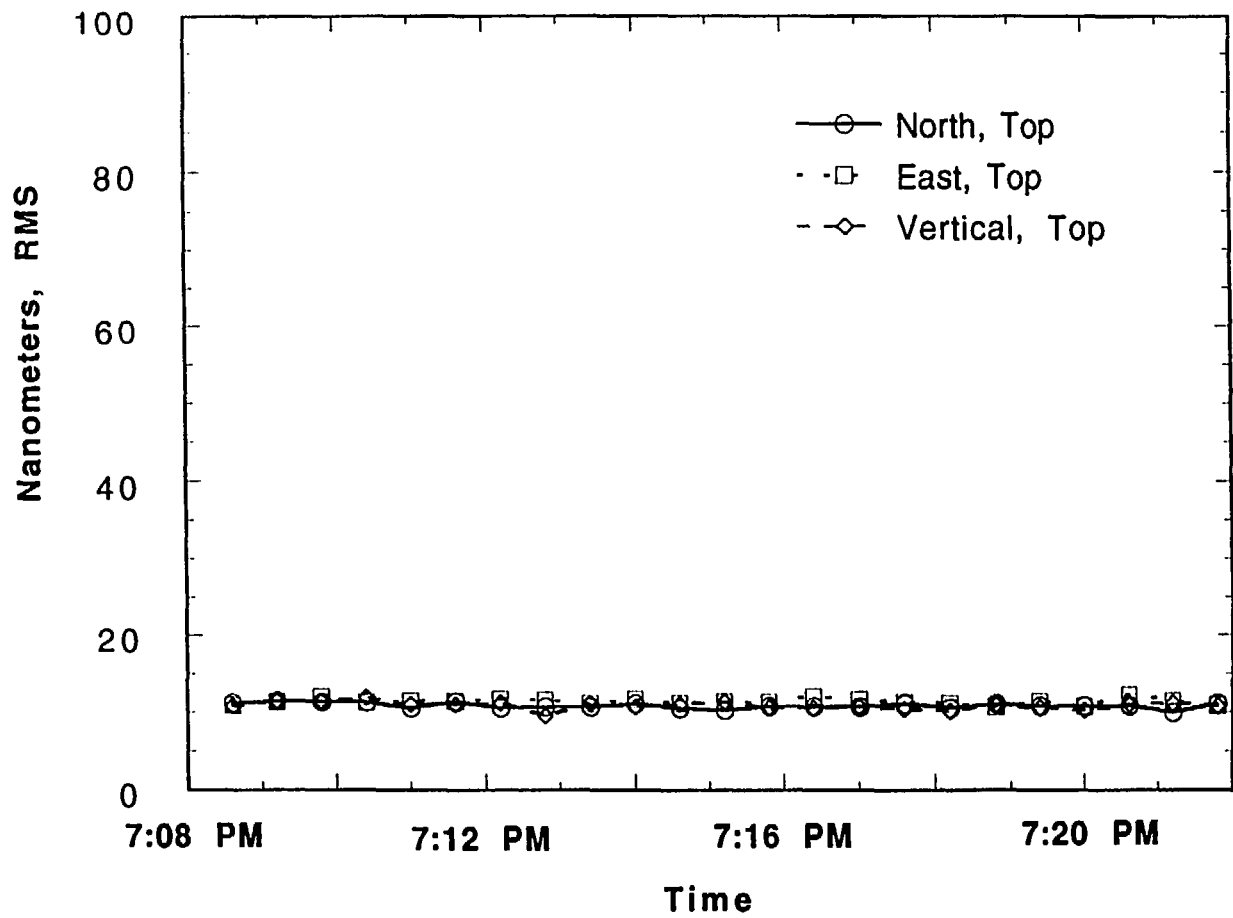


Fig. 57. Displacement response, Condition 3, on roof, 10-100 Hz

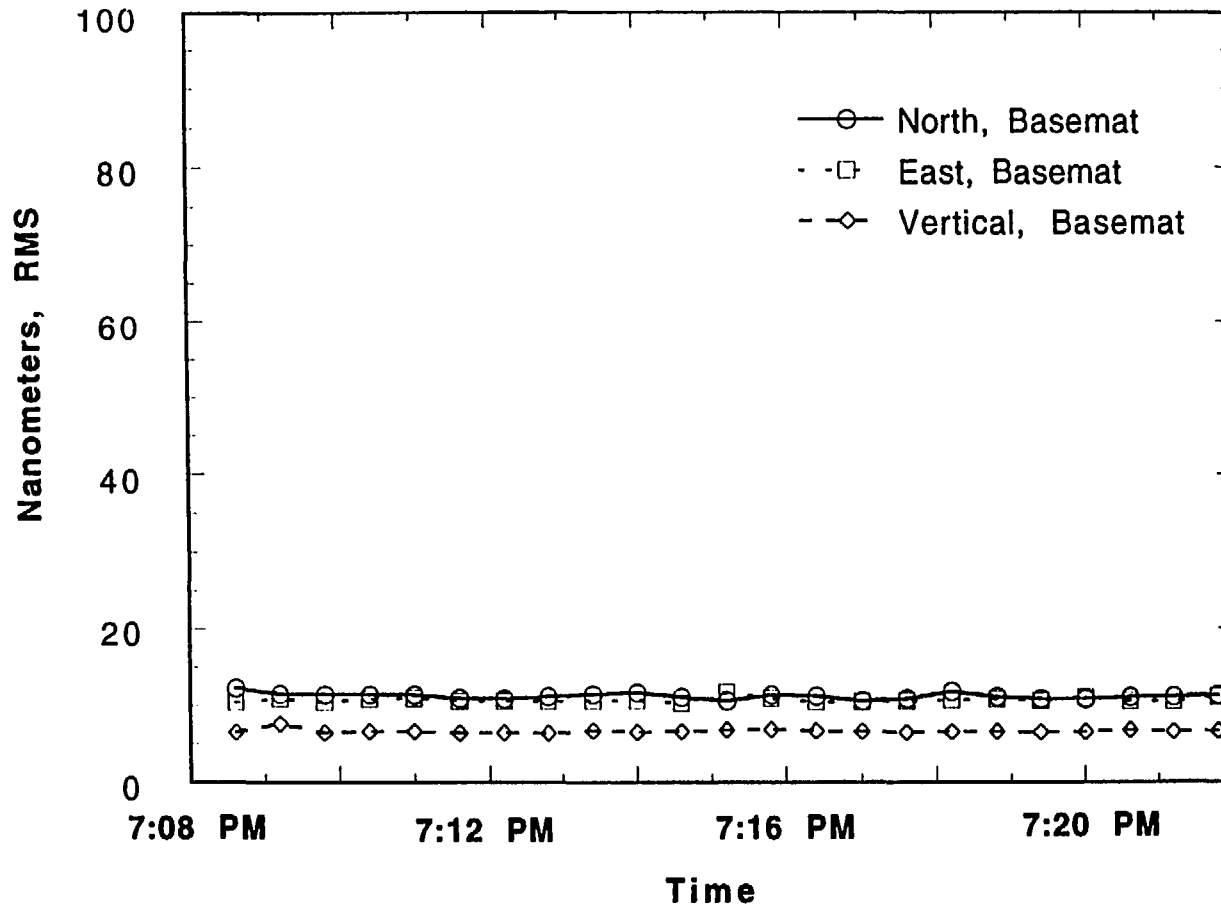


Fig. 58. Displacement response, Condition 3, on basemat, 10-100 Hz

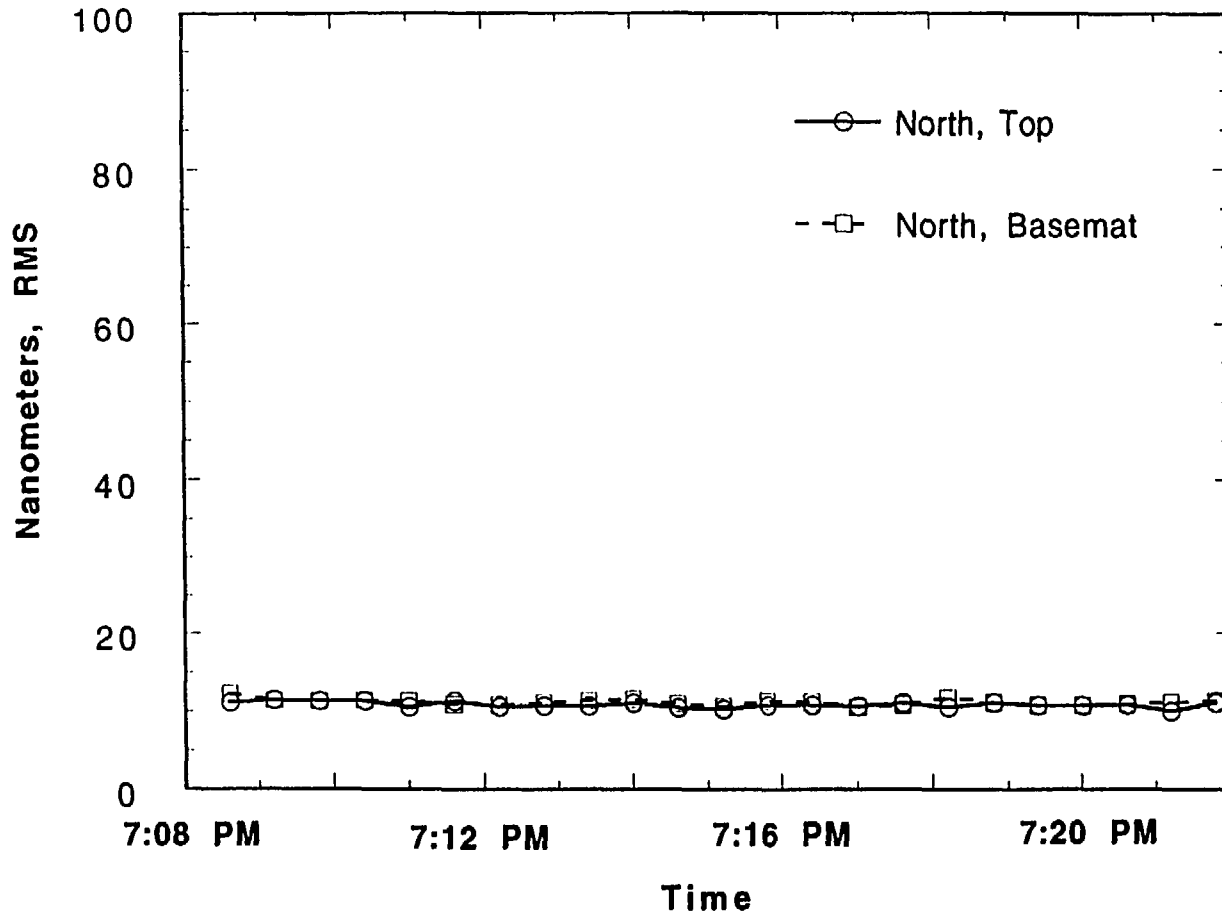


Fig. 59. Comparison of displacements, north roof to north basemat, 10-100 Hz

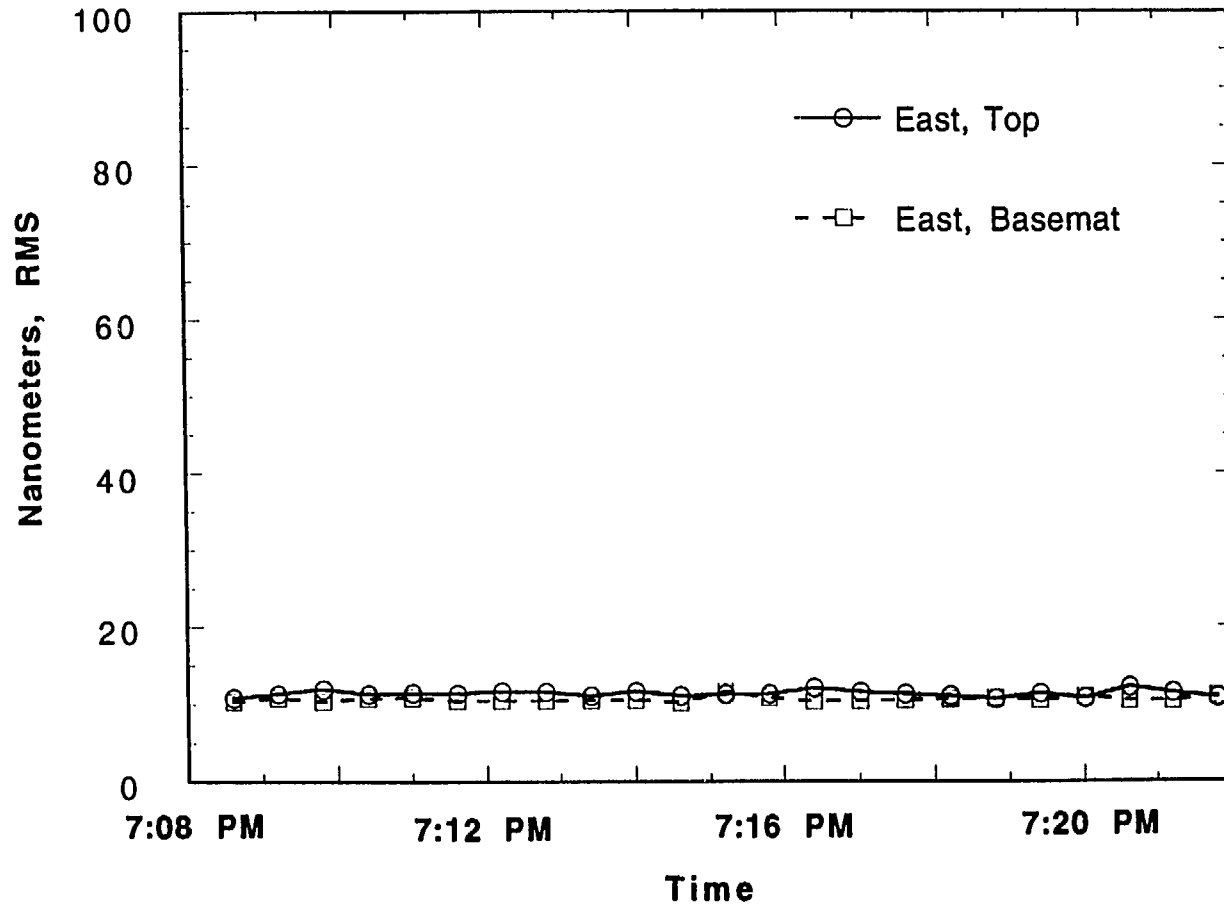


Fig. 60. Comparison of displacements, east roof to east basemat, 10-100 Hz

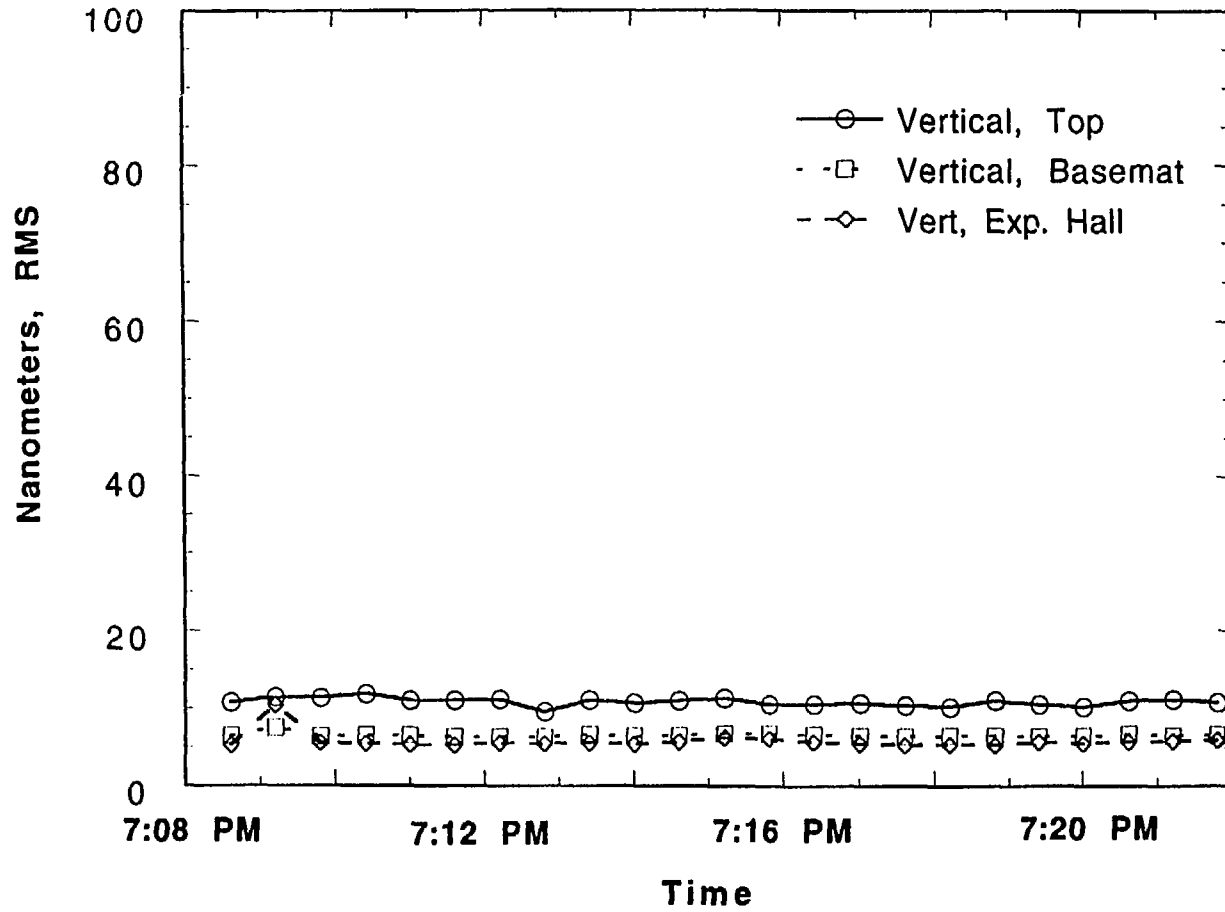


Fig. 61. Vertical displacements, Condition 3, 10-100 Hz

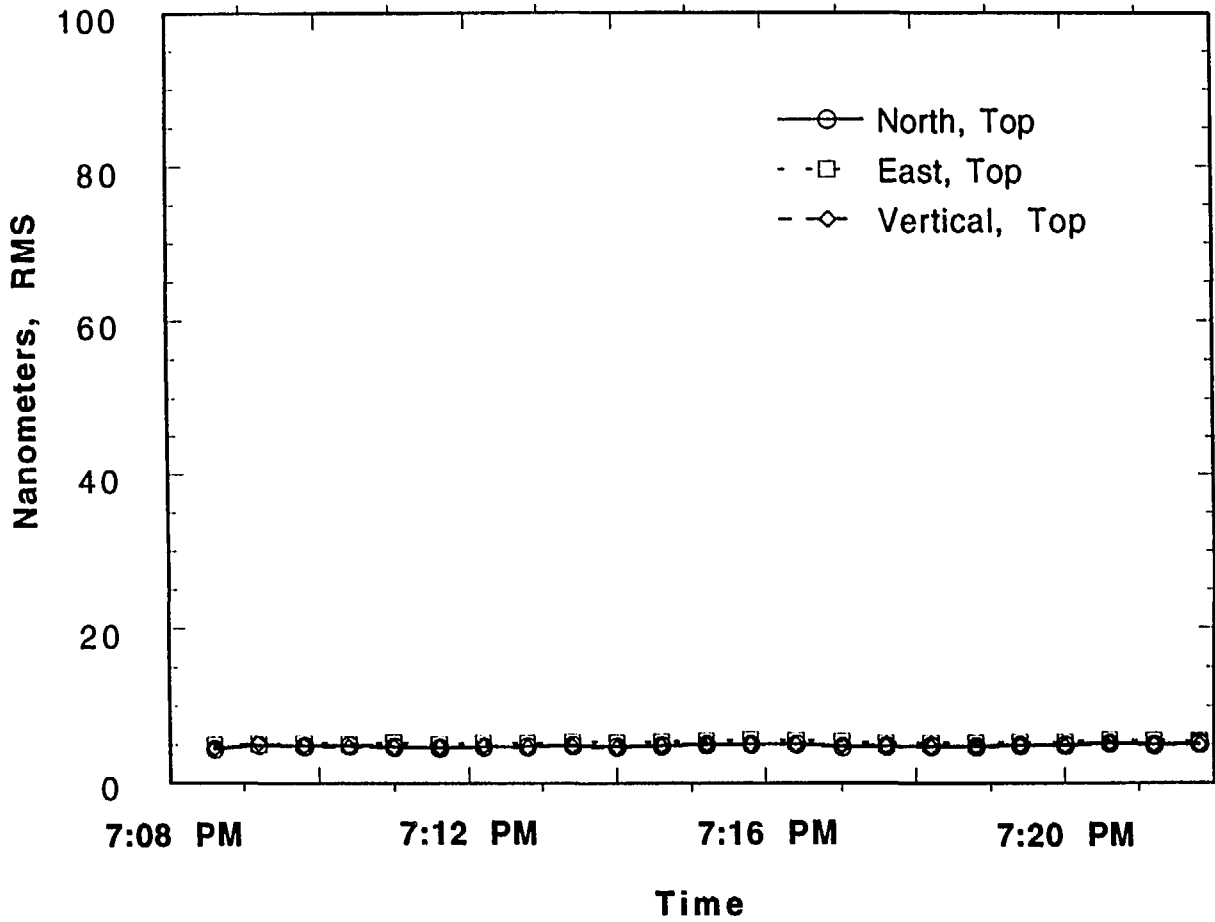


Fig. 62. Displacement response, Condition 3, on roof, 20-100 Hz

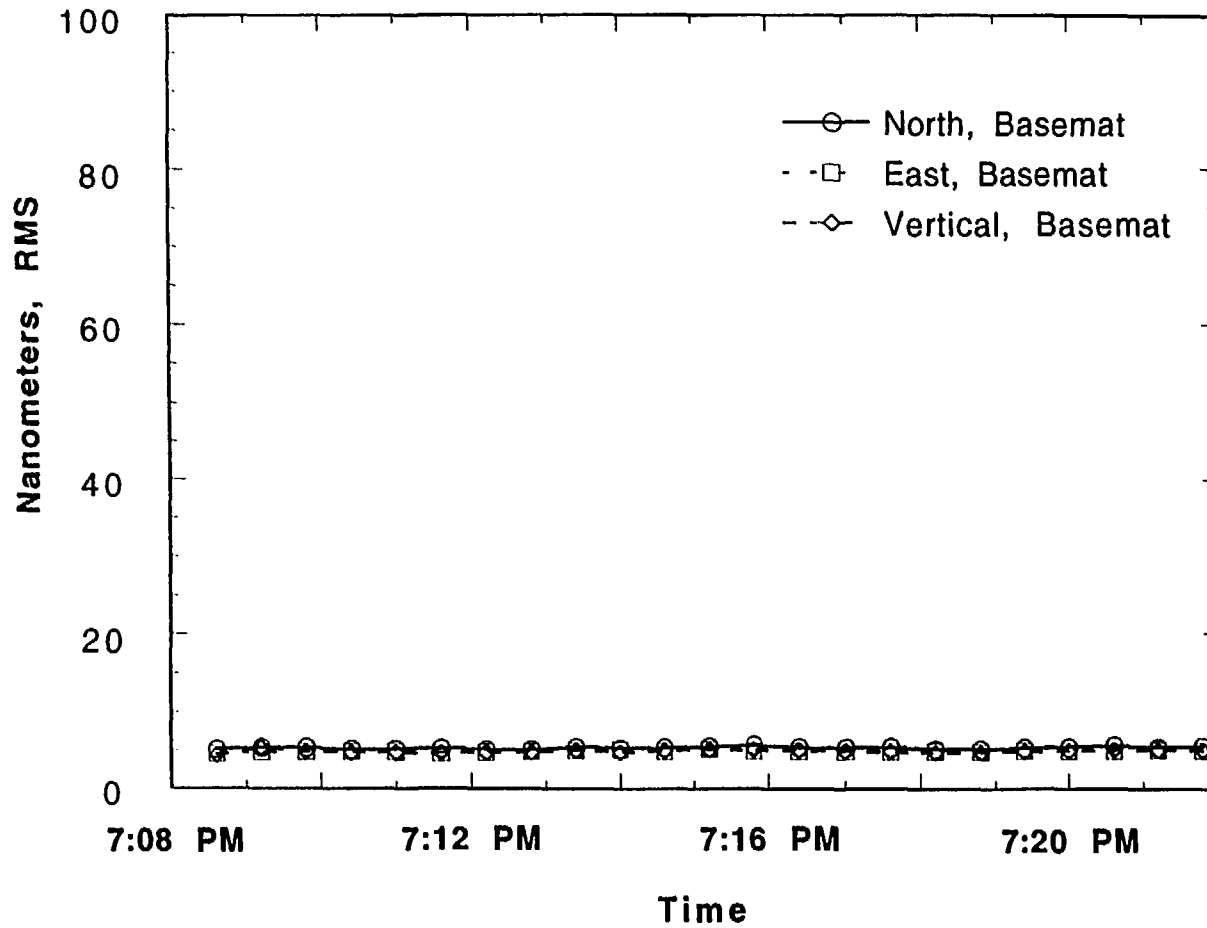


Fig. 63. Displacement response, Condition 3, on basemat, 20-100 Hz

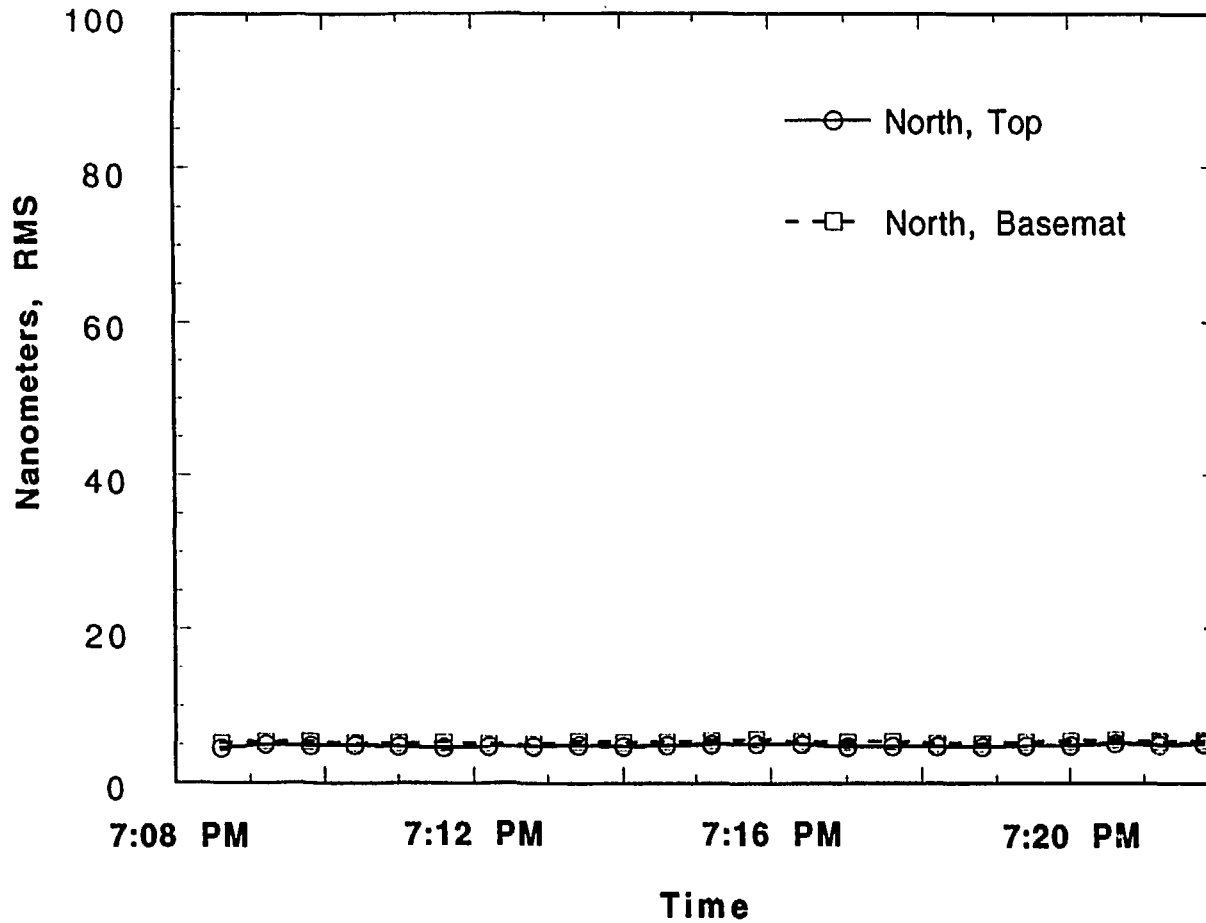


Fig. 64. Comparison of displacements, north roof to north basemat, 20-100 Hz

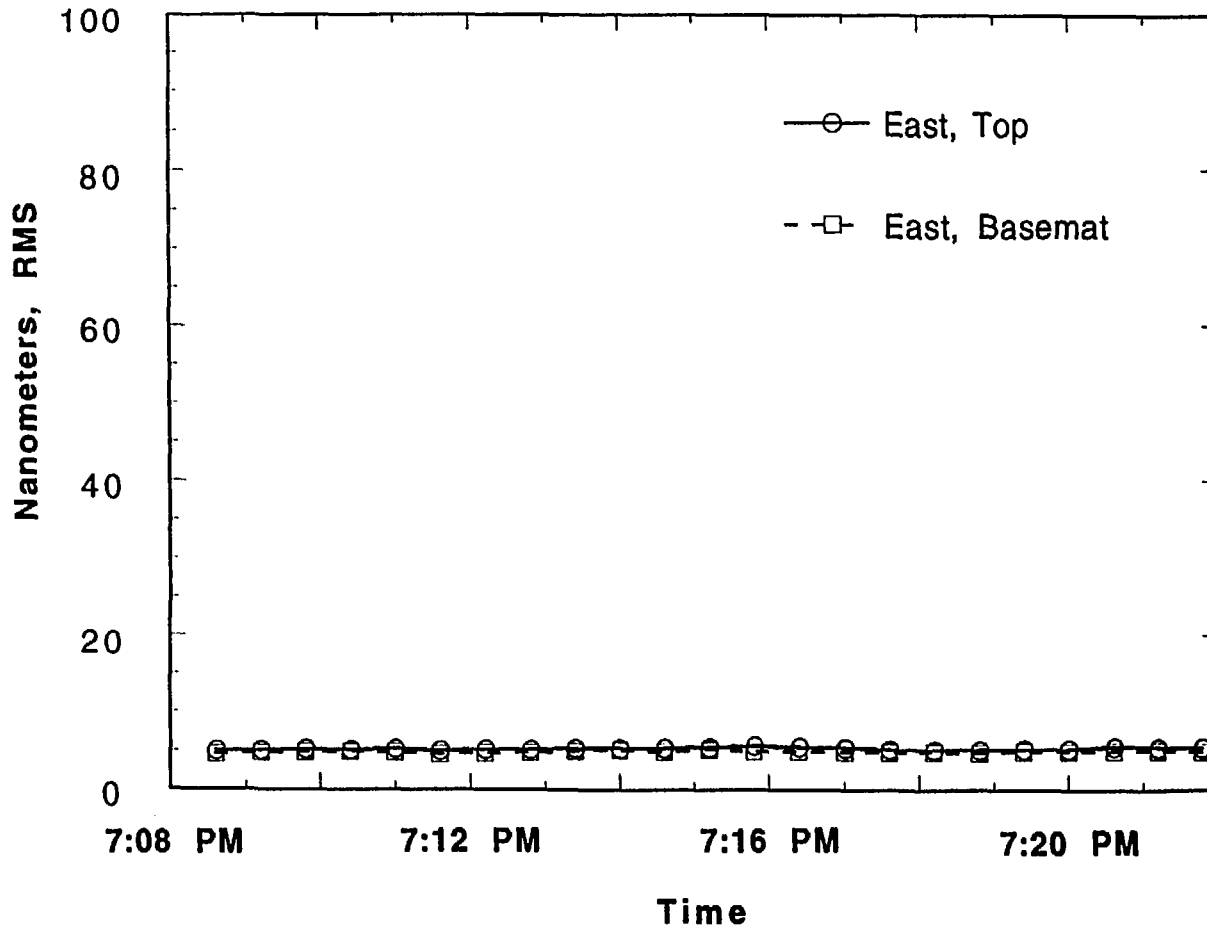


Fig. 65. Comparison of displacements, east roof to east basemat, 20-100 Hz

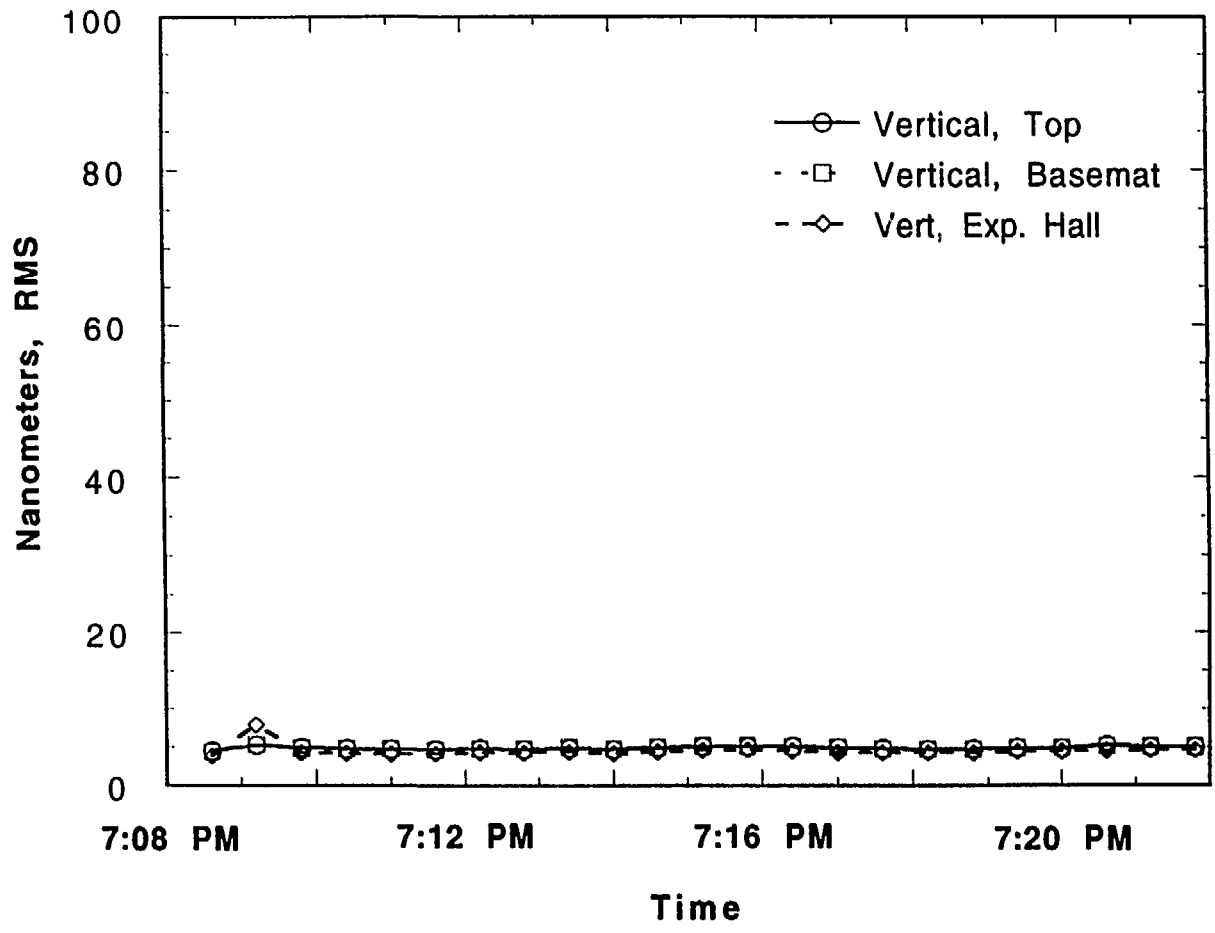


Fig. 66. Vertical displacements, Condition 3, 20-100 Hz

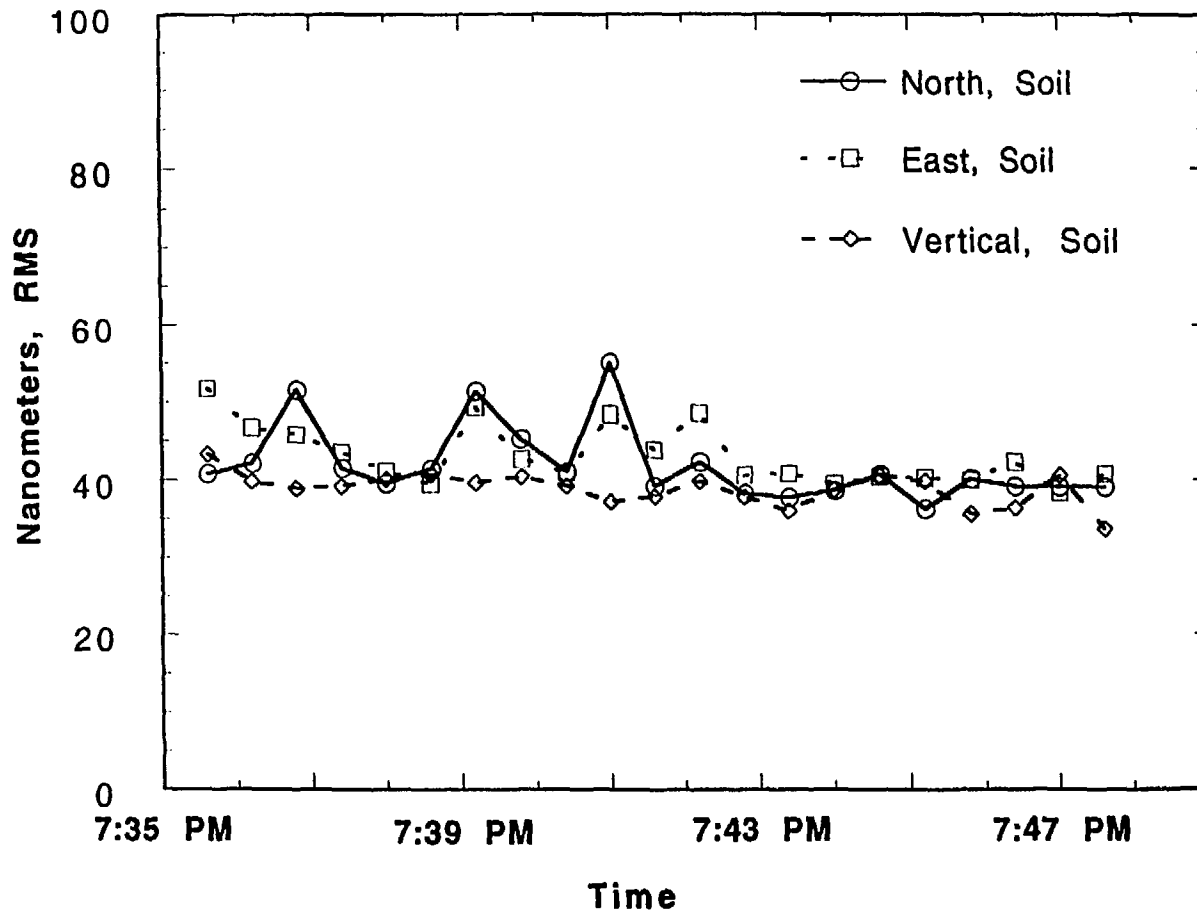


Fig. 67. Displacement response, Condition 4, north, soil, 4-100 Hz

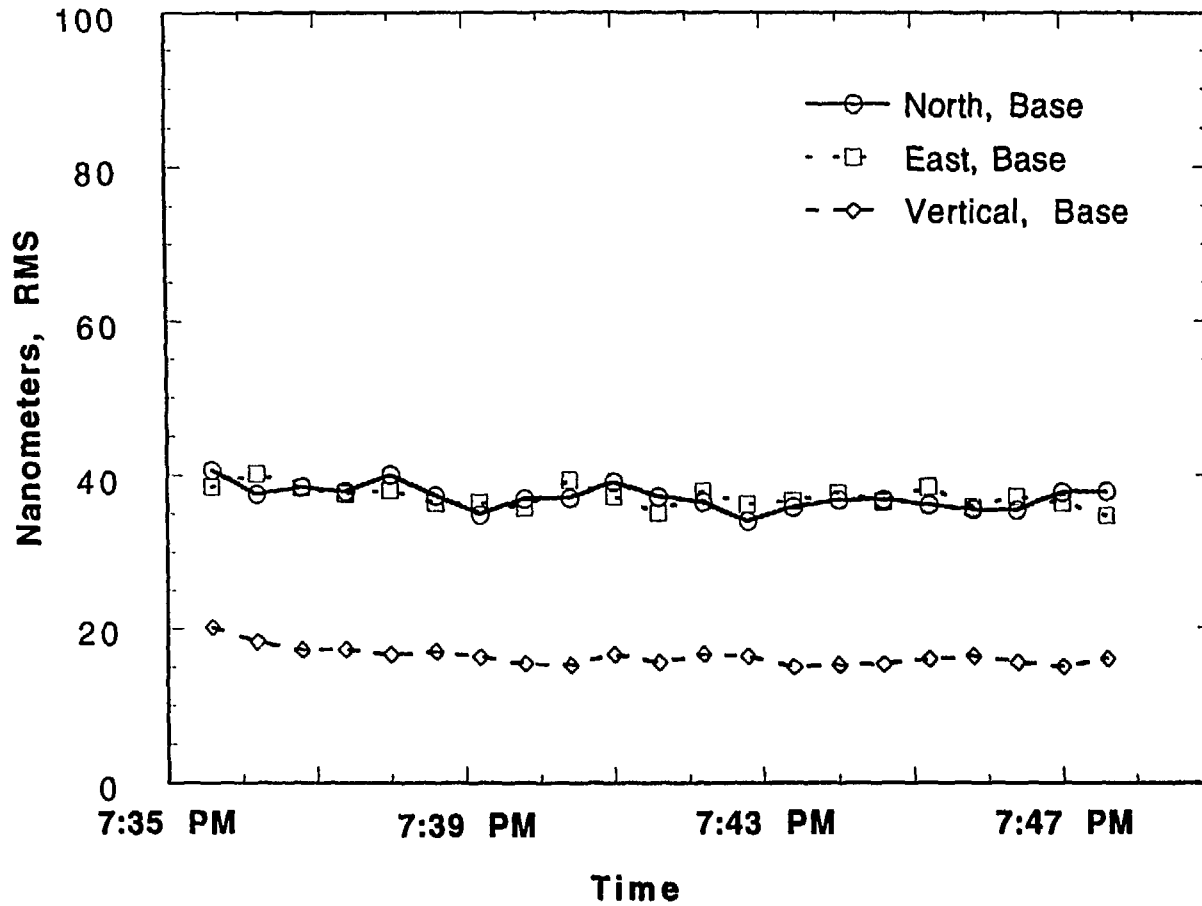


Fig. 68. Displacement response, Condition 4, north, basemat, 4-100 Hz

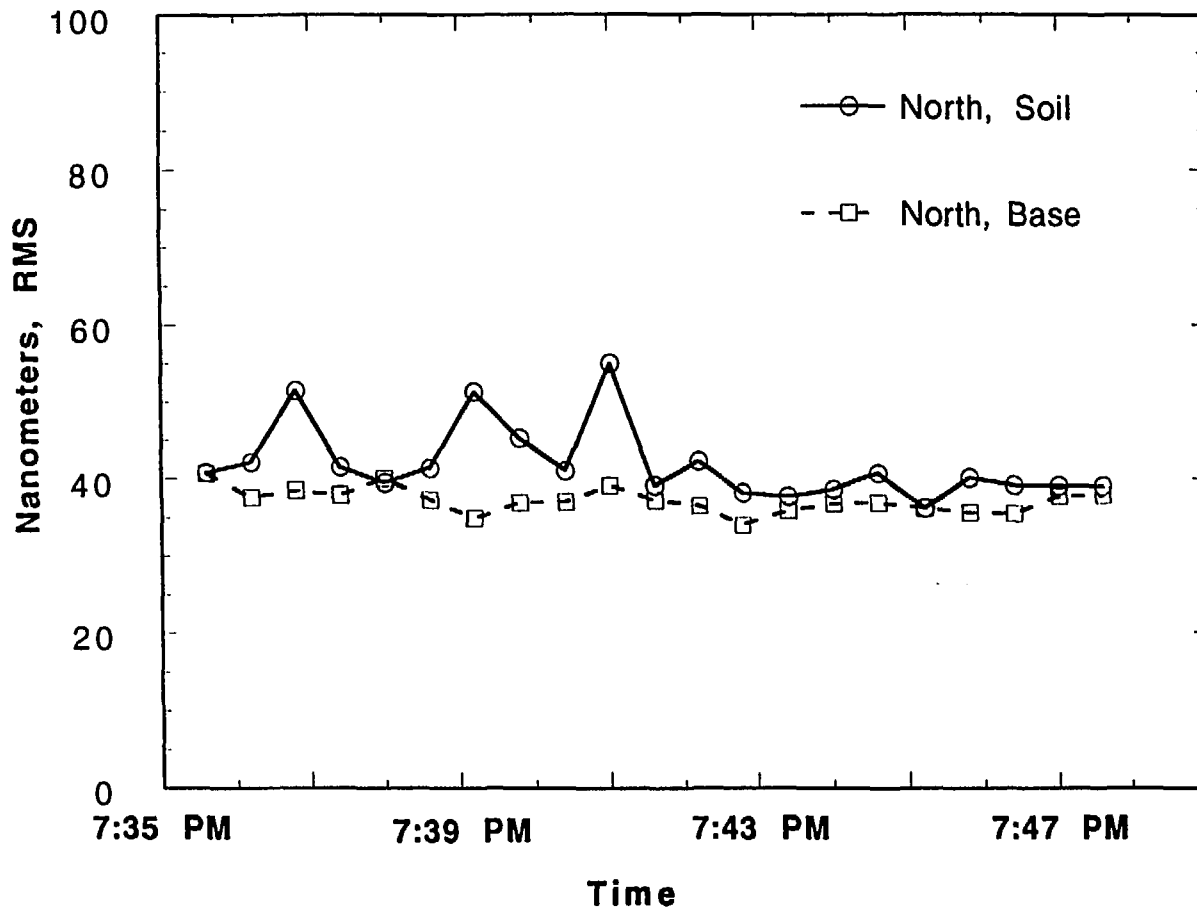


Fig. 69. Comparison of displacements, north basemat to north soil, 4-100 Hz

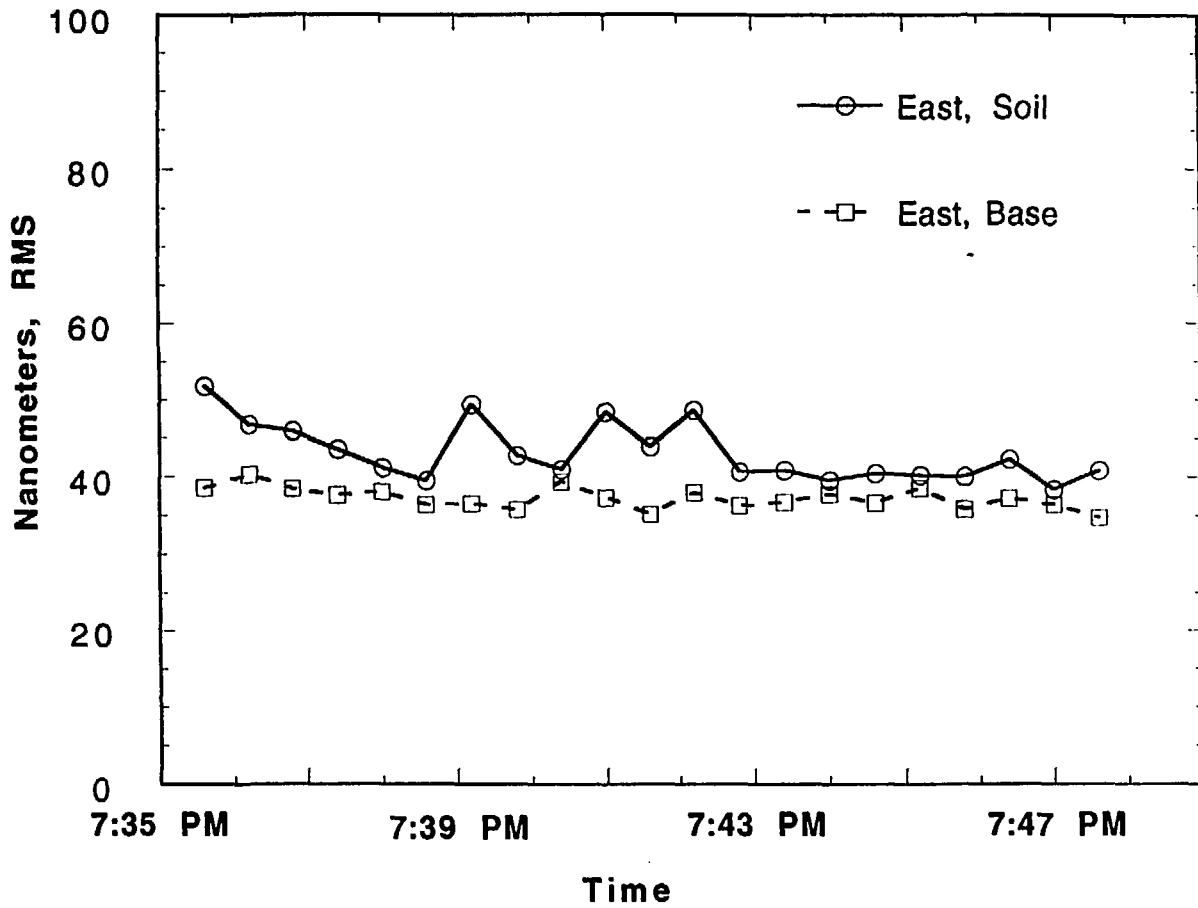


Fig. 70. Comparison of displacements, east basemat to east soil, 4-100 Hz

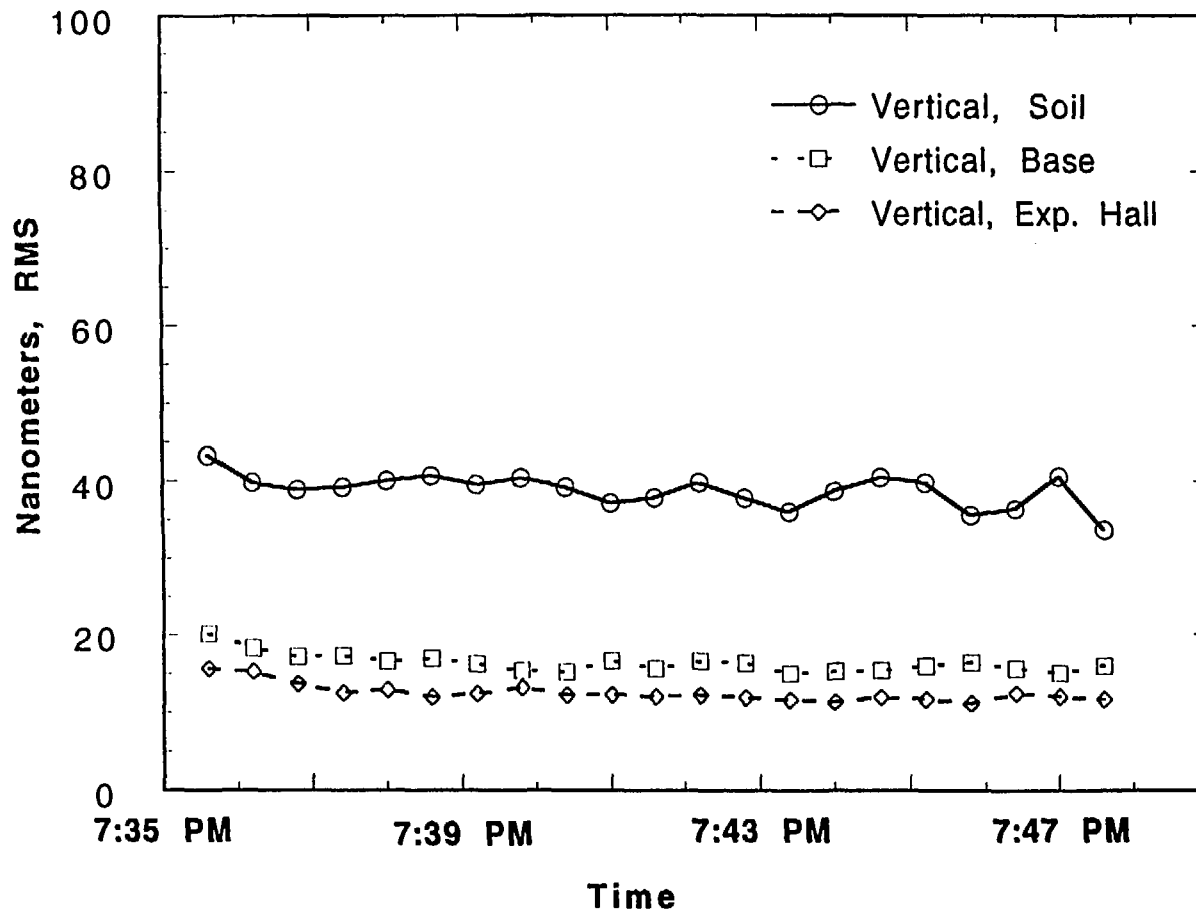


Fig. 71. Vertical displacements, Condition 4, 4-100 Hz

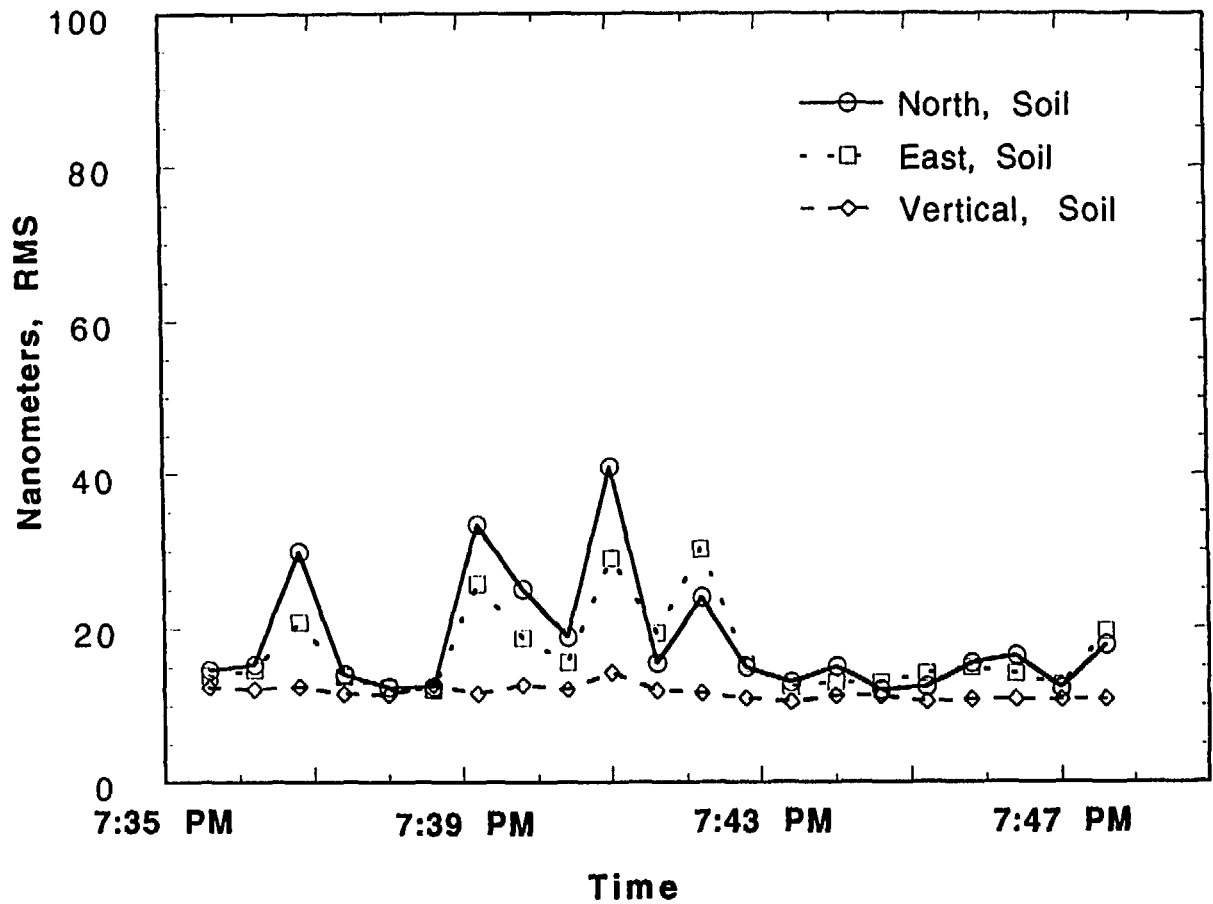


Fig. 72. Displacement response, Condition 4, north, soil, 10-100 Hz

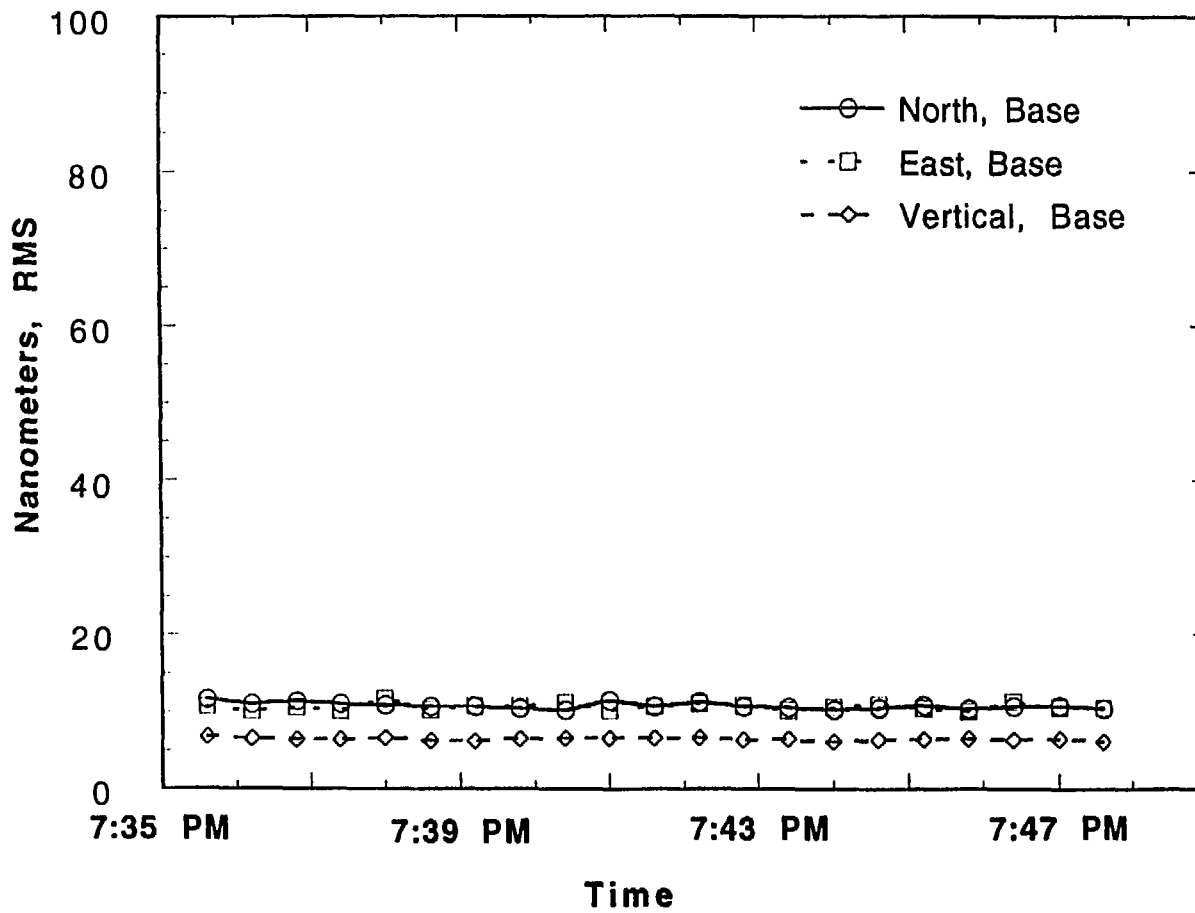


Fig. 73. Displacement response, Condition 4, north, basemat, 10-100 Hz

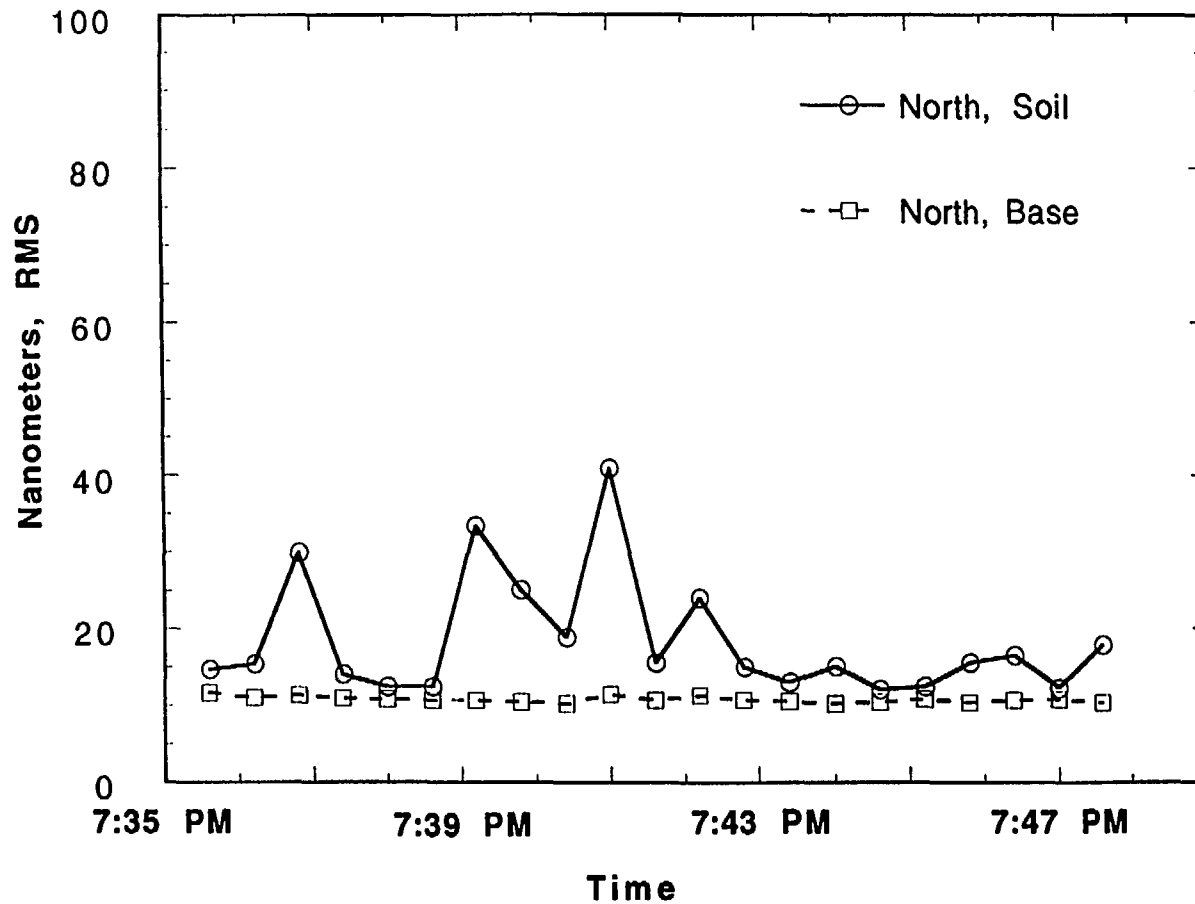


Fig. 74. Comparison of displacements, north basemat to north soil, 10-100 Hz

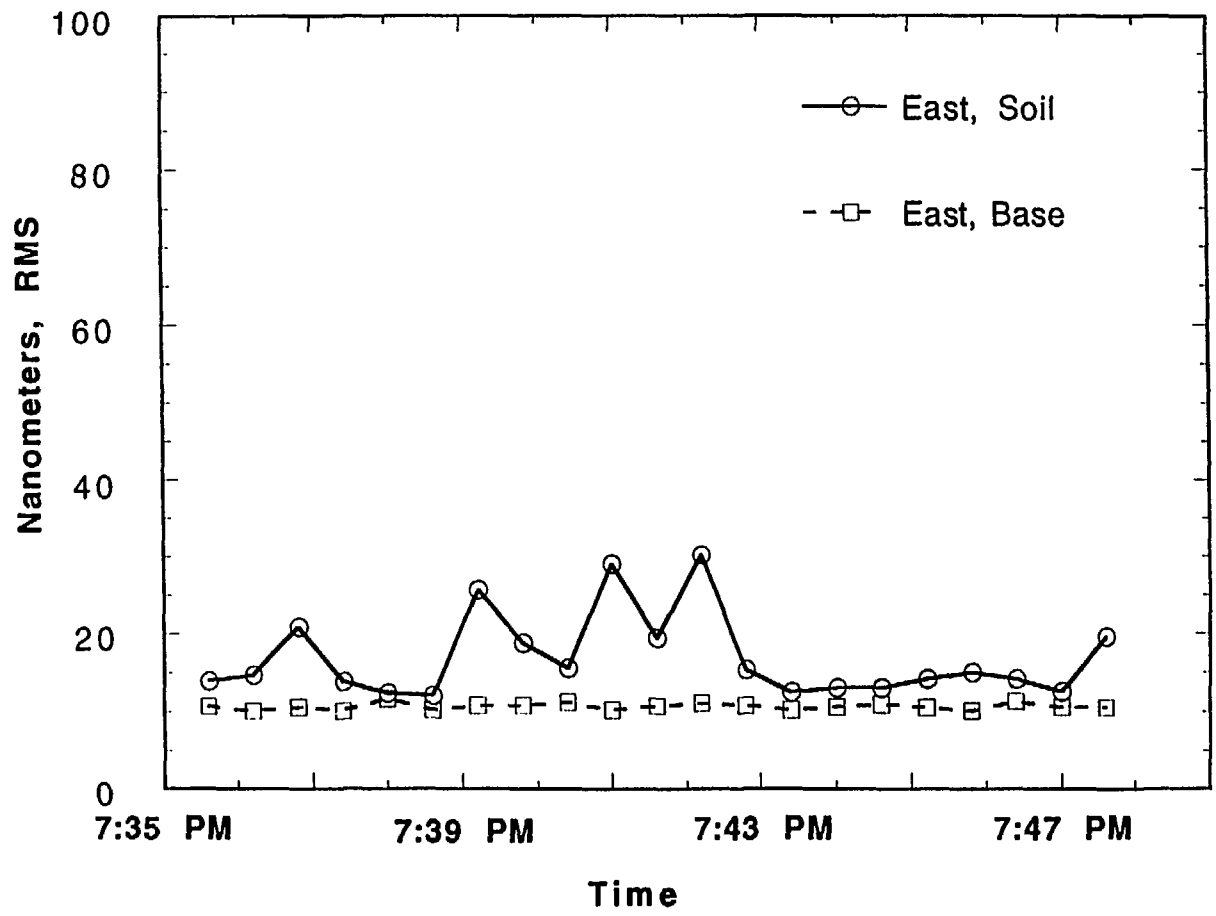


Fig. 75. Comparison of displacements, east basemat to east soil, 10-100 Hz

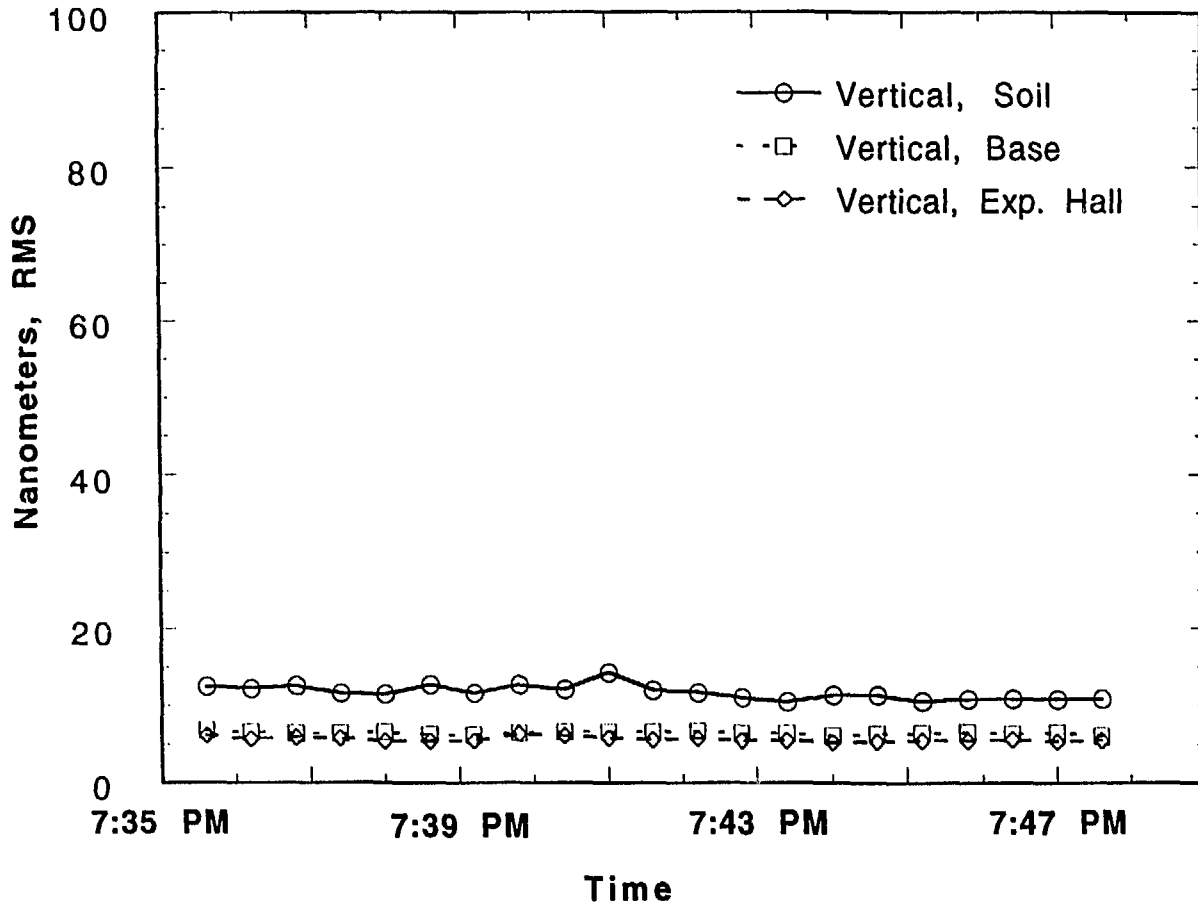


Fig. 76. Vertical displacements, Condition 4, 10-100 Hz

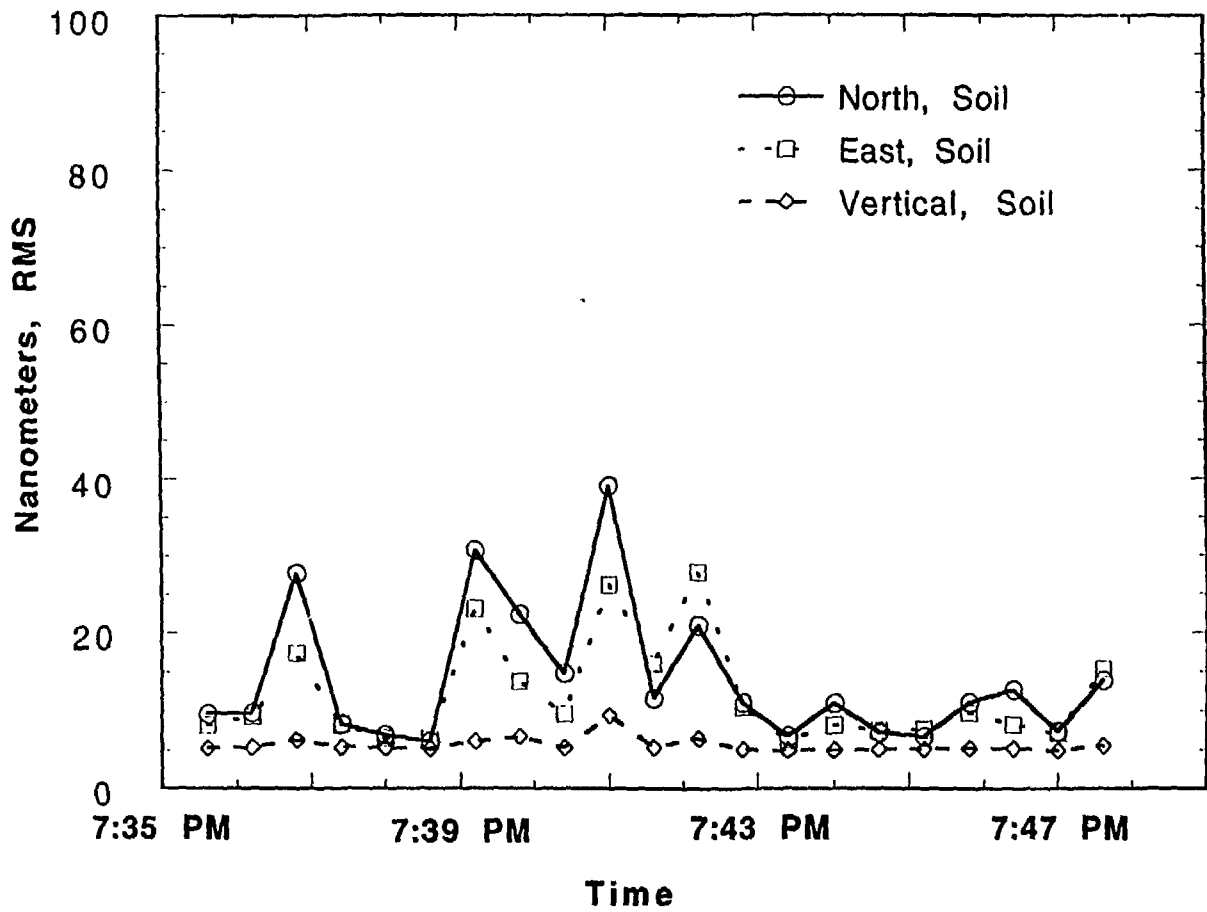


Fig. 77. Displacement response, Condition 4, north, soil, 20-100 Hz

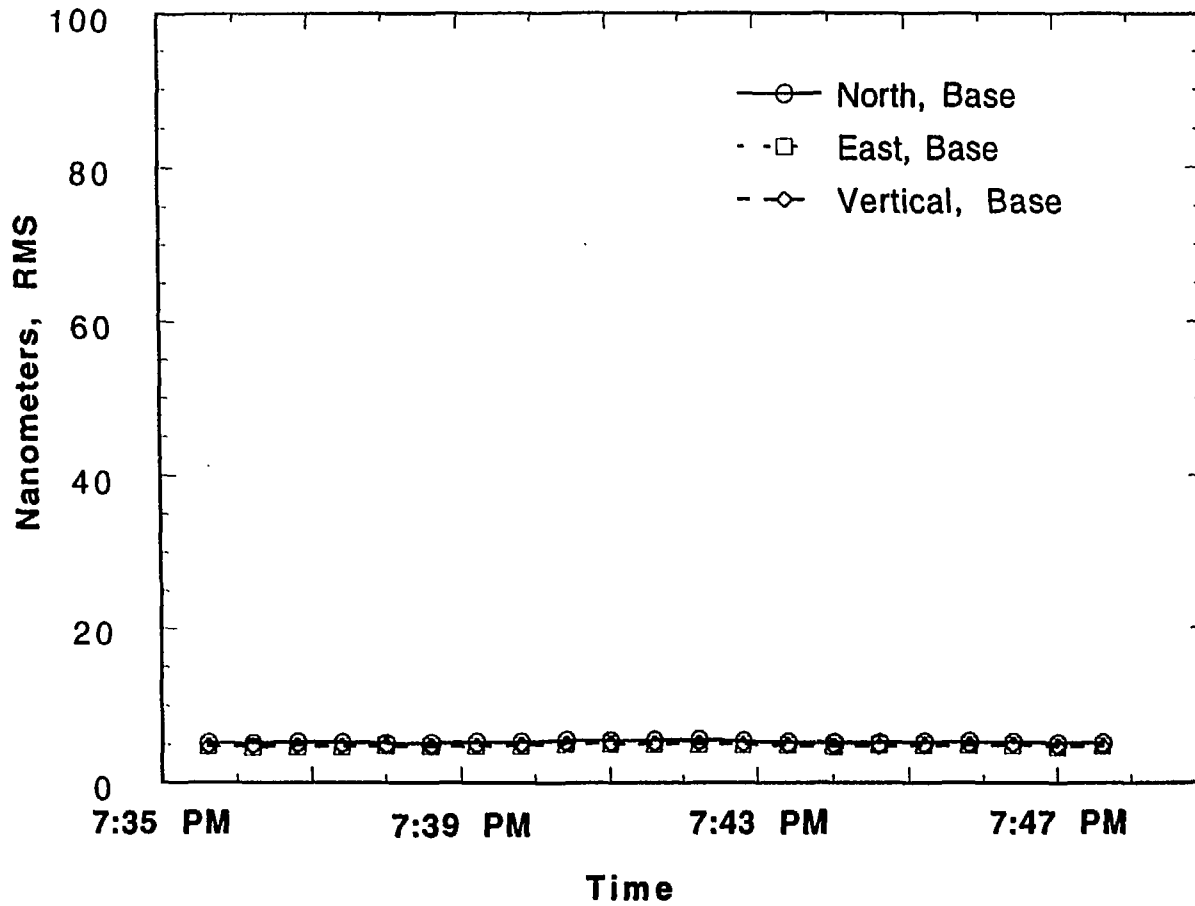


Fig. 78. Displacement response, Condition 4, north, basemat, 20-100 Hz

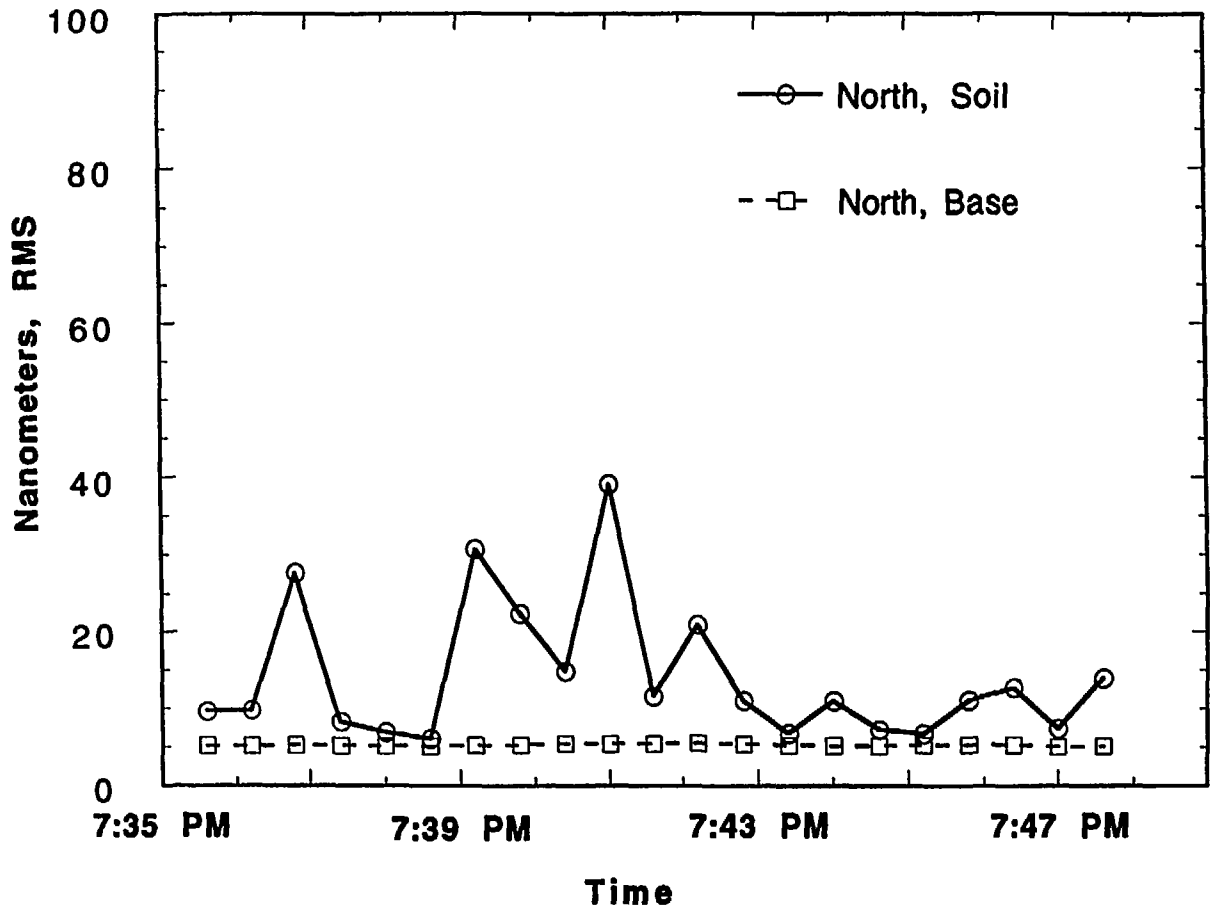


Fig. 79. Comparison of displacements, north basemat to north soil, 20-100 Hz

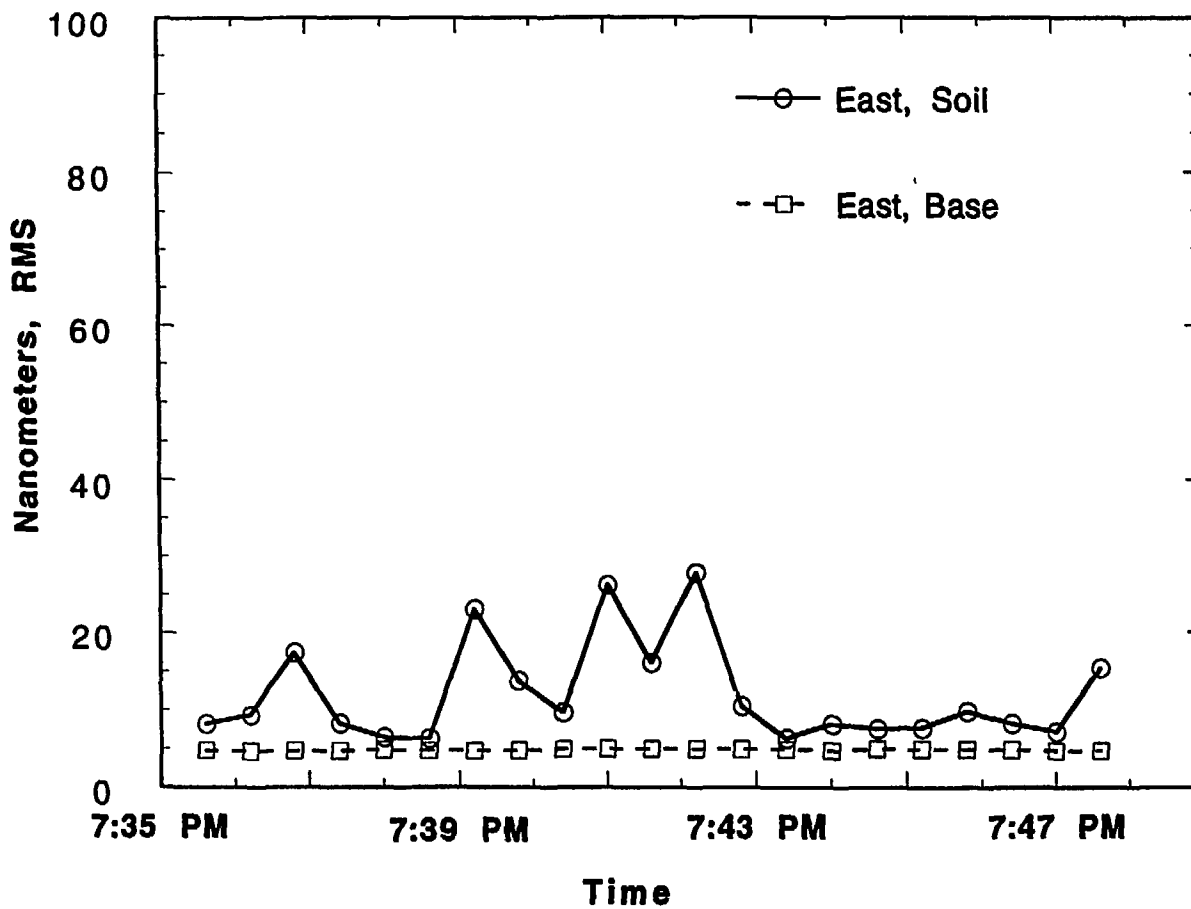


Fig. 80. Comparison of displacements, east basemat to east soil, 20-100 Hz

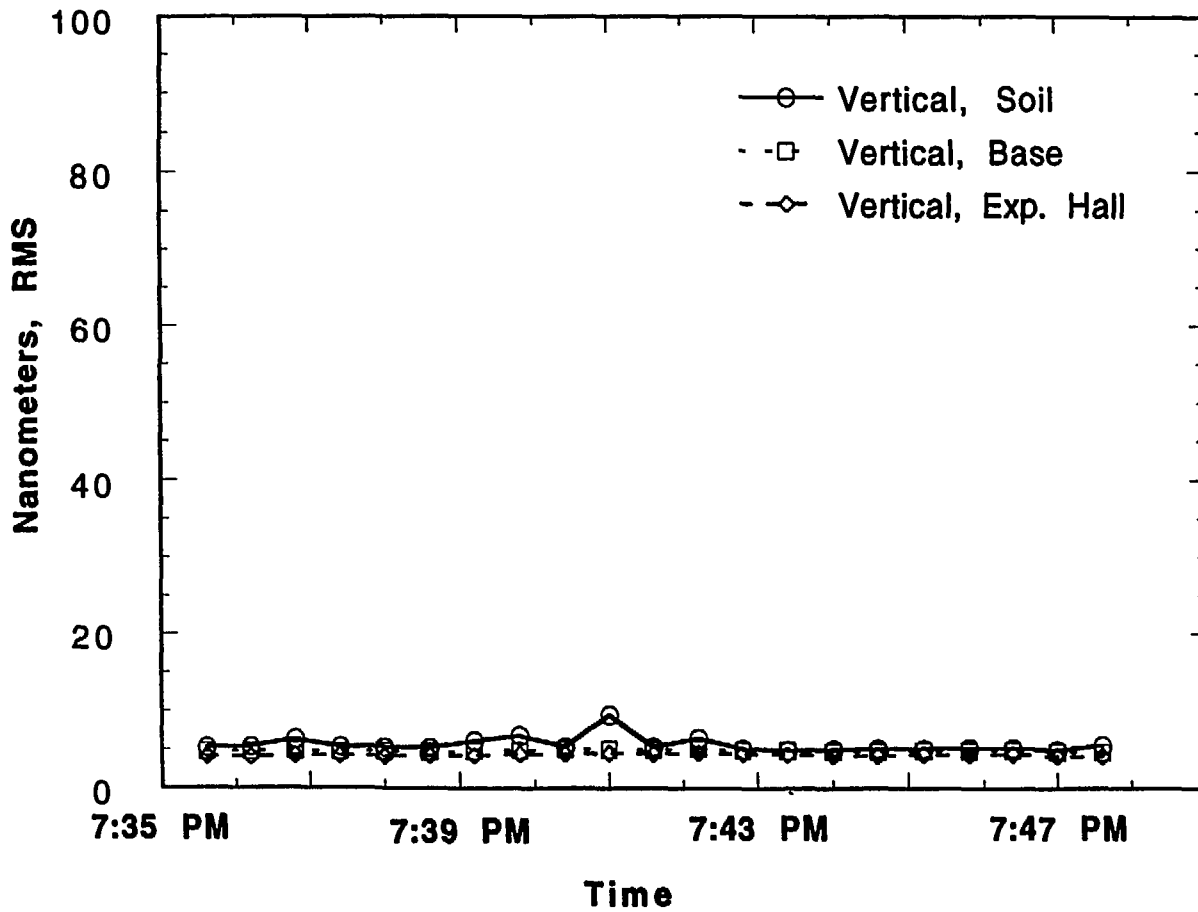


Fig. 81. Vertical displacements, Condition 4, 20-100 Hz